LITTORAL DRIFT AND THE PREDICTION OF SHORELINE CHANGES

Richard L. Pfeffer
Principal Investigator

The Geophysical Fluid Dynamics Institute
Florida State University
Tallahassee, Florida

The information contained in this paper was developed under the auspices of the Florida Sea Grant College Program, with support from the NOAA Office of Sea Grant, U. S. Department of Commerce, grant number 04-6-158-44 . This document is a Technical Paper of the State University System of Florida Sea Grant College Program, 2001 McCarty Hall, University of Florida, Gainesville, FL 32611. Technical Papers are duplicated in limited quantities for specialized audiences requiring rapid access to information, which may be unedited.

December 1976

PREFACE

This report consists of two parts. Part I contains 5 technical papers* by Barcilon, Lau, Miller, Tam and Travis, all of which are published in scientific journals with high standards of review. The first four of these cover results of our early work under the Sea Grant program. These papers provide insight into the mechanisms of formation of transverse sand bars, submarine longshore bars and rip currents. The fifth paper is a thorough review paper in which theoretical and experimental modelling of physical processes pertaining to the near shore are discussed and compared with field observations. Part II, by Christopher Miller, presents *the final computer model* for predicting changes in the plan shape of shorelines due to the littoral drift component. This part of the report includes a discussion of how the sediment transport rate is related empirically to the water flow; the range of incident wave angles for which the governing equations are stable, the finite difference scheme, as well as a *listing of the computer program*. It also includes a test of the model on specific coastal sites in Florida.

PART I: The study of longshore bars has led to the conviction that the dredging of certain submarine longshore bar systems may actually lead to severe erosion of the shoreline. A further suggestion has been made concerning the possibility of reversing erosion trends in some beach locations by properly

*Editorial note: The five papers are included by reference only, as they appear in the literature already.

References

Barcilon, A., and J. P. Lau. 1973. A Model for Formation of Transverse Bars. J. Geophys. Res. 78(15):2656-2664.

Lau, J. P., and B. Travis. 1973. Slowly-varying Stokes Waves and Submarine Longshore Bars. J. Geophys. Res. 78(21):4489-4497.

Lau, J. P., and A. Barcilon. 1973. Harmonic Generation of Shallow Water Waves over Topography. J. Phys. Ocean. 2(4):405-410.

Miller, C., and A. Barcilon. 1976. The Dynamics of the Littoral Zone. Rev. Geophys. Space Phys. 14(1):81-91.

Tam, C. K. W. 1973. The Dynamics of Rip Currents. J. Geophys. Res. 78(12):1937-1943.

contouring the bottom topography to conform with wave-resonant equilibrium patterns determined by the theory. It remains, however, to determine the logistics and economics of such a venture. Specific abstracts of each of the 5 individual papers in this part of the final report are as follows:

The paper by Lau and Barcilon (1972) investigates the reflection and *non-linear* interaction between the first and second harmonics of a two-dimensional Boussinesq wave train. Effects of topography are included, with the depth departing from a constant in a finite region. It is found that topography can speed up or retard energy transfer between the first and second harmonics. The reflection coefficient is significantly different from the one obtained by using linear theory.

In the paper by Barcilon and Lau (1973) an extension of Kennedy's potential model is used to investigate the formation of sand bars normal to a gently sloping beach. The results show that the spacing between the transverse bars depends upon the inverse of the beach slope and upon the square of the drift velocities across the bars. In spite of certain drawbacks the theoretical predictions compare well with several observational studies.

The paper by Lau and Travis (1973) investigates the mass transport velocity in the Stokes boundary layer due to slowly varying Stokes waves impinging on and reflecting from a plane-sloping beach. The resulting mass transport velocity distribution is interpreted to indicate the possible locations of submarine longshore sand-bar formation. It is found that the number of bars is likely to increase when the bottom gradient is slight and that the spacing between the crests of the bars increases seaward for some distance offshore. These results are in qualitative agreement with field observations.

The paper by Tam (1973) investigates the dynamics of rip currents using shallow water equations with a horizontal eddy viscosity term. In this paper similarity solutions of the model equations are found which appear to give reasonable representations of the velocity profile and other characteristics of rip currents.

The *comprehensive review paper* by Miller and Barcilon (1976) covers the present knowledge concerning the dynamics of rip currents, longshore currents and *computer modelling* of beach deformation due to wave-induced erosion and accretion.

PART II: As mentioned above, this part of the Final Report (by Miller) contains the final predictive computer model including a listing of the computer program and a test of the model on specific coastal sites in Florida. The numerical model is based upon recent developments in the theory of longshore currents and Lagrangian description of shoreline deformation. The computer program requires as input data the breaker characteristics (i.e., height, angle and duration for each wave considered) computed from raw data. The choice of sites for testing the predictive characteristics of this program was dependent on the availability of wave and bathymetric data. During 1975 deep water ship wave data for the Gulf of Mexico were analyzed for long-term (100 years) study of St. George Island. In addition, a beach nourishment project at Jupiter Island provided the opportunity for a short-term (8 months to 5 years) study. The field observations on wave climate and transverse profiles gathered by our collaborators at the University of Florida were provided to our group for analysis during the course of the year. Observed changes in the St. George and Jupiter Island plan profiles were compared with test predictions of the computer model and are presented in this part of the Final Report. Moreover, the computer prediction was extended beyond the present time for these beaches by 20 years and 5 years, respectively, and will require further monitoring of the beach morphology to verify the future predictions.

One result of the study was the definition of a reasonable range for the empirical coefficient linking the sediment and water motions. It was found for St. George Island that, over the time period of interest, the longshore mode of sand transport dominated and therefore, good predictions could be made if the nearshore wave field were known well. For Jupiter Island, on the short term, the onshore-offshore component of sand movement predominated, thus making it possible to model only general trends due to the re-working of the strandline by the longshore drift. Special attention is afforded the endpoint condition in each case.

The major conclusion of this study is that the present numerical model is a viable predictor of shoreline movement if (1) the predominant direction of sand transport is longshore (2) the nearshore wave climate can be adequately resolved (3) endpoint boundaries are treated in a physically realistic manner.

The Numerical Prediction of Shoreline Changes Due to Wave-Induced Longshore Sediment Transport

Christopher D. Miller

Geophysical Fluid Dynamics Institute
Florida State University
Tallahassee, Florida

1975

Acknowledgements

The author would like to extend his appreciation to the following people:

Dr. Charles Quon of the Bedford Institute of Oceanography, Dr. Paul Schwarztrauber of NCAR for helpful discussions; Todd L. Walton of the University of Florida for the use of his wave modification program; Ziya Ceylanli of the University of Florida for valuable advice and assistance on the Jupiter Island project; Dr. Richard Pfeffer for making available the facilities and resources of the Geophysical Fluid Dynamics Institute, Florida State University.

Abstract

We have attempted to quantify numerically the changes which occur in the plan shape of beaches due to wave-induced longshore sand transport. The approach of this study has been to draw upon recent developments in the theory of longshore currents, beach deformation, and sediment transport to synthesize a numerical model which can be calibrated in accordance with field observation and laboratory studies and, subsequently, used to make predictions of shifts in a shoreline, given certain bathymetric and wave data as input. The work of Longuet-Higgins (1970a,b) on longshore currents and that of LeBlond (1972) on shoreline evolution constitute the framework within which we build our numerical model. The model is applied to two Florida coastal regions, the Apalachicola Bay region in the Panhandle and Jupiter Island on the southeast coast.

Table of Contents

I. Introduction

A beach face can only achieve a state of quasi-equilibrium. Acted on by varying wave climate, wave-induced circulations, tidal currents, wind-generated currents, etc., it undergoes modification on both short and long time scales. Movements of sediment are induced in both the onshore-offshore direction and the longshore direction. There is much evidence that the sediment motion normal to shore is cyclical in nature (e.g., the classic winter-summer variations in the transverse profile) and that over the course of a year the net loss or gain of sand to the beach system in this direction approximates zero. Exceptions to this tenuous rule occur when the sand moved offshore is made unavailable for eventual transport shoreward, for instance, when a nearshore canyon acts as a sink for the sand flow (as in Southern California) or when storm waves remove the sand to such a depth that the 'summer' (accretive) waves cannot effect the shoreward migration of the resulting semi-permanent offshore sand bars (e.g., off the west coast of Florida), etc. In this study we are concerned with time scales of, at least, 1 year and longer. We assume implicitly that over the period of a year there is no net displacement of the shoreline due to the onshore-offshore shifting of sand. If this were not the case then we would have to establish criteria, both theoretical and empirical, governing the movement of sand normal to the beach; examples of such approaches are provided in section III.

There are several agents which can be responsible for the introduction of sand into or the removal of sand from a beach system. A river can discharge enormous quantities of sediment into the coastal zone replenishing the beaches continuously. A tidal inlet with its delicate balance between currents and sand transport can act as an impasse to the longshore 'river of sand' flowing by its mouth, trapping a substantial amount in shoals both outside and inside of the inlet channel. Violent storms (e.g., hurricanes) with their associated surge and high waves can carry beach sand landward ('washover') or far seaward making it inaccessible to the normal accretive processes. The refraction and diffraction of waves around barriers, man-made (jetties, groins) and natural (tips of islands and spits), conveys sand into quiescent 'shadow' regions where it is sheltered from wave attack. In other words, in order to model correctly the changes in a coastal area, one must be familiar with the hydrodynamics and marine geomorphology peculiar to that locale.

Confining our attention to the longshore drift of sand which we view in this study to be the principal means by which the particulate matter at the coast is redistributed we seek to apply recent developments in the theory of longshore currents (Longuet-Higgins, 1970a,b) and shoreline deformation (LeBlond, 1972) to the practical problem of predicting the change in the shape of a shoreline over a period of time. The procedure entails choosing a coastal site for which adequate data on wave climate and shoreline development exist. With wave and bathymetric data serving as inputs the distribution of breaker wave characteristics along the shore is computed; using this information a forcing function for the longshore flux of water and sand can be derived. The longshore divergence of these flows leads to local accumulations or deficits of sediment and the subsequent movement in time of the strandline can be monitored. A predictive computer model is developed based on these simple concepts and is applied to St George Island, a barrier island fronting the Apalachicola Bay, Florida, and Jupiter Island on the south-east coast of Florida. St. George Island is presently undergoing developmental pressures. Jupiter Island, plagued by erosion problems, is the site of a recent beach fill project; the question naturally arises as to whether or not the local beach system can retain this artificially deposited sand. Our approach to each site differs because of the nature of the inputs (source and analysis of wave data, bathymetry), the scale of the motions, and the time period of interest. We elaborate on these points in sections VII and VIII.

Previous numerical studies on the molding of a coastline composed of loose material by wave-induced forces include Price, et al. (1972), Komar (1973), and LeBlond (1972). Price, et al. and Komar formulated one-dimensional Lagrangian descriptions for beach change, i.e., the translation of the coordinate points which define the shoreline was restricted to to-and-fro motion along a line parallel to one of the fixed coordinate axes. Figure 1 from Komar indicates how the shoreline is represented and its movement normal to itself. In LeBlond's model the beach points

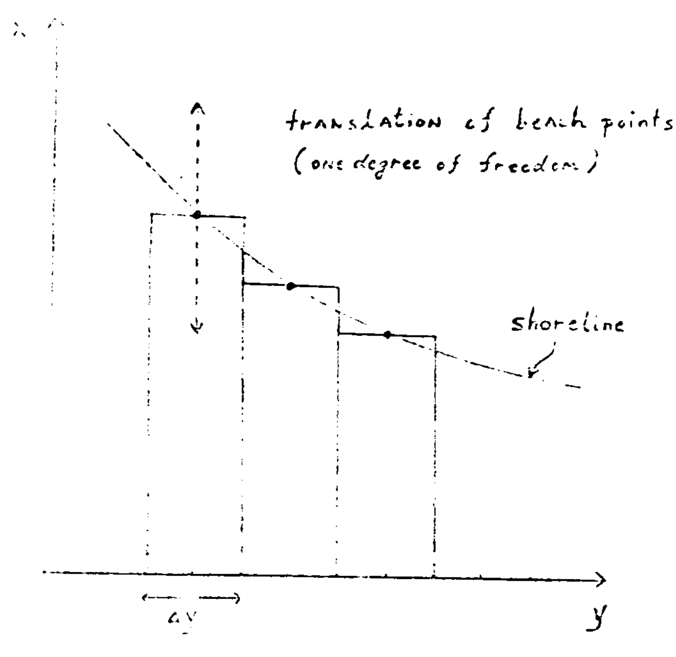

Figure [illegible] [illegible] of shoreline according to Komar (1973).

are free to move in the entire horizontal plane (a two-dimensional Lagrangian formulation); this allows for a more accurate tracking of the evolving beach shape as well as a truer modeling of end point boundary conditions (see Figure 4). Among the disadvantages are the possibility of very irregular spacing between points and the merging of adjacent points (note: our computer model allows for 're-setting' the beach if this is warranted).

The general format for this study involves a discussion of the equations governing the fluid and sediment motions, the finite-difference form of these equations and a scheme for their integration, a treatment of the empiricism which links the magnitude of the sand flow to the longshore current, an explanation and listing of the computer program, application of this numerical model to specific beaches and conclusions.

II. Longshore Currents and Beach Deformation

1. Longshore Currents

Over the years various approaches have been adopted in attempts to describe how the orbital motion of water waves is converted into the circulation velocities found in and near the surf zone. Longshore currents, which are prominent when wave crests break skew to the bathymetric contours, have been treated theoretically by considering the balances of mass, momentum, and/or energy in the wave-breaking region. Galvin (1967) has provided a summary of longshore current theory and supporting lab and field data up to 1967. Galvin's conclusion that both theory and data are wholly inadequate led to more sophisticated theoretical models by Thornton (1969), Bowen (1969) and Longuet-Higgins (1970a,b). Based on the conservation of momentum and the "radiation stress" concepts introduced by Longuet-Higgins and Stewart (1960,1961,1962,1964) these three researchers independently developed models to explain how the longshore current is generated and what accounts for its cross-stream (shore-normal) profile. Each postulated that the main forcing for this current is the oblique approach of a long-crested breaking wave front. The steady state balance was taken to be between the shore-normal gradient of the component of excess momentum flux (radiation stress) parallel to shore and retarding bottom and lateral friction. Bowen used a bottom friction term proportional to the longshore current, v, and a constant horizontal eddy viscosity coefficient. Thornton and Longuet-Higgins derived expressions for the bottom stress and lateral coupling terms which differ from Bowen's and which are more plausible physically. They showed that the bottom friction is proportional to the product uv where u is the amplitude of the local orbital velocity perpendicular to the shoreline. The eddy coefficient was assigned an offshore dependence, tending to zero at the shore and increasing monotonically toward the breaker line, where maximum mixing is to be expected. In Thornton's model the mixing coefficient was allowed to realistically decay seaward of the breaker line, whereas in Longuet-Higgins' model it increased continuously from shore seaward. Thornton solved his equations numerically; Bowen and Longuet-Higgins obtained analytical solutions. The longshore current profiles in each study were supported by the available data, such as the laboratory results of Galvin and Eagleson (1965).

For our purposes the equations of Longuet-Higgins seem the most appropriate because of the physical bases for his derivation and the ease of applying his results. To be specific, his expression for the longshore current as a function of the non-dimensional offshore coordinate, $x^* = x/x_b$ (modified slightly by inverting the x-axis so as to have a positive depth gradient) is

$$v = \frac{K x^{*p_1} \sin\phi_b}{P(p_1-p_2)(p_1-1)} + \frac{2K x^* \sin\phi_b}{(5P-2)} \qquad 0 \le x^* \le 1$$

$$= \frac{K x^{*p_2}}{P(p_1-p_2)(p_2-1)} \qquad 1 < x^* < \infty \tag{1}$$

where x_b = width of surf zone

$K = \frac{5\pi}{8}\frac{\alpha}{C} g^{1/2} x_b^{1/2} s^{3/2}$

α = ratio between the wave amplitude and the local mean depth in the surf zone, ≈0.4

C = bottom stress coefficient ≈0.01

g = gravitational constant

s = beach slope = tan β, where β is the beach angle

ϕ_b = angle between the gradient of the local depth contours and the wave propogation vector at the breaker line

P = $\pi NS/(2\alpha C)$ is a measure of the strength of lateral mixing relative to bottom friction where N is a number indicating the magnitude of the eddy coefficient.

P equal to 0.4 is a special case in which (1) is modified to include a logarithmic term.

$$P_i = -3/4 \pm (9/16 + 1/P)^{1/2}$$

Equation (1) is strictly valid only when ϕ_b is small so that $\cos \phi_b \sim 1$. It is worthwhile to take note of the assumptions and simplifications which lead to (1). To enumerate:

1. Linear shallow water theory is employed in the surf zone and immediately seaward.
2. The wave amplitude in the surf zone is taken to be a constant fraction of the water depth (as corroborated by experimental and field data).
3. The beach is plane and constant sloping and is acted on by a monochromatic wave train.
4. The angle of wave incidence is assumed to vary little across the surf zone (due to such influence as refraction, wave-current interaction, etc.).
5. The horizontal eddy viscosity coefficient is set proportional to ρuL where ρ is the density, u a characteristic velocity taken to be the wave velocity [illegible]

characteristic length taken to be the horizontal coordinate, x, i.e.,

$$\mu = \rho N x (gh)^{1/2}$$

where h is the local depth. N is dependent on the level of turbulence in the water, a reasonable range based on field measurements (Inman, et al, 1971) being $0 \le N \le 0.05$. If the condition of small ϕ_b is relaxed (as it must be for any practical study) then the expressions in (1) are multiplied by $\cos \phi_b$. We will return to some of these points later as they affect our model.

The merit of Longuet-Higgins' model is that it removes much of the previous dependence on empiricism. Battjes (1972) and Earle (1974) have extended Longuet-Higgins' analysis to include a wave field characterized by a Rayleigh wave amplitude distribution.

Under special circumstances non-uniformities of the wave field in the longshore direction can produce non-negligible gradients in the radiation stress at the breaker line and force a longshore current. O'Rourke and LeBlond (1972) have studied the nature of these additional functions in the setting of an idealized semi-circular bay and concluded that, whereas the stress due to the obliqueness of long-crested waves is dominant, the contribution made by a longshore modulation in the wave height can be significant, with a longshore variation in the angle of wave incidence playing a minor role. LeBlond (1972) has expanded on Longuet-Higgins' (1970b) analytical expressions for a longshore current to take into account all three types of drive.

The quantities of interest to us are the volume transport rates of the longshore current and its sediment load. We assume that the major portion of this transport is confined to the surf zone. Outside the turbulent wave breaking region the wave-induced bottom stresses exerted on the sand grains decrease rapidly as does the mean (longshore) current (Thornton, 1969). We expect, therefore, for the sediment transport rate to decay rapidly seaward of the breaker line. Furthermore, Longuet-Higgins' formulation tends to overestimate the magnitude of lateral friction in the seaward zone (due to the artificially high mixing coefficient) as well as the role of bottom friction (since shallow water theory magnifies the true orbital velocities in this region). Multiplying (1) by x^* and $\cos\phi_b$ and integrating across the surf zone, $0 \leq x^* \leq 1$, we get for the volume of water transported per unit time

$$V = \tfrac{1}{2} s x_b^2 K \sin 2\theta_b \left\{ \frac{2}{3(5P-2)} + \frac{1}{(p_1+2)(p_1-1)(p_1-p_2)P} \right\} \qquad (2)$$

If, as with LeBlond (1972), we assume that the volume transport of sand which accompanies this longshore flow is simply a fraction of the total water transport then we have

$$Q = \tau V \qquad (3)$$

The determination of T in terms of meaningful physical quantities measured in the laboratory and field is discussed in section III.

2. Shoreline Movement

There is no rigid boundary separating the beach from the ocean. Where they meet at any moment defines the instantaneous shoreline. A function of space and time this line undulates in response to wave run-up, the presence of edge waves, wind and wave-induced set-up, the tidal cycle, surge, etc. For our purposes we consider it to be the mean water level with respect to the local tidal conditions. Mathematically at any time, t, this line can be described by an equation of the form (see Figure 2)

$$\vec{F}(y, x, t) = 0 \tag{4}$$

We can establish the following relations for the local normal, $\hat{n}$, and tangential, $\hat{t}$, unit vectors:

$$\hat{n} = \frac{\nabla \vec{F}}{|\nabla \vec{F}|} = \frac{\frac{\partial F}{\partial x}\hat{i}_x + \frac{\partial F}{\partial y}\hat{i}_y}{\left[\left(\frac{\partial F}{\partial x}\right)^2 + \left(\frac{\partial F}{\partial y}\right)^2\right]^{1/2}} \tag{5}$$

and since $\hat{n}$ and $\hat{t}$ are orthogonal ($\hat{n} \cdot \hat{t} = 0$)

$$\hat{t} = \frac{-\frac{\partial F}{\partial y}\hat{i}_x + \frac{\partial F}{\partial x}\hat{i}_y}{\left[\left(\frac{\partial F}{\partial x}\right)^2 + \left(\frac{\partial F}{\partial y}\right)^2\right]^{1/2}} \tag{6}$$

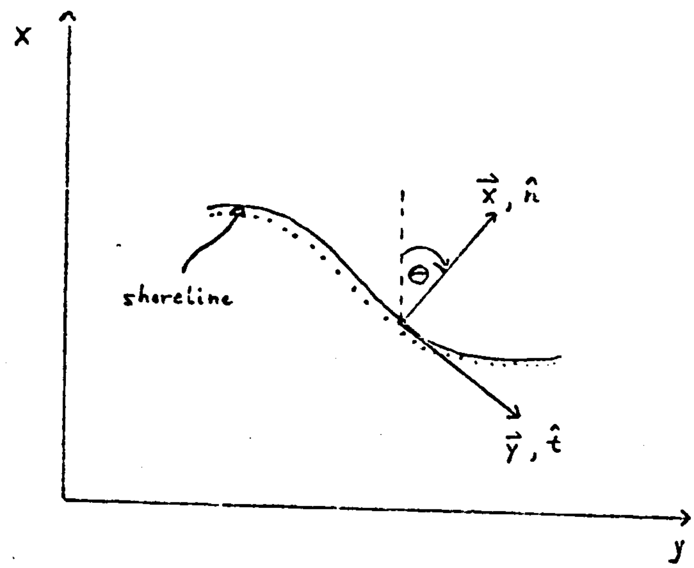

Figure 2. Definition of relation between fixed and local coordinate systems.

The movement of the shoreline normal to itself will be a function of both the magnitude and the longshore variability of the littoral drift. The beach will prograde if more sand is deposited in an area than removed over some time interval and will retreat if the sand extracted exceeds that supplied. In other words, local erosion and accretion depend on the sign of the longshore divergence of the sand transport; this quantity is expressed in terms of the longshore coordinate, $\vec{y}$, as

$$\frac{\partial Q}{\partial \vec{y}} = \hat{t} \cdot \nabla Q = \frac{-\frac{\partial F}{\partial y}\frac{\partial Q}{\partial x} + \frac{\partial F}{\partial x}\frac{\partial Q}{\partial y}}{\left[\left(\frac{\partial F}{\partial x}\right)^2 + \left(\frac{\partial F}{\partial y}\right)^2\right]^{1/2}} \tag{7}$$

The displacement of the shoreline in the x-direction depends solely on the variation of Q in the y-direction and any displacement in the y-direction depends only on the x-component of $\frac{\partial Q}{\partial \vec{y}}$. With reference to the right-hand coordinate system of Figure 2 we see that the projection of $\frac{\partial Q}{\partial \vec{y}}$ on the y axis is given by

$$(\hat{t} \cdot \hat{\imath}_y) \left| \frac{\partial Q}{\partial \vec{y}} \right| = \cos\theta \left| \frac{\partial Q}{\partial \vec{y}} \right| = \frac{\frac{\partial F}{\partial x}}{\left[\left(\frac{\partial F}{\partial x}\right)^2 + \left(\frac{\partial F}{\partial y}\right)^2\right]^{1/2}} \left| \frac{\partial Q}{\partial \vec{y}} \right| \tag{8}$$

and its x-component resolution is

$$(\hat{t} \cdot \hat{\imath}_x) \left| \frac{\partial Q}{\partial \vec{y}} \right| = -\sin\theta \left| \frac{\partial Q}{\partial \vec{y}} \right| = \frac{-\frac{\partial F}{\partial y}}{\left[\left(\frac{\partial F}{\partial x}\right)^2 + \left(\frac{\partial F}{\partial y}\right)^2\right]^{1/2}} \tag{9}$$

where θ is positive counterclockwise.

Therefore we can express the temporal change in the horizontal coordinates of any beach point (y,x) as a balance

$$\frac{\partial x}{\partial t} \propto -\cos\theta \frac{\partial Q}{\partial \bar{y}} = \frac{-\partial F/\partial x}{\left(\frac{\partial F}{\partial x}\right)^2 + \left(\frac{\partial F}{\partial y}\right)^2} \left(-\frac{\partial F}{\partial y}\frac{\partial Q}{\partial x} + \frac{\partial F}{\partial x}\frac{\partial Q}{\partial y}\right) \tag{10}$$

$$\frac{\partial y}{\partial t} \propto \sin\theta \frac{\partial Q}{\partial \bar{y}} = \frac{\partial F/\partial y}{\left(\frac{\partial F}{\partial x}\right)^2 + \left(\frac{\partial F}{\partial y}\right)^2} \left(-\frac{\partial F}{\partial y}\frac{\partial Q}{\partial x} + \frac{\partial F}{\partial x}\frac{\partial Q}{\partial y}\right) \tag{11}$$

We follow the approach of LeBlond (1972) and cast (10) and (11) into forms more appropriate for application to arbitrarily-shaped shorelines. Referring to the vertical cross-section of the plane-sloping beach in Figure 3 it is assumed that the profile remains unchanged in time, i.e., the slope at a particular point along the beach is constant. In response to erosion or accretion the entire profile shifts laterally inward or outward, respectively. This is a convenience and implies that either: (1) The distribution of sand transport capacity across the surf zone is such as to maintain the profile, or (2) there may be a smoothing effect normal to shore due to waves re-working the sediment into an 'equilibrium' profile. Neither of these hypothesized factors is considered explicitly here. The amount of sand gained or lost is proportional to the area of the parallelogram EFGH. 'D' represents the depth beyond which there is little or no sand transport (in this study, D is the depth at which waves begin to break). The initial plan shape of the beach is specified by a set of discrete points (see Figure 4) whose movement in the

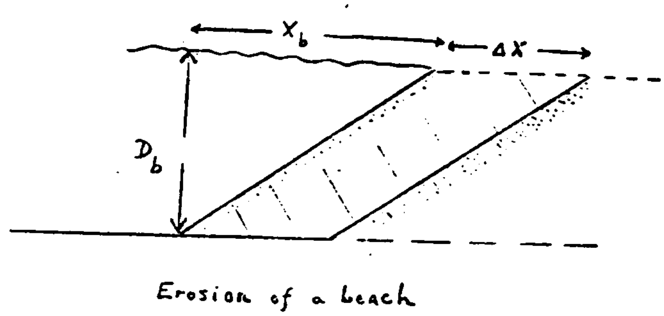

Figure 3. Cross-sectional profile of lateral movement of a beach point.

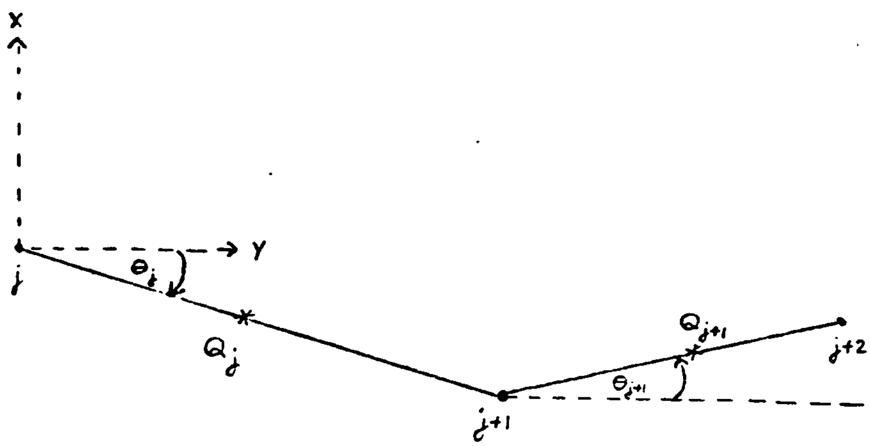

Figure 4. Representation of strandline in LeBlond (1972).

horizontal plane is determined by the net amount of sediment transported into or out of the control volumes. These control volumes are bounded at the mean shoreline by line segments joining adjacent beach points, by the plane-sloping bottom, and by a line parallel to shore at an offshore depth, D. A simple continuity equation relates the translation of the beach points, normal to the local shoreline, to the longshore divergence of sand transport, i.e.,

$$\frac{\partial Q}{\partial \vec{y}} + D\frac{\partial \vec{x}}{\partial t} = 0 \qquad (12)$$

In terms of the fixed coordinate system (y,x) and in view of (10) and (11), (12) becomes

$$\frac{\partial x}{\partial t} = \frac{-\cos\theta}{D}\frac{\partial Q}{\partial \vec{y}} \qquad (13a)$$

$$\frac{\partial y}{\partial t} = \frac{\sin\theta}{D}\frac{\partial Q}{\partial \vec{y}} \qquad (13b)$$

where D is a function of position along the beach, i.e., $D = D(\vec{y})$ [Note: There is a typographical error in LeBlond's (1972) equation 14b.] Equation (13) is valid for a right-hand coordinate system with θ positive counterclockwise or a left-hand coordinate system with θ positive clockwise.

It is obvious that there will be seaward discharges of water and sediment (e.g., in rip currents) interrupting the longshore flow. In a strict 'control volume' approach these transports have to be accounted for to satisfy mass balances. We are assuming that on large spatial and time scales their contribution is minor.

III. Longshore Transport of Sediment

In and near the surf zone the waves provide a large part of the stress required to dislodge sand particles and make them available for transport by the mean currents. There are two modes of sediment movement which can result, 'suspended' transport or 'bedload' transport. Suspension of sand particles in the fluid column can occur in response to the turbulent action of the breaking waves and the presence of a small current is sufficient to advect these sand grains. 'Bedload' motion is the creep of sediment particles in constant or intermittent contact with the bed and requires a threshold shear stress to overcome static friction and initiate motion. The dominance of one mode over the other is largely dependent on incident wave type and to a smaller extent on the sand characteristics. Suspended material is more likely to be associated with plunging breakers whereas bedload movement often predominates when the breakers are spilling or surging. Spilling breakers invariably occur when large waves break on a mild slope. As the incident wave height decreases and/or the beach slope increases in a continuous fashion the spilling breaker evolves successively into a plunging, collapsing, and surging breaker. Galvin (1972) has provided both descriptive and parametric classifications for these breaker types. The transition in the direction spilling→plunging→collaspsing→surging is an inverse function of the deep-water wave steepness (or breaker height) and a direct function of the beach slope.

For some time it has been recognized that a parameter critical to the question of whether sand is moved onshore or offshore (resulting in a 'summer-swell' profile or a 'winter-storm' profile, respectively) is the deep-water wave steepness, H_o/L_o where H_o is the deep-water wave height and L_o is the deep-water wavelength. Laboratory experiments by Johnson (1949), Rector (1954), Scott (1954), Saville (1959) point to a value of H_o/L_o = 0.025 as marking the transition between winter and summer profiles. Values greater than this correspond to erosion and values less than this to deposition, although this is not a stringent rule. Saville's (1950) experiments suggest that the suspended mode of sand transport dominates over the bedload mode for large wave steepness and that this relation is reversed when the wave steepness is low. However, it cannot be stated that there exists general agreement as to which mode is predominant in the surf zone.

Presently there are no definitive experimental studies relating deep-water wave steepness <u>and</u> breaker type to the sand transport mode and its direction.

We are restricting our attention to the littoral drift component. Dean (1973) has formulated a relation between the longshore transport of suspended material and the longshore component of energy flux. By assuming that a fraction (empirical) of the energy flux is consumed by the falling sand grains, determining a volumetric suspended concentration and using Longuet-Higgins' (1970a) expression for the average longshore velocity he obtains

$$Q = G_0(C_D, s, \rho_s, \rho_w, w)\, H_b^{1/2} \cos\phi_b\, E_a \tag{14}$$

where Q = volume transport rate of sand

C_D = bottom drag coefficient

s = beach slope

ρ_s, ρ_w = density of sand and water respectively

w = fall velocity of sand grains which is a function of grain diameter

H_b = wave height at breaking

ϕ_b = wave angle at breaking

E_a = longshore flux of wave energy = $C_{g_b} E_b \sin \phi_b$ where E_b is the wave energy density and C_{g_b} the group velocity at the breaker line.

In contrast, by considering only bedload motion, Komar and Inman (1970) followed Inman and Bagnold (1963) and expressed the longshore transport rate as an immersed weight transport, I_ℓ,

$$I_\ell = (\rho_s - \rho_w)\, g\, a\, Q \tag{15}$$

where g = gravitational constant

a = correction factor for pore space

Laboratory and field studies indicated that I_ℓ could be set proportional to the product $F_b c_b$ where F_b = lateral wave thrust at breaker line = $\frac{E_b}{2} \sin 2\phi_b$ (see Longuet-Higgins (1972));

c_b = phase velocity at breaker line, i.e.,

$$I_\ell = K_o F_b c_b \tag{16}$$

where K_o is the empirically determined non-dimensional constant of proportionality. If we re-arrange (15) we get an expression for Q

$$Q = \frac{K_o F_b c_b}{(\rho_s - \rho_w) g a} \tag{17}$$

If we expand equations (14) and (17) and use the theoretical-empirical breaking criterion

$$H_b = \gamma h_b \tag{18}$$

where h_b = breaking depth

$\gamma \approx 0.8$

we obtain, respectively,

$$Q = G_1 (C_D, s, \rho_s, \rho_w, w, g, \gamma) H_b^3 \sin 2\phi_b \tag{19}$$

and

$$Q = G_2 (\rho_s, \rho_w, g, \gamma, a) H_b^{5/2} \sin 2\phi_b \tag{20}$$

Equation (19) in comparison to (20) contains the additional parametric dependencies on c_D, s and w and therefore offers the possibility of modeling the effect of these parameters. There is also to be noted the difference in the exponents of H_b. It is instructive to compare the expression for Q given in section II, equation (3), with the above results. Equation (3) can be re-written as

$$Q = \frac{5\pi\alpha g^{1/2}}{16 C_D \gamma^{5/2}} T \Psi H_b^{5/2} \sin 2\phi_b \tag{21}$$

where

$$\psi = \left\{ \frac{2}{3(5P-2)} + \frac{1}{P(p_1+2)(p_1-1)(p_1-p_2)} \right\}$$

We note that the functional dependence on the breaker height, H_b, and angle of breaking, ϕ_b, is the same in (20) and (21). Furthermore, the product $F_b c_b$, contained in (20), is the quantity against which many laboratory and field observations are taken (see Shore Protection Manual Vol. 1, U.S. Army Coastal Engineering Research Center, 1973). Equating (20) and (21) we obtain an expression for our unknown proportionality coefficient, T, i.e.,

$$T = \frac{C_D \gamma^2 \rho_w K_o}{5\pi\alpha\,\psi(\rho_s-\rho_w)a} \tag{22}$$

If we insert typical values

$c_D = 0.01$

$K_o = 0.5$ (see Das (1972))

$\rho_w = 1.02\ g/cm^3$

$\rho_s = 2.65\ g/cm^3$ (quartz)

$a = 0.6$ (packed sand)

$\psi = -0.2$ corresponding to $P = 0.13$

we get $T = -0.0026$. Physically this means that for each cubic meter of water transported across a plane perpendicular to the shoreline 0.0026 cubic meters of sand will accompany it. There is considerable scatter in the data and, therefore, in the estimates of K_o. Measurements have been made by various means under a variety of test conditions (e.g., differing wave spectra, beach bathymetry, duration of record, instrumentation, interpretation, etc.). Das (1971, 1972) has described several of the methods employed in the lab and field for determining the rate of sediment transport and summarized much of the data on K_o. Noda (1971) has reviewed the techniques presently available for measuring littoral drift in the field.

In view of the order-of-magnitude uncertainty in the value of K_o we treat this quantity as a control variable subject to adjustment over a reasonable range. It seems unlikely that K_o will assume a single value appropriate for all beaches since there are beach parameters (such as w in (19)) whose significance has not been guaged.

IV. Stability Analysis of Governing Equations

It is customary and worthwhile to determine if one's working equations are subject to any intrinsic instabilities for some range of the parameters involved. If the instabilities of the analytic form of the equations can be identified, then, spurious results appearing in their numerical integration can be labeled and/or avoided. We consider, again, equations (13) in the coordinate system defined in Figure 4. To avoid unnecessary and lengthy computations we postulate that the original (unperturbed) shoreline is straight and lies parallel with the horizontal axis. By superposing small perturbations on this configuration and examining under what conditions these disturbances grow, decay, or remain unchanged we can determine when our equations will behave peculiarly, i.e., admit oscillatory solutions that "blow up".

We express Q, the transport rate, as

$$Q = \beta \sin(\phi_o - \theta)\cos(\phi_o - \theta) \tag{23}$$

where β contains implicitly all empirical constants as well as the functional form of H_b which is assumed independent of the longshore coordinate; $\phi_o - \theta = \phi_b$ where ϕ_o is some constant initial value for ϕ_b adjusted due to changes in beach orientation (θ). Upon expansion this becomes

$$Q = \beta\left(\sin\phi_o\cos\theta - \cos\phi_o\sin\theta\right)\left(\cos\phi_o\cos\theta + \sin\phi_o\sin\theta\right) \tag{24}$$

We note that (see Figure 2)

$$\frac{dx}{d\vec{y}} = \sin\theta \tag{25}$$

and

$$\frac{dy}{d\vec{y}} = \cos\theta \tag{26}$$

so that we can write the longshore derivative of Q as

$$\frac{\partial Q}{\partial \vec{y}} = \beta\left(T_1\frac{\partial T_2}{\partial \vec{y}} + T_2\frac{\partial T_1}{\partial \vec{y}}\right), \tag{27}$$

where

$$T_1 = \sin\phi_o\frac{dy}{d\vec{y}} - \cos\phi_o\frac{dx}{d\vec{y}} \tag{28}$$

$$T_2 = \cos\phi_o\frac{dy}{d\vec{y}} + \sin\phi_o\frac{dx}{d\vec{y}} \tag{29}$$

Now, let $\vec{y}$ be a function of the original (t = 0) arc length 's_o' (linear) and the time 't', i.e.,

$$\vec{y} = \vec{y}(s_o, t)$$

Then we can evaluate the derivatives in (27) as

$$\frac{\partial x}{\partial \vec{y}} = \frac{\partial x/\partial s_o}{\partial \vec{y}/\partial s_o} \quad , \quad \frac{\partial y}{\partial \vec{y}} = \frac{\partial y/\partial s_o}{\partial \vec{y}/\partial s_o} \tag{30}$$

and

$$\frac{\partial^2 x}{\partial \vec{y}^2} = \frac{\frac{\partial \vec{y}}{\partial s_o}\, \partial^2 x/\partial s_o^2 - \frac{\partial x}{\partial s_o}\, \partial^2 \vec{y}/\partial s_o^2}{(\partial \vec{y}/\partial s_o)^3}$$

$$\frac{\partial^2 y}{\partial \vec{y}^2} = \frac{\frac{\partial \vec{y}}{\partial s_o}\, \partial^2 y/\partial s_o^2 - \frac{\partial y}{\partial s_o}\, \partial^2 \vec{y}/\partial s_o^2}{(\partial \vec{y}/\partial s_o)^3} \tag{31}$$

In view of the following relations

$$\partial \vec{y}/\partial s_o = \left[(\partial x/\partial s_o)^2 + (\partial y/\partial s_o)^2 \right]^{1/2} \tag{32}$$

$$\frac{\partial^2 \vec{y}}{\partial s_o^2} = \frac{\partial x/\partial s_o\, \partial^2 x/\partial s_o^2 + \frac{\partial y}{\partial s_o}\, \partial^2 y/\partial s_o^2}{\partial \vec{y}/\partial s_o} \tag{33}$$

we can rewrite (30) and (31) as

$$\frac{\partial x}{\partial \vec{y}} = \frac{\partial x/\partial s_o}{\left[\left(\frac{\partial x}{\partial s_o}\right)^2 + \left(\frac{\partial y}{\partial s_o}\right)^2 \right]^{1/2}} \quad , \quad \frac{\partial y}{\partial \vec{y}} = \frac{\partial y/\partial s_o}{\left[\left(\frac{\partial x}{\partial s_o}\right)^2 + \left(\frac{\partial y}{\partial s_o}\right)^2 \right]^{1/2}} \tag{34}$$

and

$$\frac{\partial^2 x}{\partial \vec{y}^2} = \frac{(\partial y/\partial s_0)^2 \, \partial^2 x/\partial s_0^2 - \frac{\partial x}{\partial s_0} \frac{\partial y}{\partial s_0} \, \partial^2 y/\partial s_0^2}{\left[\left(\frac{\partial y}{\partial s_0} \right)^2 + \left(\frac{\partial x}{\partial s_0} \right)^2 \right]^2}$$

(35)

$$\frac{\partial^2 y}{\partial \vec{y}^2} = \frac{(\partial x/\partial s_0)^2 \, \partial^2 y/\partial s_0^2 - \frac{\partial y}{\partial s_0} \frac{\partial x}{\partial s_0} \, \partial^2 x/\partial s_0^2}{\left[\left(\frac{\partial x}{\partial s_0} \right)^2 + \left(\frac{\partial y}{\partial s_0} \right)^2 \right]^2}$$

Our original governing equations (13a), (13b) become

$$\frac{\partial x}{\partial t} = - \frac{\partial y/\partial s_0}{D\left[\left(\frac{\partial x}{\partial s_0} \right)^2 + \left(\frac{\partial y}{\partial s_0} \right)^2 \right]^{1/2}} \frac{\partial Q}{\partial \vec{y}} \tag{36}$$

$$\frac{\partial y}{\partial t} = \frac{\partial x/\partial s_0}{D\left[\left(\frac{\partial x}{\partial s_0} \right)^2 + \left(\frac{\partial y}{\partial s_0} \right)^2 \right]^{1/2}} \frac{\partial Q}{\partial \vec{y}} \tag{37}$$

where $\partial Q/\partial \vec{y}$ is defined by (27), (28), (29), (34) and (35).

We now introduce expansions of the form

$$x(s_0, t) = \varepsilon x_1(s_0, t) + \varepsilon^2 x_2(s_0, t) + \ldots$$

$$y(s_0, t) = s_0 + \varepsilon y_1(s_0, t) + \varepsilon^2 y_2(s_0, t) + \ldots \tag{38}$$

and establish the following relations valid to $0(\varepsilon)$

$$\frac{\partial x}{\partial s_0} = \varepsilon \frac{\partial x_1}{\partial s_0} \qquad \frac{\partial y}{\partial s_0} = 1 + \varepsilon \frac{\partial y_1}{\partial s_0} \tag{39}$$

$$\frac{\partial^2 x}{\partial s_0^2} = \varepsilon \frac{\partial^2 x_1}{\partial s_0^2} \qquad \frac{\partial^2 y}{\partial s_0^2} = \varepsilon \frac{\partial^2 y_1}{\partial s_0^2}$$

Substituting (39) into the x equation, (36), we obtain

$$\varepsilon \frac{\partial x_1}{\partial t} = \frac{1+\varepsilon\, \partial y_1/\partial s_0}{\left\{1+2\varepsilon \frac{\partial y_1}{\partial s_0}+\varepsilon^2\left[\left(\frac{\partial x}{\partial s_0}\right)^2+\left(\frac{\partial y}{\partial s_0^2}\right)^2\right]\right\}} \left\{\left[\sin\phi_0\left(1+\varepsilon\frac{\partial y_1}{\partial s_0}\right) - \right.\right.$$

$$\left.\varepsilon\cos\phi_0\, \partial x_1/\partial s_0\right]\left[\cos\phi_0\left(O(\varepsilon^2)\ \text{term}\right)+\varepsilon\sin\phi_0\, \partial^2 x_1/\partial s_0^2\right] +$$

$$\left[\cos\phi_0\left(1+\varepsilon\, \partial y_1/\partial s_0\right)+\varepsilon\sin\phi_0\, \partial x_1/\partial s_0\right]\left[\sin\phi_0\left(O(\varepsilon^2)\ \text{term}\right) - \right.$$

$$\left.\left.\varepsilon\cos\phi_0\, \partial^2 x_1/\partial s_0^2\right]\right\} \tag{40}$$

The $O(\varepsilon)$ equation extracted is

$$\frac{\partial x_1}{\partial t} = \frac{-\left[\sin^2\phi_0-\cos^2\phi_0\right]}{D}\ \frac{\partial^2 x_1}{\partial s_0^2}$$

or

$$\frac{\partial x_1}{\partial t} = \frac{-\left(1-2\cos^2\phi_0\right)}{D}\ \frac{\partial^2 x_1}{\partial s_0^2} \tag{41}$$

This is of the form of a one-dimensional heat (diffusion) equation which is a well-studied linear second-order partial differential equation. A fundamental property of this equation is that initial value information can only be propagated in one direction, i.e., it is not possible to integrate this equation backwards in time to determine the initial distribution of x_1. For this reason the coefficient on the right-hand side of (41) must always be positive. We identify the regions of stability and instability according to

$$\begin{array}{lll} |\phi_0| \le 45^\circ, & -\left(1-2\cos^2\phi_0\right) \ge 0, & \text{stability} \\ |\phi_0| > 45^\circ, & -\left(1-2\cos^2\phi_0\right) < 0, & \text{instability} \end{array} \tag{42}$$

Thus, for breaker angles greater than $\pm 45°$ the shoreline will be unstable to perturbations of all wavelengths and will undergo oscillations of increasing amplitude. This has been confirmed numerically. A small disturbance of arbitrary wavelength is imposed on an initially straight beach such that ϕ_b assumes values greater than $\pm 45°$. It is found that the shoreline is stable to the disturbance if ϕ_b does not exceed $\pm 45°$ and is unstable otherwise.

It is interesting to speculate whether such an instability occurs in the field. Bowen (personal communication) has noted that wind-generated waves in small lakes can break on the beach at very acute angles and cause the shoreline to deform in a wave-like manner, i.e., be responsible for periodically spaced shoreline protuberances. Aerial photographs of coastal areas frequently show undulations of the shoreline with definite wavelengths. However, Dolan (1970,71) and Vincent (1973) have correlated the existence of these meanders with inner and outer submarine bar rhythms. These bar systems may represent in themselves an instability of the submarine bed to longshore currents as suggested by Sonu (1972) and theorized by Barcilon and Lau (1973).

In our model we exclude angles, ϕ_b, which fall within the unstable range of (42). It is conceivable that a second-order term in Q added to the right-hand side of (36) and (37) might damp the growing oscillation. However, the physical justification of such an "artificial viscosity" term is not clear. The omission of $|\phi_b|>45°$ is not considered serious. It is usually true, especially for swell waves on mild slopes, that refraction will limit the breaking angle to the stable regime. This may not be the case for local sea on steep slopes. An analysis of our study results indicates that over 95% of the ϕ_b's generated satisfied the stability criterion.

V. Finite Difference Form of Equations

We wish to express our governing equations in a form appropriate for numerical integration. Equations (13a) and (13b) are discretized according to LeBlond (1972) as

$$x_j^{n+1} - x_j^n = -\frac{\cos\beta_j}{D_j}\left(\frac{Q_j - Q_{j-1}}{\Delta_j/2}\right) \tag{43a}$$

$$y_j^{n+1} - y_j^n = \frac{\sin\beta_j}{D_j}\left(\frac{Q_j - Q_{j-1}}{\Delta_j/2}\right) \tag{43b}$$

where the superscript n denotes the time level and the subscript j the space level. Referring to Figure (4) we make the following comments:

1. θ_j is the orientation of the beach segment, j, in the fixed coordinate system (y,x). The θ's, of course, are altered as the beach points migrate.

2. β_j is the 'effective' (averaged) angle at a point, j, given by

$$\beta_j = \frac{(\theta_j + \theta_{j-1})}{2}$$

3. Δ_j is the sum of the distances between point j and adjacent points j-1 and j+1, i.e.,

$$\Delta_j = \left[(x_{j+1} - x_j)^2 + (Y_{j+1} - Y_j)^2\right]^{1/2} + \left[(x_j - x_{j-1})^2 + (Y_j - Y_{j-1})^2\right]^{1/2}$$

4. The transports Q are evaluated at mid-segment points and are characteristic of a segment (not a point).

At endpoints these definitions of β, Δ, and Q need to be modified.

The general class of integration schemes we adopt is 'predictor-corrector'. A predictor-corrector method represents an iterative approximation to a fully implicit scheme. Kurihara (1965), Lilly (1965), and Baer and Simons (1970) have discussed the performance (e.g., stability, conservation properties, accuracy, phase errors, etc.) of several of the more widely used predictor-corrector schemes (leapfrog-trapezoidal, Adams-Moulton, Milne). The advantage of such multi-step methods lies in their ease of application and speed (provided the proper step size, Δt, is chosen). We employ Hamming's (1962) predictor-corrector method which consists of the fourth-order Milne predictor and Hamming corrector. The Hamming corrector is favored over more traditional correctors (Milne, Moulton) because it exhibits stronger stability, although at the price of an increase in the magnitude of the truncation error.

Predictor: $$z^{n+1} = z^{n-3} + \frac{4\Delta t}{3}\left(2f^{n} - f^{n-1} + 2f^{n-2}\right) \tag{44}$$

Corrector: $$z^{n+1} = \frac{9}{8} z^{n} - \frac{1}{8} z^{n-2} + \frac{3}{8}\Delta t\left(f^{n+1} + 2f^{n} - f^{n-1}\right) \tag{45}$$

where z = (y,x) and f represents the right-hand side of (43a,b). It is obvious that, in addition to the initial datum, 3 values of z and the corresponding f's are required at the n-1, n-2, and n-3 time levels. Since these are not available a special method is required to generate them. We revert to a numerical method based on a Lagrangian interpolation formula (Ralston, 1965, p. 191) which yields estimates for z_1, z_2, z_3, given z_o, namely

$$z_1 = z_0 + \frac{\Delta t}{24}\left(9f_0 + 19f_1 - 5f_2 + f_3\right) \tag{46}$$

$$z_2 = z_0 + \frac{\Delta t}{3}\left(f_0 + 4f_1 + f_2\right) \tag{47}$$

$$z_3 = z_0 + \frac{\Delta t}{8}\left(3f_0 + 9f_1 + 9f_2 + 3f_3\right) \tag{48}$$

The error term is $0(\Delta t^5)$. We guess values for z_1, z_2, z_3, calculate the corresponding f_1, f_2, f_3 and use (46), (47), and (48) to compute new values of z_1, z_2, z_3. This procedure is then iterated to convergence. (An alternative method for furnishing starting values is the Runge-Kutta scheme.) Ralston (1965) has provided a careful analysis of the properties of predictor-corrector methods as well as their merit in relation to other schemes.

The step size, Δt, must satisy several criteria. In a physical sense it is controlled by the spatial increment $\Delta\vec{y}_j$

(the distance between neighboring beach points) and by the average speed of the sand particles, v_s (a function of the longshore current strength and the grain characteristics). Linear computational stability requires that

$$\Delta t \leq \Delta \vec{y}_j / v_s \tag{49}$$

A rough estimate for v_s can be had by noting that the triangular wedge through which the longshore current flows has a cross-sectional area of 1/2 $D_b x_b$ and therefore the sand transport rate equals

$$s x_b^2 v_s / 2$$

Equating this to (3) we obtain

$$v_s = 2TV / s x_b^2 \tag{50}$$

A more rigorous requirement than (49) is that the increment, Δt, be small enough to meet the convergence condition on the corrector equation, (45), preferably small enough so as to achieve convergence in one or two interations; it must also be sufficiently small to satisfy any restrictions on the magnitude of the local truncation error which is given approximately by (Ralston, p. 189)

$$\sigma = \frac{9}{121}\left(z_{n+1} - z^{o}_{n+1}\right) \tag{51}$$

where z^{o}_{n+1} is the predicted value and z_{n+1} the corrected value. In addition, the step size should be large enough so that round-off errors and the number of derivative evaluations is minimized; otherwise, the multi-step method loses its chief advantage, namely, speed. Ideally one would like to adjust Δt so that only one application of the corrector equation is necessary. Equation (51) is helpful in two ways: 1. knowledge of ε, as the integration proceeds, can suggest in which direction Δt should be adjusted for efficiency; 2. ε can be used to actually modify the solution of the corrector equation. The proper choice of the step size is a function of the geometry of a beach site and the incident wave energy levels.

VI. Computer Program

Structure

The program is divided into 11 sections—a core and ten subroutines. We note below the designation and function of each part:

1. Main Program

   a. Read input parameters (which run program)
   b. Establish shoreline
   c. Call working subroutines
   d. Execute Hamming predictor-corrector (repeat)

2. Subroutine EMPIRCL

   a. Set value of constants appearing in expression for longshore current
   b. Compute coefficient, T, the ratio between the sand and water transport rates

3. Subroutine ADJUST

   a. Read in values of breaker height, angle, and duration (fractional) of a particular wave type for each beach segment; compute transport rates
   b. We expect the angle of wave attack to change as the beach orientation is altered. An "adjustment" angle, the difference between the old and new beach angles, is added to the original ϕ_b and a revised transport figure is calculated. This is done at time intervals chosen by the user. Any accompanying refractive modification of wave height is considered secondary and is neglected.

4. Subroutine INITL

   Generate all necessary starting values for use by the Hamming scheme as outlined in section V.

5. Subroutine DERIV

   a. Given the beach coordinates compute the beach segment angles and the spacing between adjacent points.
   b. Given the volume transport rates of sand along the beach compute the incremental change in position of each beach point over a time interval, Δt. A Fortran ENTRY statement links DERIV with that part of subroutine ADJUST that re-computes the incident angles on some regular basis because of the re-shaping of the shoreline.

6. Subroutine AREA

   a. The surface area of the beach is an important quantity. Its change can be monitored by computing the areal difference between two successive strandlines. In Figure 4a the calculation is straightforward since the y coordinate of each endpoint remains constant. Figure 4b represents the more general case wherein the endpoints are allowed to move freely. A rough estimate of the net areal change (additions due to accretion minus depletions due to erosion) can be had in the following way: (i) connect the endpoints A, B and E, F as shown, (ii) compute area under curves AF and BE (summations over a series of trapezoids); these are the exact areas under a discrete beach which is itself an approximation to the real strandline, (iii) compute the areas of trapezoids ABCD and EFGH, (iv) subtract the two numbers in (ii) and, then, from this result subtract the areas computed in (iii); this number represents crudely the increase or decrease in beach area. If the positive or negative contribution near an endpoint is desired we can estimate this at the left end to be ABA' where A' is the point on curve AF at which a line dropped from B parallel to the vertical axis intersects. The x coordinate of point A' is determined by linearly interpolating between the beach points on either side. The area, then, is just the area under AA' minus the area ABCD. Similarly, the area EFE' can be computed.

b. Approximate volumetric changes can be obtained by multiplying the discrete trapezoidal areas by the local value of D_b (see Figure 2).

7. Subroutine RESET

If, for some reason, it is desirable to have the spacing between neighboring beach points more or less equal, it is possible to reset the beach points to accomplish this. The circumstances which might dictate this action are many: (i) a more rational control over the size of Δt would result; (ii) a few beach points may be moving at an anomalous rate compared to their neighbors (e.g., the point at the tip of a rapidly expanding spit); (iii) equal increments might be more compatible with the longshore resolution of the wave field, etc.

With reference to Figure 4c we shift only interior points; endpoints must retain their positions if the beach shape is not to be disturbed. All or only part of the shoreline can be reset.

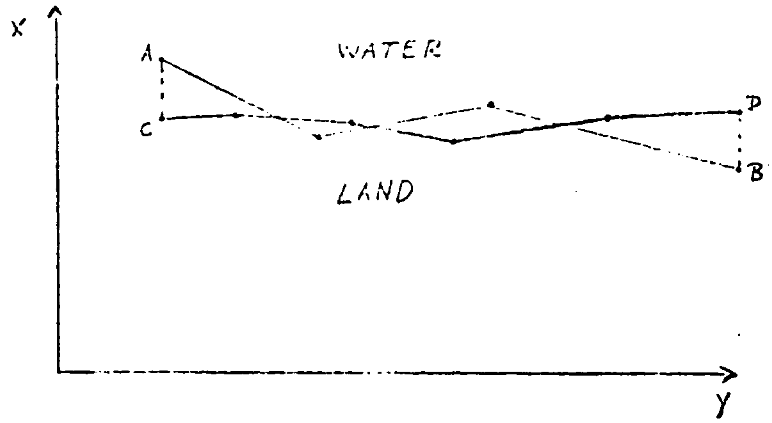

Figure 4a. The difference in area between successive strandlines whose endpoints have the same abscissal coordinate.

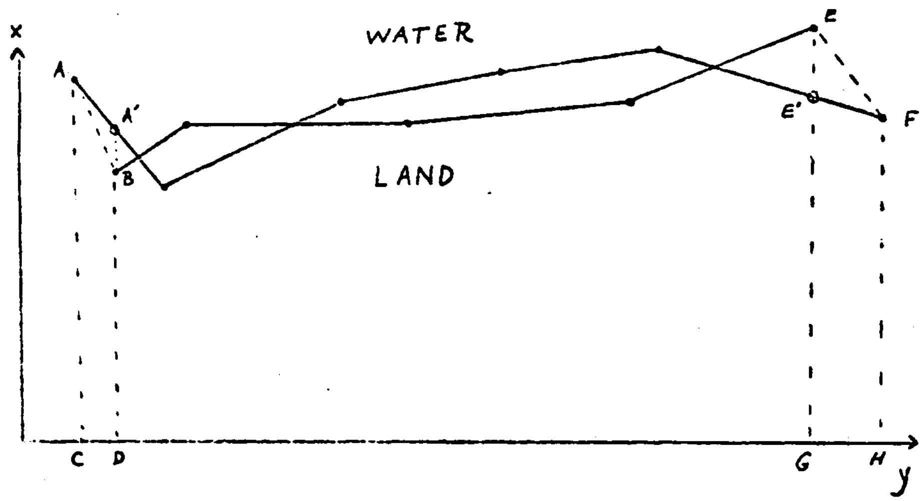

Figure 4b. The difference in area between successive strandlines of arbitrary shape and orientation.

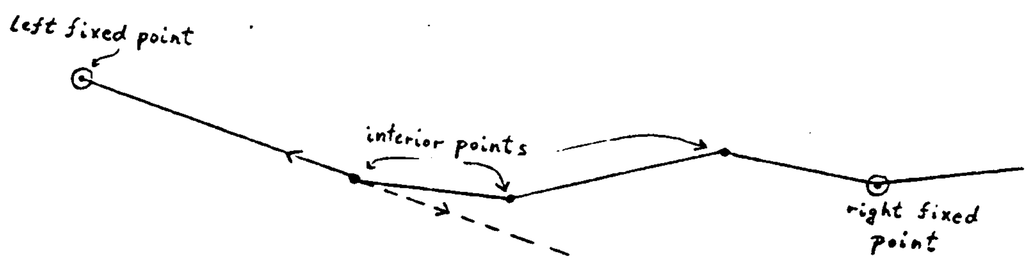

Figure 4c. Schematic diagram defining beach points and their movement in the 're-setting' process.

Over that portion of the beach which is to be re-defined the lengths of the discrete longshore segments are summed over and divided by the total number of segments to yield an "average" spatial increment. The first interior point is moved along the segment immediately to its left (like a bead on a string) until the distance between it and the fixed point on its left side is the "average" increment. This interior point now becomes the fixed point for the next interior point, i.e., the second interior point is moved along the line segment joining it to the new fixed point until the distance between them is, again, the average increment. (note: movement along these segments can be forward or backward). This process is repeated until the fixed point on the right hand side is reached (either the right endpoint or the point defining the right boundary of that portion of beach to be reset). Because the right boundary point is not allowed to move this procedure must be iterated 4 or 5 times before all the beach increments converge toward one value. This method must be applied thoughtfully; otherwise, the resultant shoreline may deviate too much from its former shape.

8. Subroutine RESULTS

Display results of computationsin print-out form

9. Subroutine PLOTTER

Use the Florida State University plotting package (Fortran callable, calcomp-like routines) for displaying the shoreline evolution graphically.

10. Subroutine ROTATE

Rotate the N-S, E-W axes if beach points are desired in a new coordinate system. This is used for plotting purposes, i.e., to show direction of maximum beach change.

11. Subroutine ERROR

Calculate error between actual and predicted quantities.

Below we provide a listing of the program with accompanying comments .

```
      PROGRAM SHORLIN(TAPE1,INPUT,OUTPUT,TAPE5=INPUT,TAPE6=OUTPUT,PLOT)
C
C**** THIS PROGRAM MONITORS THE CHANGE IN THE PLAN SHAPE OF A SHORELINE
C     DUE TO THE DIFFERENTIAL LONGSHORE TRANSPORT OF SEDIMENT INDUCED BY
C     WAVES BREAKING AT AN ANGLE TO THE SHORE.NECESSARY INPUTS ARE THE
C     WAVE CHARACTERISTICS(HEIGHT,ANGLE OF INCIDENCE,DURATION)AT THE
C     BREAKER LINE AS A FUNCTION OF LONGSHORE POSITION AND THE HORIZONTAL
C     COORDINATES OF THE POINTS WHICH DEFINE THE SHORELINE AS RECORDED
C     AT VARIOUS TIMES.
C     THESE QUANTITIES ARE ASSUMED TO HAVE BEEN GENERATED IN ANOTHER
C     PROGRAM.IN ADDITION IT IS ASSUMED THAT THE BREAKER ANGLES WHOSE
C     ABSOLUTE VALUE IS GREATER THAN 45 DEGREES HAVE BEEN EXCLUDED.
C     AB HAS UNITS OF DEGREES.
C
C
C     THIS PROGRAM IS WRITTEN IN FORTRAN IV LANGUAGE FOR THE CDC 6500
C     COMPUTER.SAMPLE VALUES FOR MANY OF THE PROGRAM PARAMETERS ARE USED.
C     PLOTTING ROUTINES ARE WRITTEN FOR THE GOULD PLOTTER.
C
C     THE LETTERS A.D.I.T. AS THEY APPEAR THROUGHTOUT STAND FOR THE PHRASE
C    =AS DEFINED IN TEXT=.
C
      DIMENSION FRAC(50)
      DIMENSION DXX(90),DYY(90),H1(90),H2(90),Z1(90),Z2(90),X(90),Y(90)
      COMMON DEL(90),BETA(90),THETA(90)
      COMMON     X0(90),X1(90),X2(90),X3(90),Y0(90),Y1(90),Y2(90),Y3(90)
      COMMON DY0(90),DX0(90),DY1(90),DX1(90),DY2(90),DX2(90),DY3(90),
     *DX3(90)
      COMMON/BLOC/HB(50,90)
      COMMON/BLK/AB(50,90)
      COMMON/BLK1/XX(90),YY(90)
      COMMON/BLK4/KOUNT,IIT,NPC(50)
      COMMON/BLK5/L(10),M(10)
      COMMON/BLOC0/II
      COMMON/BLOC1/PI
      COMMON/BLOC2/LIMIT,LIM1,LIM2
      COMMON/BLOC3/CVPT1,CVPT2
      COMMON/BLOC6/DIFA,DIFV,DIFA1,DIFV1
      COMMON/BLOC7/IV,DT
      COMMON/BLOC11/COEFF
   50 FORMAT(1X,15F5.2)
   51 FORMAT(2I2,2I3,I5,F4.0)
   52 FORMAT(1H ,2(2X,I2),2X,2(2X,I3),2X,I5,2X,F4.0)
   55 FORMAT(1X,10I3)
   60 FORMAT(2X,7(3X,I4),5X,F5.1)
   61 FORMAT(3X,I4)
C
C**** THE PLOTTING MODE IS ENTERED INTO-PLOTLIB AND GOULD LIBRARY
C     ROUTINES ARE CALLED.
      CALL PLOTS(0.0,0.0,4HPLOT,0)
C
C**** THE INTEGER VARIABLES L AND M ARE USED IN SUBROUTINE ADJUST
C     TO PICK OUT THE BEACH POINTS OF INTEREST IN COMPUTING NET
C     TRANSPORT RATES FOR VARIABLE STRETCHES OF SHORELINE.
      READ(5,55)(L(I),M(I),I=1,10)
C
C**** COEFF IS USED IN SUBROUTINE ADJUST.

      COEFF=0.5
C
```

```
C**** READ PROGRAM PARAMETERS:N1 IS THE NUMBER OF WAVE DATA SETS:
C     N2 IS THE NUMBER OF TIMES THE CORRECTOR EQUATIONS ARE APPLIED:
C     LIM IS THE NUMBER OF POINTS WHICH MAKE UP THE BASE SHORELINE:
C     MAX IS THE NUMBER OF POINTS WHICH MAKE UP THE SHORELINE AS
C     OBSERVED AT A LATER TIME:IPRINT IS THE INTERVAL(EXPRESSED AS
C     NUMBER OF TIME STEPS)AT WHICH RESULTS ARE DISPLAYED:DT IS THE
C     TIME STEP.
      READ(6,51)N1,N2,LIM,MAX,IPRINT,DT
      WRITE(6,52)N1,N2,LIM,MAX,IPRINT,DT
C
C**** SOME WORKING DEFINITIONS:
      LIMIT=LIM+1
      LIM1=LIM-1
      LIM2=LIM-2
C
C**** FRAC IS THE FRACTION OF THE TOTAL TIME OF RECORD(EXPRESSED AS
C     THE UNIT 1)DURING WHICH A PARTICULAR WAVE ACTS.HB AND AB ARE THE
C     BREAKER HEIGHT AND ANGLE,RESPECTIVELY,FOR THAT WAVE AS
C     COMPUTED FOR EACH BEACH SEGMENT.

      READ(1)(FRAC(I),I=1,N1)

      READ(1)((HB(II,J),AB(II,J),II=1,N1),J=1,LIM1)
C
C**** THE DURATION OF A PARTICULAR WAVE TYPE OVER THE PERIOD OF A YEAR
C     IS COMPUTED IN TERMS OF NUMBER OF TIME STEPS.IF THE INTEGRATION
C     PROCEEDS LESS THAN A YEAR THEN THIS CALCULATION MUST BE MODIFIED.
      DO 54 I=1,N1
   54 NDC(I)=FRAC(I)*365.*24./DT
C
C**** THE TOTAL NUMBER OF TIME STEPS IS COMPUTED.YEAR IS THE NUMBER OF
C     YEARS OVER WHICH THE INTEGRATION PROCEEDS.
      YEAR=5.
      NUMDT=YEAR*365.*24./DT
C
C***DEFINE FACTORS FOR CONVERTING FROM RADIANS TO DEGREES AND BACK***
      PI=4.*ATAN(1.)
      CVRT1=PI/180.
      CVRT2=1./CVRT1
C
C**** READ INITIAL VERTICAL-HORIZONTAL COORDINATES OF BEACH POINTS.
C     ALSO READ THE COORDINATES AS RECORDED AT SOME LATER TIME IF THESE
C     ARE AVAILABLE(FOR COMPARISON WITH PREDICTED VALUES).
      READ(5,50)(X0(I),Y0(I),I=1,LIM)
      READ(5,50)(XX(I),YY(I),I=1,MAX)
C
C**** CV CONVERTS OUTSTANDING UNITS TO METERS-IN THIS CASE,FEET TO
C     METERS.
      CV=1./3.28
      DO 1 I=1,LIM
      X0(I)=CV*X0(I)
      Y0(I)=CV*Y0(I)
C**** THE INITIAL VERTICAL AND HORIZONTAL COORDINATES ARE DESIGNATED
C     X AND Y,RESPECTIVELY.
      X(I)=X0(I)
    1 Y(I)=Y0(I)
      DO 12 I=1,MAX


      XX(I)=CV*XX(I)
   12 YY(I)=CV*YY(I)
C
C**** THE ATAN2 FUNCTION ALLOWS FOR UNAMBIGUOUS EVALUATION OF
C     THE ANGULAR ORIENTATION OF BEACH SEGMENTS IRRESPECTIVE OF
C     QUADRANT LOCATION.THETA AND BETA ARE A.O.I.T.
      DO 17 I=1,LIM1
   17 THETA(I)=ATAN2(X(I+1)-X(I),Y(I+1)-Y(I))
C
C**** THETA(0),THETA(LIM) ARE DEFINED AS THEY WERE FOR THE JUPITER
C     ISLAND PROJECT.A ZERO SUBSCRIPT IS PERMITTED IF A PROPER STORAGE
C     LOCATION IS ALLOTTED THE ZERO-SUBSCRIPTED VARIABLE.
      THETA(0)=THETA(1)-(THETA(2)-THETA(1))
      THETA(LIM)=THETA(LIM1)-(THETA(LIM2)-THETA(LIM1))
      DO 18 I=1,LIM
   18 BETA(I)= (THETA(I)+THETA(I-1))/2.
C
```

```
C**** THE EMPIRICAL SEDIMENT TRANSPORT COEFFICIENT IS COMPUTED
      CALL EMPIRCL
C
C**** WE CALL ADJUST TO ESTABLISH THE FIRST SET OF BREAKER HEIGHTS AND
C     ANGLES.
C**** II IS THE WAVE DATA SET NUMBER.
      II=1
      CALL ADJUST(LIM)
C
C**** KOUNT IS A FLAG USED IN SUBROUTINE DERIV
      KOUNT=1
C
C**** DERIV COMPUTES THE CHANGE IN THE (Y,X) COORDINATES OVER 1 TIME STEP.
      CALL DERIV(X0,Y0,DX0,DY0,LIM)
      KOUNT=0
C
C**** ALL REQUIRED STARTING VALUES FOR THE COORDINATES (Y,X) ARE
C     GENERATED IN INITL.
      CALL INITL(LIM,IND)
C
C**** IND IS AN INDICATOR OF CONVERGENCE OR LACK OF CONVERGENCE IN INITL.
      IF(IND.EQ.1)GO TO 100
      WRITE(6,200)
  200 FORMAT(3X,*NO CONVERGENCE*)
      GO TO 102
  100 CALL DERIV(X1,Y1,DX1,DY1,LIM)
      CALL DERIV(X2,Y2,DX2,DY2,LIM)
      CALL DERIV(X3,Y3,DX3,DY3,LIM)
C
COMPUTE THE DIFFERENCE IN PLAN AREA OF THE BEACH AS OBSERVED
C      INITIALLY AND AS OBSERVED AT SOME LATER TIME (DIFA1) AS WELL AS

C      THE VOLUMETRIC CHANGE (DIFV1)
       CALL AREA(Y,X,LIM,YY,XX,MAX)
       DIFA1=DIFA
       DIFV1=DIFV
       WRITE(6,67) DIFA1,DIFV1
   67 FORMAT(2X,*THE OBSERVED CHANGE IN BEACH AREA OVER SOME TIME
     $INTERVAL=*,F10.1//2X,*THE OBSERVED CHANGE IN BEACH VOLUME OVER
     *SOME TIME INTERVAL=*,F10.1)
C
C**** INITIALIZE THE TIME STEP COUNTERS III,IV: III REGULATES THE


C      TRANSITION BETWEEN WAVE DATA SETS:IV MONITORS THE TOTAL NUMBER
C      OF TIME STEPS.
       III=0
       IV=0
       GO TO 3
     2 II=II+1
       CALL ADJUST(LIM)
C
C**** IF ALL DATA SETS HAVE BEEN USED,WE RETURN TO DATA SET NO.1.
       IF(II.EQ.N1+1) II=1
       III=0
     3 III=III+1
       IV=IV+1
       IF(IV.GE.NUMDT)GO TO 4
       IF(III.EQ.NDD(II)+1)GO TO 2
C
C**** IP DETERMINES THE INTERVALS AT WHICH RESULTS ARE PRINTED OUT AND
C      PLOTS MADE.
       IP=(IV/IPRINT)*IPRINT-IV
       IF(IP)5,4,5
     4 CALL AREA(Y,X,LIM,Z1,Z2,LIM)
       WRITE(6,66)DIFA,DIFV
   66 FORMAT(1H ,*CHANGE IN THE SURFACE AREA OF THE SUBAERIAL BEACH=*,
     1F10.1//2X,*VOLUMETRIC CHANGE IN THE SUBAERIAL BEACH=*,F10.1)
       CALL RESULTS(X,Y,Z2,Z1,LIM,MAX)
       CALL PLOTTER(X,Y,Z2,Z1,LIM)
C
C**** IF AN INSPECTION OF THE RESULTS LEADS TO THE CONCLUSION THAT
C      THE BEACH POINTS SHOULD BE RESET THEN WE SET THE INDICATOR IND1
C      EQUAL TO 1. J1 AND J2 ARE THE LEFT AND RIGHT BOUNDARY POINTS FOR
C      THE SECTION OF BEACH TO BE RESET.
       IND1=1
       J1=10
       J2=20
       IF(IND1.EQ.1) CALL RESET(Z2,Z1,J2,J1)
       IF(IV.GE.NUMDT) GO TO 102
```

```
C**** THE PREDICTOR EQUATIONS ARE APPLIED
    5 DO 7 J=1,LIM
      H1(J)= Y0(J)+4./3.*DT*(2.*DY3(J)-DY2(J)+2.*DY1(J))
    7 H2(J)= X0(J)+4./3.*DT*(2.*DX3(J)-DX2(J)+2.*DX1(J))
      CALL DERIV(H2,H1,DXX,DYY,LIM)
C
C**** LCOUNT IS A COUNTER WHICH SPECIFIES NUMBER OF TIMES THE CORRECTOR
C     EQUATIONS ARE APPLIED.
      LCOUNT=0
C
C**** THE CORRECTOR EQUATIONS ARE APPLIED
    6 DO 8 J=1,LIM
      Z1(J)= 9./8.*Y3(J)-1./8.*Y1(J)+3./8.*DT*(DYY(J)+2.*DY3(J)-DY2(J))
    8 Z2(J)= 9./8.*X3(J)-1./8.*X1(J)+3./8.*DT*(DXX(J)+2.*DX3(J)-DX2(J))
      LCOUNT=LCOUNT+1
      IF(LCOUNT.EQ.N2)GO TO 10
    9 CALL DERIV(Z2,Z1,DXX,DYY,LIM)
      GO TO 6
C
C**** AS THE INTEGRATION IS ADVANCED 1 TIME STEP ALL PERTINENT VARIABLES
C     ARE UPDATED.


   10 DO 11 J=1,LIM
      DY0(J)=DY1(J)
      DX0(J)=DX1(J)
      DY1(J)=DY2(J)
      DX1(J)=DX2(J)
      DY2(J)=DY3(J)
      DX2(J)=DX3(J)
      X0(J)=X1(J)
      Y0(J)=Y1(J)
      X1(J)=X2(J)
      Y1(J)=Y2(J)
      Y2(J)=Y3(J)
      X2(J)=X3(J)

      Y3(J)=Z1(J)
   11 X3(J)=Z2(J)
      CALL DERIV(Z2,Z1,DX3,DY3,LIM)
      GO TO 3
  102 PRINT 103
  103 FORMAT(1H ,*THIS IS THE END OF THE CURRENT RUN*)
      END


      SUBROUTINE EMPIRCL
C***EMPIRCL ASSIGNS VALUES TO ALL PARAMETERS WHICH APPEAR IN THE EXPRESSION
C    FOR THE SEDIMENT TRANSPORT COEFFICIENT***
      REAL K0,N
      COMMON/BLOC1/PI
      COMMON/BLOC9/T,TV
      COMMON/BLOC10/GAMMA
C***DEFINITIONS: A=ALLOWANCE FOR PORE SPACE
C               CD=BOTTOM DRAG COEFFICIENT
C               K0=CONSTANT OF PROPORTIONALITY BETWEEN THE IMMERSED
C                   WEIGHT TRANSPORT RATE AND THE QUANTITY F(9)C(3) AS
C                   DEFINED IN THE TEXT
C                N=A MEASURE OF THE EFFECTIVENESS OF LATERAL MIXING
C                G=GRAVITATIONAL CONSTANT (MKS)
C            GAMMA=RATIO BETWEEN WAVE HEIGHT AND MEAN DEPTH AT BREAKING
C            ALPHA=RATIO BETWEEN WAVE AMPLITUDE AND LOCAL DEPTH IN THE
C                   SURF ZONE. ALPHA,AS SUPPORTED BY MEASUREMENTS,IS
C                   USUALLY SET EQUAL TO GAMMA/2.
C                S=AN AVERAGE SLOPE FOR THE COASTAL SITE BEING CONSIDERED
C        RHOW,RHOS=DENSITY OF WATER AND SAND,RESPECTIVELY
```

```
C                     TV=TRANSPORT COEFFICIENT FOR THE WATER MOTION
C                     T=SEDIMENT TRANSPORT COEFFICIENT
C        P,P1,P2,PSI ARE A.D.I.T.
      A=0.6
      CD=0.01
      KO=0.3
      N=0.052
      G=9.81
      GAMMA=0.78
      ALPHA=0.39
      S=0.02
      P=PI*N*S/(2.*ALPHA*CD)
      P1=-.75+SQRT(9./16.+1./P)
      P2=-.75-SQRT(9./16.+1./P)
      PSI= (1./(P*(P1+2.)*(P1-P2)*(P1-1.))+2./((5.*P-2.)*3.))
      RHOW=1.02
      RHOS=2.65
      TV=PSI*5.*PI*ALPHA*SQRT(G)/(16.*CD*GAMMA**(5./2.))
      T=KO*GAMMA*GAMMA*CD*RHOW/(PI*PSI*A*ALPHA*5.*(RHOS-RHOW))
C***NOTE: IF,IN THE COORDINATE SYSTEM ESTABLISHED,THE DEPTH GRADIENT IS
C         NEGATIVE,THEN,THE SIGN OF TV AND T IS REVERSED
      WRITE(6,1) N,P,PSI,TV,T
    1 FORMAT(2X,*N=*,F7.4//2X,*P=*,F7.4//2X,*PSI=*,F7.4//2X,*TV=*,F10.3
     2//2X,*T=*,F7.4)
      RETURN
      END


      SUBROUTINE ADJUST(N)
C**** ADJUST SERVES THREE PURPOSES:
C             (1) IT UPDATES THE INCIDENT WAVE CLIMATE.
C             (2) AS THE SHORELINE EVOLVES IT ADJUSTS THE INPUT BREAKER
C                 ANGLES AND RECOMPUTES THE LONGSHORE TRANSPORT RATES.
C             (3) A NET TRANSPORT FIGURE IS CALCULATED FOR PRE-SPECIFIED
C                 STRETCHES OF SHORELINE.THIS HAS SIGNIFICANCE WITH RESPECT
C                 TO A DETERMINATION OF WHETHER THE SEDIMENT FLOW IS
C                 CONFINED TO MORE OR LESS CLOSED CELLS OR IS A CONTINUOUS
C                 STREAM INTERRUPTED ONLY OCCASIONALLY.
      DIMENSION PHI(90),QNET(25)
      COMMON DEL(90),BETA(90),THETA(90)
      COMMON     X0(90),X1(90),X2(90),X3(90),Y0(90),Y1(90),Y2(90),Y3(90)
      COMMON DY0(90),DX0(90),DY1(90),DX1(90),DY2(90),DX2(90),DY3(90),
     *DX3(90)
      COMMON/BLOC/HB(50,90)
      COMMON/BLK/AB(50,90)
      COMMON/BLOC0/II
      COMMON/BLOC2/LIMIT,LIM1,LIM2
      COMMON/BLOC3/CVRT1,CVRT2
      COMMON/BLOC4/V0,V(90)
      COMMON/BLOC5/Q0,Q(50)
      COMMON/BLOC9/T,TV
      COMMON/BLOC10/GAMMA
      COMMON/BLOC11/COEFF
      COMMON/BLK2/PHI0,PHI(90)
      COMMON/BLK3/DB0,DB(90)
      COMMON/BLKF/L(10),M(10)
C     (1)
      DO 7  J=1,LIM1
      DB(J)=HB(II,J)/GAMMA
    7 PHI(J)=CVRT1*AB(II,J)
C**** WE MAKE THE FOLLOWING ASSUMPTIONS:
      DB(0)=DB(1)
      DB(LIM)=DB(LIM1)
      PHI(0)=PHI(1)-(PHI(2)-PHI(1))
      PHI(LIM)=PHI(LIM1)-(PHI(LIM2)-PHI(LIM1))
C****NOTE:IF THE END BOUNDARY CONDITIONS WERE Q=0.,WE WOULD SET PHI(0)=
C         PHI(LIM)=PI/2.,CORRESPONDING TO THE INCIDENT WAVE CRESTS BEING
C         PERPENDICULAR TO THE SHORELINE.
      RETURN
      ENTRY TRANSPT
```

```
C     (2)
C        COEFF IS A SOMEWHAT ARBITRARILY CHOSEN FRACTIONAL COEFFICIENT
C        WHICH TRANSLATES A CHANGE IN LOCAL BEACH ORIENTATION INTO A
C        CHANGE IN LOCAL BREAKER ANGLE.LEBLOND(1972) SET IT EQUAL TO 1.
      DO 3 J=1,LIMIT
      I=J-1
    3 PHI(I)=PHI(I)+COEFF*(CHI(I)-BETA(I))
C**** A WORD OF CAUTION: THE ABOVE ADJUSTMENT OF THE BREAKER ANGLE MUST BE
C     MADE THOUGHTFULLY.IF THE SHORELINE EXHIBITS SHARP HORIZONTAL CURVATUR
C     AND IS A REGION OF RAPID CHANGE THEN THE APPLICATION OF THIS FORMULA
C     MAY LEAD TO INSTABILITIES.IN THIS CASE IT IS BETTER TO RECOMPUTE THE
C     NEARSHORE WAVE FIELD MORE FORMALLY OR OMIT THE ADJUSTMENT PROCEDURE
C     ALTOGETHER.****
C
C**** Q AND V ARE A.D.I.T.


      DO 1 J=1,LIMIT
      I=J-1
      V(I)=TV*(GAMMA*DR(I))**(5./2.)*SIN(2.*PHI(I))
    1 Q(I)=T*V(I)
C**** SET CHI EQUAL TO PRESENT VALUE OF BETA.
      DO 4 J=1,LIMIT
      I=J-1
    4 CHI(I)=BETA(I)
C     (3)
C        L(I) AND M(I) REPRESENT THE LEFT AND RIGHT BOUNDARY POINTS
C        ON AN INTERVAL FOR WHICH WE WISH TO COMPUTE A NET TRANSPORT RATE.
      PRINT 9
      DO 5 I=1,10
      QNET(I)=0.
      L1=L(I)
      M1=M(I)
      DO 6 J=L1,M1
      QNET(I)=QNET(I)+(Q(J)-Q(J-1))
    6 CONTINUE
      WRITE(6,8)L1,M1,QNET(I)
    5 CONTINUE
    8 FORMAT(6X,I3,15X,I3,15X,F7.1)
    9 FORMAT(1H ,*LEFT POINT*,5X,*RIGHT POINT*,5X,*NET RATE*)
      RETURN
      END

      SUBROUTINE INITL(N,IND)
C
C**** INITL IS A SELF-EXPLANATORY SUBROUTINE THAT GENERATES ALL NECESSARY
C     STARTING VALUES FOR THE COORDINATES,(X,Y),OF THE BEACH POINTS FOR USE
C     IN THE FINITE-DIFFERENCED EQUATIONS.THE METHOD IS DESCRIBED IN THE TEX
C
      DIMENSION XX1(90),XX2(90),XX3(90),YY1(90),YY2(90),YY3(90)
      COMMON DEL(90),BETA(90),THETA(90)
      COMMON    X0(90),X1(90),X2(90),X3(90),Y0(90),Y1(90),Y2(90),Y3(90)
      COMMON DY0(90),DX0(90),DY1(90),DX1(90),DY2(90),DX2(90),DY3(90),
     $DX3(90)
      COMMON/BLOC2/LIMIT,LIM1,LIM2
      COMMON/BLOC7/TV,DR
C**** IMAX IS THE MAXIMUM NUMBER OF ITERATIONS ALLOWED
      IMAX=25
C**** EPS IS THE LARGEST PERMITTED DIFFERENCE BETWEEN COORDINATE VALUES
C     GENERATED ON SUCCESSIVE ITERATIONS(CONVERGENCE CRITERION).
      EPS=1.E-6
C**** GUESS IS AN ARBITRARY NUMBER USED TO YIELD INITIAL GUESSES FOR THE
C     COORDINATE VALUES.
      GUESS=.3
      CALL DERIV(X0,Y0,DX0,DY0,N)
      DO 2 I=1,N
      Y1(I)=Y0(I)-GUESS
    2 X1(I)=X0(I)-GUESS
      CALL DERIV(X1,Y1,DX1,DY1,N)
      DO 3 I=1,N
      Y2(I)=Y1(I)-GUESS
    3 X2(I)=X1(I)-GUESS
      CALL DERIV(X2,Y2,DX2,DY2,N)
      DO 4 I=1,N
      Y3(I)=Y2(I)-GUESS
    4 X3(I)=X2(I)-GUESS
      CALL DERIV(X3,Y3,DX3,DY3,N)
      ITER=0
    5 ITER=ITER+1
      IF(ITER.EQ.IMAX) GO TO 16
```

```
      DO 6 I=1,N
      XX1(I)=X1(I)
      XX2(I)=X2(I)
      XX3(I)=X3(I)
      YY1(I)=Y1(I)
      YY2(I)=Y2(I)
    6 YY3(I)=Y3(I)
      DO 7 I=1,N
      X1(I)=X0(I)+DT/24.*(9.*DX0(I)+19.*DX1(I)-5.*DX2(I)+DX3(I))
      Y1(I)=Y0(I)+DT/24.*(9.*DY0(I)+19.*DY1(I)-5.*DY2(I)+DY3(I))
      X2(I)=X0(I)+DT/3.*(DX0(I)+4.*DX1(I)+DX2(I))
      Y2(I)=Y0(I)+DT/3.*(DY0(I)+4.*DY1(I)+DY2(I))
      X3(I)=X0(I)+DT/8.*(3.*DX0(I)+9.*DX1(I)+9.*DX2(I)+3.*DX3(I))
    7 Y3(I)=Y0(I)+DT/8.*(3.*DY0(I)+9.*DY1(I)+9.*DY2(I)+3.*DY3(I))
    8 I=1
    9 IF(ABS(XX1(I)-X1(I)).LE.EPS.AND.ABS(YY1(I)-Y1(I)).LE.EPS)GO TO 10
      GO TO 13
   10 IF(ABS(XX2(I)-X2(I)).LE.EPS.AND.ABS(YY2(I)-Y2(I)).LE.EPS)GO TO 11
      GO TO 13
   11 IF(ABS(XX3(I)-X3(I)).LE.EPS.AND.ABS(YY3(I)-Y3(I)).LE.EPS)GO TO 12

      GO TO 13

   12 I=I+1
      IF(I.EQ.LIMIT)GO TO 14
      GO TO 9
   13 CALL DERIV(X1,Y1,DX1,DY1,N)
      CALL DERIV(X2,Y2,DX2,DY2,N)
      CALL DERIV(X3,Y3,DX3,DY3,N)
      GO TO 5
   14 IND=1
      GO TO 17
   18 IND=0
  200 FORMAT(1H ,8(4X,F10.3))
   17 RETURN
      END

      SUBROUTINE DERIV(X,Y,DX,DY,LIM)
C
C**** DERIV COMPUTES THE INCREMENTAL CHANGES,DY AND DX,IN THE (Y,X)
C     COORDINATES GIVEN BEACH SEGMENT ANGLES,THE DISTANCE BETWEEN ADJACENT
C     BEACH POINTS(DEL/2.),THE BREAKER DEPTHS AND THE TRANSPORT RATES.
C
      DIMENSION DX(90),DY(90),X(90),Y(90)
      DIMENSION FACTOR(90)
      COMMON    X0(90),X1(90),X2(90),X3(90),Y0(90),Y1(90),Y2(90),Y3(90)
      COMMON DY0(90),DX0(90),DY1(90),DX1(90),DY2(90),DX2(90),DY3(90),
     *DX3(90)
      COMMON DEL(90),BETA(90),THETA(90)
      COMMON/BLOC1/PI
      COMMON/BLOC2/LIMIT,LIM1,LIM2
      COMMON/BLOC5/Q0,Q(90)
      COMMON/BLOC7/IV,DT
      COMMON/BLK3/DB0,DB(90)
      COMMON/BLK4/KOUNT,III,NDC(50)
      DO 1 I=1,LIM1
    1 THETA(I)=ATAN2(X(I+1)-X(I),Y(I+1)-Y(I))
      THETA(0)=THETA(1)-(THETA(2)-THETA(1))
      THETA(LIM)=THETA(LIM1)-(THETA(LIM2)-THETA(LIM1))
      DO 2 I=1,LIM
    2 BETA(I)=(THETA(I)+THETA(I-1))/2.
C**** IF WE ARE AT THE START OF THE PROGRAM(KOUNT=1) OR THE WAVE DATA
C     SET IS CHANGING WE ENTER SUBROUTINE ADJUST TO RECOMPUTE TRANSPORT
C     FIGURES.
      IF(KOUNT.EQ.1.OR.III.EQ.NDC(II)) CALL TRANSPT(LIM)
```

```
      DO 3 I=1,LTM2
    3 DEL(I+1)=SQRT((X(I+2)-X(I+1))**2+(Y(I+2)-Y(I+1))**2)+SQRT((X(I+1)-
     *X(I))**2+(Y(I+1)-Y(I))**2)
C**** DEL(1) AND DEL(LIM) ARE DEFINED IN A SPECIAL WAY.
      DEL(1)=SQRT((X(2)-X(1))**2+(Y(2)-Y(1))**2)*2.
      DEL(LIM)=SQRT((X(LIM)-X(LIM1))**2+(Y(LIM)-Y(LIM1))**2)*2.
      DO 5 I=1,LIM
      FACTOR(I)=2./D3(I)*(Q(I)-Q(I-1))/DEL(I)
      DY(I)= SIN(BETA(I))*FACTOR(I)
    5 DX(I)=-COS(BETA(I))*FACTOR(I)
C**** NOTE:IF,IN THE COORDINATE SYSTEM CHOSEN,THE DEPTH GRADIENT IS
C           NEGATIVE THEN THE SIGNS PRECEDING THE SIN AND COS FUNCTIONS
C           ABOVE ARE REVERSED.HOWEVER THE SIGN OF V (EQUIVALENTLY,T) ALSO
C           CHANGES.THE NET EFFECT IS TO LEAVE THE EQUATIONS UNCHANGED.
      RETURN
      END


      SUBROUTINE AREA(Y,X,LTM,A,B,N)
C
C**** GIVEN THE COORDINATES OF THE BEACH POINTS AT 2 DIFFERENT TIMES THE
C     CHANGE IN SUBAERIAL SURFACE AREA OVER THAT TIME INTERVAL IS COMPUTED.
C     COORDINATES (Y,X) REFER TO THE FORMER SHORELINE POSITION (CURVE 1)
C     COORDINATES (A,B) REFER TO THE MORE RECENT POSITION (CURVE 2).
C
C     AN APPROXIMATE CALCULATION IS PERFORMED ALSO FOR THE CHANGE IN THE
C     VOLUME OF MATERIAL.
C
C     NOTE THAT ABSOLUTE VALUES OF AREA AND VOLUME ARE NOT COMPUTED BUT
C     RATHER THE RELATIVE CHANGE IN EACH.
C
C     THIS SUBROUTINE CAN BE MODIFIED TO COMPUTE CHANGES OVER ANY DISCRETE
C     LENGTH OF BEACH.
C
C     THE SIGN CONVENTIONS ESTABLISHED IN THIS SUBROUTINE ARE FOR A
C     COORDINATE SYSTEM IN WHICH THE DEPTH GRADIENT IS POSITIVE.
C     IF THE DEPTH GRADIENT IS NEGATIVE THE RESULTS CITED BELOW NEED
C     TO BE MODIFIED.
C
      DIMENSION YDEL(90),X(90),Y(90),B(90),A(90)
      LOGICAL A1,A2,A3,A4,B1,B2,B3,B4
      COMMON DEL(90),BETA(90),THETA(90)
      COMMON    X0(90),X1(90),X2(90),X3(90),Y0(90),Y1(90),Y2(90),Y3(90)
      COMMON DY0(90),DX0(90),DY1(90),DX1(90),DY2(90),DX2(90),DY3(90),
     *DX3(90)

      COMMON/BLOC2/LIMIT,LIM1,LIM2
      COMMON/BLK3/D30,D3(90)
C     COMPUTE AREA UNDER CURVE 1
      AREA1=0.
      VOL1=0.
      DO 1 I=1,LTM1
      AREA1=AREA1+.5*(Y(I+1)-Y(I))*(X(I+1)+X(I))
    1 VOL1=VOL1+.5*(Y(I+1)-Y(I))*(X(I+1)+X(I))*D3(I)
C     COMPUTE AREA UNDER CURVE 2
      N1=N-1
      AREA2=0.
      VOL2=0.
      DO 2 I=1,N1
      AREA2=AREA2+.5*(A(I+1)-A(I))*(B(I+1)+B(I))
    2 VOL2=VOL2+.5*(A(I+1)-A(I))*(B(I+1)+B(I))*D3(I)
C     COMPUTE THE AREA OF THE FAR LEFT TRAPEZOID A.D.I.T.
      TRAP1=ABS(.5*(Y(1)-A(1))*(X(1)+B(1)))
      VOL3=TRAP1*D3(1)
C     COMPUTE THE AREA OF THE FAR RIGHT TRAPEZOID A.D.I.T.
      TRAP2=ABS(.5*(Y(LTM)-A(N))*(X(LIM)+B(N)))
      VOL4=TRAP2*D3(LIM)
C     COMPUTE THE CONTRIBUTION DUE TO THE EXTENSION OF THE ENDPOINTS(LEFT)
      IF(Y(1).GT.A(1))GO TO 3
      DO 4 I=1,25
      IF(Y(I+1).GT.A(1))GO TO 5
    4 CONTINUE
    5 K=I+1
C**** A NEW X(K) IS DEFINED (SOLELY FOR THE PURPOSES OF THIS
C     SUBROUTINE) BY LINEAR INTERPOLATION.A NEW Y(K) IS ALSO DEFINED.
C     THE OLD VALUES ARE STORED.
```

```
      XK=X(K)
      X(K)=X(K)+(X(K-1)-X(K))*(A(1)-Y(K))/(Y(K-1)-Y(K))
      YK=Y(K)
      Y(K)=A(1)
      K1=K-1
      AREA3=0.
      VOL5=0.
      DO 6 I=1,K1
      AREA3=AREA3+.5*(Y(I+1)-Y(I))*(X(I+1)+X(I))
    6 VOL5=VOL5+.5*(Y(I+1)-Y(I))*(X(I+1)+X(I))*DB(I)
      X(K)=XK
      Y(K)=YK
    3 DO 7 I=1,25
      IF(A(I+1).GT.Y(1))GO TO 8
    7 CONTINUE
    8 K=I+1
C**** A NEW B(K) IS DEFINED BY LINEAR INTERPOLATION.A NEW A(K) IS ALSO
C     DEFINED.THE OLD VALUES ARE STORED.
      BK=B(K)
      B(K)=B(K)+(B(K-1)-B(K))*(Y(1)-A(K))/(A(K-1)-A(K))
      AK=A(K)
      A(K)=Y(1)
      K1=K-1
      AREA3=0.
      VOL5=0.
      DO 9 I=1,K1
      AREA3=AREA3+.5*(A(I+1)-A(I))*(B(I+1)+B(I))
    9 VOL5=VOL5+.5*(A(I+1)-A(I))*(B(I+1)+B(I))*DB(I)
      B(K)=BK
      A(K)=AK
COMPUTE THE CONTRIBUTION DUE TO THE EXTENSION OF THE ENDPOINTS(RIGHT).
      IF(Y(LIM).GT.A(N))GO TO 11
      DO 12 I=1,25
      IF(A(N-I).LT.Y(LIM))GO TO 13
   12 CONTINUE
   13 K=N-I
C**** A NEW B(K) IS DEFINED BY LINEAR INTERPOLATION.A NEW A(K) IS ALSO
C     DEFINED.THE OLD VALUES ARE STORED.
      BK=B(K)
      B(K)=B(K)+(B(K+1)-B(K))*(Y(LIM)-A(K))/(A(K+1)-A(K))
      AK=A(K)
      A(K)=Y(LIM)
      AREA4=0.
      VOL6=0.
      DO 14 I=K,N1
      AREA4=AREA4+.5*(A(I+1)-A(I))*(B(I+1)+B(I))
   14 VOL6=VOL6+.5*(A(I+1)-A(I))*(B(I+1)+B(I))*DB(I)
      B(K)=BK
      A(K)=AK
   11 DO 15 I=1,25
      IF(Y(LIM-I).LT.A(N))GO TO 16
   15 CONTINUE
   16 K=LIM-I

C**** A NEW X(K) IS DEFINED BY LINEAR INTERPOLATION.A NEW Y(K) IS ALSO
C     DEFINED .THE OLD VALUES ARE STORED.
      XK=X(K)
      X(K)=X(K)+(X(K+1)-X(K))*(A(N)-Y(K))/(Y(K+1)-Y(K))
      YK=Y(K)


      Y(K)=A(N)
      AREA4=0.
      VOL6=0.
      DO 17 I=K,LIM1
      AREA4=AREA4+.5*(Y(I+1)-Y(I))*(X(I+1)+X(I))
   17 VOL6=VOL6+.5*(Y(I+1)-Y(I))*(X(I+1)+X(I))*DB(I)
      X(K)=XK
      Y(K)=YK
C
      A=AREA2-AREA1
      VOL=VOL2-VOL1
C
C**** WE NOW COMPUTE THE AREAL (DIFA) AND VOLUMETRIC (DIFV) CHANGES.
```

```
C**** A1,A2,A3,A4,B1,B2,B3,B4 ARE LOGICAL VARIABLES WHICH DEFINE THE
      POSSIBLE RELATIONSHIPS BETWEEN THE ENDPOINTS OF 2 STRANDLINES.
      A1=A(1).GT.Y(1).AND.A(N).GT.Y(LIM)
      A2=A(1).GT.Y(1).AND.A(N).LE.Y(LIM)
      A3=A(1).LT.Y(1).AND.A(N).LT.Y(LIM)
      A4=A(1).LE.Y(1).AND.A(N).GT.Y(LIM)
      B1=B(1).GT.X(1).AND.B(N).GT.X(LIM)
      B2=B(1).GT.X(1).AND.B(N).LE.X(LIM)
      B3=B(1).LT.X(1).AND.B(N).LT.X(LIM)
      B4=B(1).LE.X(1).AND.B(N).GT.X(LIM)
C
C**** THE DEFINITIONS OF DIFA AND DIFV DEPEND ON WHICH COMBINATION
C     OF THE ABOVE LOGICAL STATEMENTS IS TRUE.
C
      IF(A2.AND.B2)  DIFA=A
      IF(A2.AND.B2)  DIFV=VOL
      IF(A4.AND.B4)  DIFA=-A
      IF(A4.AND.B4)  DIFV=-VOL
      IF(A4.AND.B1)  DIFA=A-TRAP1-TRAP2
      IF(A4.AND.B1)  DIFV=VOL-VOL3-VOL4
      IF(A2.AND.B3)  DIFA=A+TRAP1+TRAP2
      IF(A2.AND.B3)  DIFV=VOL+VOL3+VOL4
      IF(A1.AND.B4)  DIFA=A+TRAP1-TRAP2
      IF(A1.AND.B4)  DIFV=VOL+VOL3-VOL4
      IF(A3.AND.B2)  DIFA=A-TRAP1+TRAP2
      IF(A3.AND.B2)  DIFV=VOL-VOL3+VOL4
      IF(A1.AND.B1)  DIFA=A+2.*AREA3-TRAP1-TRAP2
      IF(A1.AND.B1)  DIFV=VOL+2.*VOL5-VOL3-VOL4
      IF(A3.AND.B3)  DIFA=A-2.*AREA3+TRAP1+TRAP2
      IF(A3.AND.B3)  DIFV=VOL-2.*VOL5+VOL3+VOL4
      IF(A4.AND.B2)  DIFA=A-2.*AREA4-TRAP1+TRAP2
      IF(A4.AND.B2)  DIFV=VOL-2.*VOL6-VOL3+VOL4
      IF(A2.AND.B4)  DIFA=A+2.*AREA4+TRAP1-TRAP2
      IF(A2.AND.B4)  DIFV=VOL+2.*VOL6+VOL3-VOL4
      IF(A3.AND.B1)  DIFA=A+2.*AREA4-TRAP1-TRAP2
      IF(A3.AND.B1)  DIFV=VOL+2.*VOL6-VOL3-VOL4
      IF(A1.AND.B3)  DIFA=A-2.*AREA4+TRAP1+TRAP2
      IF(A1.AND.B3)  DIFV=VOL-2.*VOL6+VOL3+VOL4
      IF(A1.AND.B2)  DIFA=A-2.*AREA4+2.*AREA3-TRAP1+TRAP2
      IF(A1.AND.B2)  DIFV=VOL-2.*VOL6+2.*VOL5-VOL3+VOL4
      IF(A3.AND.B4)  DIFA=A+2.*AREA4-2.*AREA3+TRAP1-TRAP2
      IF(A3.AND.B4)  DIFV=VOL+2.*VOL6-2.*VOL5+VOL3-VOL4
      IF(A4.AND.B3)  DIFA=A-2.*AREA3-2.*AREA4+TRAP1+TRAP2
      IF(A4.AND.B3)  DIFV=VOL-2.*VOL5-2.*VOL6+VOL3+VOL4


      IF(A2.AND.B1)  DIFA=A+2.*AREA3+2.*AREA4-TRAP1-TRAP2
      IF(A2.AND.B1)  DIFV=VOL+2.*VOL5+2.*VOL6-VOL3-VOL4
C
      RETURN
      END
C


      SUBROUTINE RESET(X,Y,L,J)
C
C*** RESET RE-ARRANGES THE BEACH POINTS FOR ANY SECTION OF THE SHORELINE
C    OR ALONG THE ENTIRE SHORELINE SUCH THAT THE SPACING BETWEEN ADJACENT
C    POINTS IS MADE MORE OR LESS EQUAL AND,AT THE SAME TIME,DISTORTION
C    OF THE BEACH SHAPE IS MINIMIZED.
C
C     L IS THE FAR RIGHT FIXED POINT A.D.I.T.
C     J IS THE FAR LEFT FIXED POINT A.D.I.T.
      DIMENSION X(90),Y(90),DELXY(90)
      COMMON DEL(90),BETA(90),THETA(90)
C**** ICOUNT IS A COUNTER FOR THE NUMBER OF TIMES THE FOLLOWING PROCEDURE
C     IS ITERATED.
      ICOUNT=0
C**** NUMIT IS NUMBER OF PERMITTED ITERATIONS.
      NUMIT=5
      J1=J+1
      L1=L-1
      L2=L-2
C     THE BEACH SEGMENT ANGLES AND THE DISTANCE BETWEEN SUCCESSIVE
C     POINTS IS COMPUTED.
   11 DO 1 I=J,L1
      THETA(I)=ATAN2(X(I+1)-X(I),Y(I+1)-Y(I))
    1 DELXY(I)=SQRT((X(I+1)-X(I))**2+(Y(I+1)-Y(I))**2)
COMPUTE A MEAN DISTANCE BETWEEN BEACH POINTS.
```

```
      SUM=0.
      DO 2 I=J,L1
    2 SUM=SUM+DELXY(I)
      DELNEW=SUM/(L1-J+1)
      I=J
C**** EXECUTE THE PROCEDURE AS DESCRIBED IN THE TEXT FOR THE
C     TRANSLATION OF THE BEACH POINTS I.E. MOVE THE FIRST POINT
C     ALONG THE BEACH SEGMENT TO ITS LEFT UNTIL THE DISTANCE BETWEEN
C     IT AND THE POINT ON ITS LEFT IS DELNEW,REDEFINE THE SEGMENT
C     BETWEEN THIS NEW POSITION AND THE POINT IMMEDIATELY TO ITS RIGHT
C     AND MOVE THIS SECOND POINT ALONG THE NEW SEGMENT...ETC.
   23 IF(DELNEW-DELXY(I))10,20,30
   10 X(I+1)=X(I+1)+(DELNEW-DELXY(I))*SIN(THETA(I))
      Y(I+1)=Y(I+1)+(DELNEW-DELXY(I))*COS(THETA(I))
      GO TO 21
   30 X(I+1)=X(I+1)+(DELNEW-DELXY(I))*SIN(THETA(I+1))
      Y(I+1)=Y(I+1)+(DELNEW-DELXY(I))*COS(THETA(I+1))
   21 DELXY(I+1)=SQRT((X(I+2)-X(I+1))**2+(Y(I+2)-Y(I+1))**2)
   20 I=I+1
      IF(I.EQ.L1)GO TO 22
      GO TO 23
   22 ICOUNT=ICOUNT+1
      IF(ICOUNT.NE.NUMTI) GO TO 11
CHECK TO SEE IF THE DISTANCE BETWEEN ADJACENT POINTS IS APPROXIMATELY
      EQUAL.
      WRITE(6,25)(DELXY(I),I=J,L1)
   25 FORMAT(2X,5(3X,F10.1))
      RETURN
      END


      SUBROUTINE RESULTS(X,Y,Z2,Z1,LIM,MAX)
C
C**** RESULTS PRINTS OUT SOME OF THE MORE IMPORTANT NUMBERS GENERATED
C     BY SHORLIN.
      DIMENSION Z1(90),Z2(90),X(90),Y(90)
      COMMON DEL(90),BETA(90),THETA(90)
      COMMON    X0(90),X1(90),X2(90),X3(90),Y0(90),Y1(90),Y2(90),Y3(90)
      COMMON DY0(90),DX0(90),DY1(90),DX1(90),DY2(90),DX2(90),DY3(90),
     $DX3(90)
      COMMON/BLK1/XX(90),YY(90)
      COMMON/BLOC2/LIMIT,LIM1,LIM2
      COMMON/BLOC5/Q0,Q(90)
      COMMON/BLOC7/IV,DT
      COMMON/BLK2/PHI0,PHI(90)
      TIME=IV*DT
      DAYS=TIME/24.
      YEARS=DAYS/365.
      PRINT 1,IV,DT,TIME,DAYS,YEARS
    1 FORMAT(3X,* NO.TIME STEPS(IV)=*,I4,5X,*TIME INCREMENT(DT)=*,F4.1,
     $1X,*HRS.*,5X,*ELAPSED TIME(IVXDT)=*,F10.1,1X,*HRS.=*,F8.1,1X,
     $*DAYS=*,F5.2,1X,*YEARS*)
      PRINT 2
    2 FORMAT(//5X,*POINT*,13X,*X(TIME=0)*,10X,*Y(TIME=0)*,10X,*X(TIME=
     $IVXDT)*,10X,*Y(TIME=IVXDT)*,5X,*X(PRESENT)*,5X,*Y(PRESENT)*/17X,
     $*METERS*,13X,*METERS*,13X,*METERS*,18X,*METERS*,15X,*METERS*,
     $10X,*METERS*)
      IF(MAX.GT.LIM)  K=MAX
      IF(MAX.LE.LIM)  K=LIM
      DO 4 I=1,K
    4 WRITE(6,3)I,X(I),Y(I),Z2(I),Z1(I),XX(I),YY(I)
    3 FORMAT(3X,1H ,I3,3X,3(7X,F10.2),16X,F10.2,8X,F10.2,5X,F10.2)
      PRINT 5
    5 FORMAT(//2X,*POINT*,10X,*BEACH ANGLE*,10X,*WAVE ANGLE*,10X,*BEACH
     $POINT SEPARATION* ,5X,*TRANSPORTS*/17X,*DEGREES*,14X,*DEGREES*,13X
     $,*METERS*,22X,*CUBIC METERS/HR*)
C**** CONVERT FROM RADIANS TO DEGREES.
      DO 8 I=1,LIMIT
      J=I-1
      PHI(J)=CVRT2*PHI(J)
    8 THETA(J)=CVRT2*THETA(J)
      DO 6 I=1,LIMIT
      J=I-1
    6 WRITE(6,7)J,THETA(J),PHI(J),DEL(J),Q(J)
C**** CONVERT FROM DEGREES BACK TO RADIANS.
      DO 10 I=1,LIMIT
      J=I-1
      PHI(J)=CVRT1*PHI(J)
   10 THETA(J)=CVRT1*THETA(J)
    7 FORMAT(1H ,2X,I3,7X,F10.2,9X,F10.2,13X,F10.2,25X,F10.2)
      CALL ERROR(X,Y,Z2,Z1,LIM,MAX)
      RETURN
      END
```

```
      SUBROUTINE ERROR(X,Y,Z2,Z1,LIM,MAX)
C
C**** ERROR CAN BE MADE MORE VERSATILE THAN IT IS NOW.AT PRESENT IT
C     COMPUTES THE PERCENT ERROR OF THE PREDICTED AREAL AND VOLUMETRIC
C     CHANGES AS COMPARED TO THOSE OBSERVED.IT ALSO CAN COMPARE OBSERVED
C     AND PREDICTED SHORELINE POSITIONS POINT BY POINT.
      DIMENSION Z1(90),Z2(90),DELTAX(90),DELTAY(90),X(90),Y(90)
      COMMON DEL(90),BETA(90),THETA(90)
      COMMON    X0(90),X1(90),X2(90),X3(90),Y0(90),Y1(90),Y2(90),Y3(90)
      COMMON DY0(90),DX0(90),DY1(90),DX1(90),DY2(90),DX2(90),DY3(90),
     *DX3(90)
      COMMON/BLK1/XX(90),YY(90)
      COMMON/BLOC6/DIFA,DIFV,DIFA1,DIFV1
C**** A SHORELINE CAN BE COMPARED WITH ITSELF AT VARIOUS STAGES IF THE
C     THE NUMBER OF POINTS WHICH CONSTITUTE THE SHORELINE IS ALWAYS THE
C     SAME(THIS COULD BE EFFECTED BY A SUBROUTINE WHICH DECREASES OR
C     INCREASES THE NUMBER OF POINTS WHILE RETAINING THE BEACH SHAPE-
C     SUCH A SUBROUTINE IS NOT PROVIDED HEREIN).
      IF(LIM.NE.MAX) GO TO 5
      DO 1 I=1,LIM
      DELTAX(I)=Z2(I)-XX(I)
    1 DELTAY(I)=Z1(I)-YY(I)
      WRITE(6,2)
    2 FORMAT(1H ,*DELTAX(I)*,7X,*DELTAY(I)*)
      WRITE(6,4)(I,DELTAX(I),DELTAY(I),I=1,LIM)
    4 FORMAT(3X,I4,2X,F9.2,5X,F9.2)
    5 PCT1= ABS((DIFA-DIFA1)/DIFA*100.)
      PCT2= ABS((DIFV-DIFV1)/DIFV*100.)
      WRITE(6,6) PCT1,PCT2
    6 FORMAT(1H ,*PER CENT ERROR IN AREAL CHANGE PREDICTION=,F4.1//1X,
     $*PER CENT ERROR IN VOLUMETRIC CHANGE PREDICTION=*,F4.1)
      RETURN
      END
```

```
      SUBROUTINE PLOTTER(X,Y,Z2,Z1,LIM)
C
C**** PLOTTER CAN MAKE AS MANY SEPARATE PLOTS AS DESIRED ON A SINGLE
C     FRAME.
C
C**** ITITLE,LABU,LABV ARE HOLLERITH LABELS.
      DIMENSION ITITLE(3),LABU(2),LABV(2)
      DIMENSION Z1(90),Z2(90),X(90),Y(90)
C
C**** U AND W ARE THE STORAGE LOCATIONS FOR ALL THE HORIZONTAL AND
C     VERTICAL COORDINATES,RESPECTIVELY,TO BE USED IN A SINGLE FRAME.
      DIMENSION U(120),W(120)
      COMMON DEL(90),BETA(90),THETA(90)
      COMMON    X0(90),X1(90),X2(90),X3(90),Y0(90),Y1(90),Y2(90),Y3(90)
      COMMON DY0(90),DX0(90),DY1(90),DX1(90),DY2(90),DX2(90),DY3(90),
     *DX3(90)
      COMMON/BLK1/XX(90),YY(90)
C**** IOB IS 1 LESS THAN THE NUMBER OF PLOTS ON A SINGLE FRAME.
C     IUBS(I) SPECIFIES THE POINTS IN THE ARRAYS U AND W AT WHICH THE
C     ONGOING PLOT IS TERMINATED AND A NEW PLOT IS BEGUN.
C
C     FOR THE SAKE OF COMPLETENESS WE INCLUDE THE OTHER SUBROUTINES
C     THAT COMPLEMENT PLOTTER,NAMELY,EASY,SCALING,GRAPH AND BORDER.
C     THESE SUBROUTINES,IN TURN,INTERFACE WITH ROUTINES(E.G.PLOT,SYMBOL,
C     NUMBER,ETC.)FROM THE PLOTLIB AND GOULD LIBRARIES.
C
C     A SAMPLE FOLLOWS.
C     COMMON/IUBS/IUBS(10),IOB
C     IUBS(1)=5
C     IUBS(2)=15
C     IOB=2
C     ITITLE(1)=5H18 ST.
```

```
      ITITLE(2)=6HSEOPG-
      ITITLE(3)=6HISL'NS
      ITITLE(4)=7H  1873,
      ITITLE(5)=7H1970
      LABU(1)=7HY COORD
      LABU(2)=4H (M)
      LABV(1)=7HX COORD
      LABV(2)=4H (M)
      DO 1 I=1,14
      W(I)=X(I)
    1 U(I)=Y(I)
      DO 2 I=1,14
      W(I+14)=XX(I)
    2 U(I+14)=YY(I)
      CALL ROTATE(W,U,28)
      CALL EASY(U,W,28,ITITLE,LABU,LABV,0)
      CALL PLOT(0,0.999)
  100 IOB=3
      IOBS(3)=19
      DO 3 I=1,14
      W(I)=Z2(I)
    3 U(I)=Z1(I)
      DO 4 I=1,14
      W(I+14)=X(I)
    4 U(I+14)=Y(I)

      CALL ROTATE(W,U,28)
      CALL EASY(U,W,28,ITITLE,LABU,LABV,0)
      CALL PLOT(0,0,999)
      RETURN
      END
C
C
C
      SUBROUTINE ROTATE(X,Y,N)
C
C***ROTATE RE-EVALUATES THE BEACH POINT COORDINATES IN A SYSTEM THAT
C    IS ROTATED THROUGH AN ANGLE ANG WITH RESPECT TO THE OLD AXES
C    ONE MOTIVATION FOR THIS OPERATION IS TO MAKE CLEARER THE DIRECTION
C    AND MAGNITUDE OF SHORELINE CHANGE I.E. ENHANCE VISUALLY THIS CHANGE
C
      DIMENSION X(N),Y(N)
      COMMON/BLOC3/CVRT1,CVRT2
C***ANG IS THE ROTATION ANGLE IN RADIANS - POSITIVE COUNTERCLOCKWISE
      ANG=20.*CVRT1
      COSA=COS(ANG)
      SINA=SIN(ANG)
      DO 1 I=1,N
      YSAVE=Y(I)
      Y(I)=Y(I)*COSA+X(I)*SINA
    1 X(I)=-YSAVE*SINA+X(I)*COSA
      RETURN
      END
```

```
      SUBROUTINE EASY(U,V,N,ITITLE,LABU.LABV,IDASH)
C THIS SUBROUTINE PLOTS A SINGLE GRAPH ON A BACKGROUND THAT IS
C CARTESIAN.  X IS THE HORIZONTAL ARRAY, Y THE VERTICAL ARRAY, N THE
C OF POINTS TO BE PLOTTED, ITITLE A HOLLERITH TITLE, LABX A HOLLERITH
C LABEL FOR X, AND LABY A HOLLERITH LABEL FOR Y.  NAME IS A FILE
C NAME IN HOLLERITH FORMAT
C EASY SUBROUTINE -- CHECK ON CALL FORVHOLLERITH VARIABLE
      DIMENSION U(N),V(N),ITITLE(5),LABU(2),LABV(2)
      UMAX=U(1)
      UMIN=U(1)
      VMAX=V(1)
      VMIN=V(1)
      DO 10 I=2,N
      IF(U(I).GT.UMAX)  UMAX=U(I)
      IF(U(I).LT.UMIN)  UMIN=U(I)
      IF(V(I).GT.VMAX)  VMAX=V(I)
      IF(V(I).LT.VMIN)  VMIN=V(I)
   10 CONTINUE
      DIFFX=UMAX-UMIN
      DIFFY=VMAX-VMIN
      UMAX=UMAX+0.03*DIFFX
      UMIN=UMIN-0.03*DIFFX
      VMAX=VMAX+0.03*DIFFY
      VMIN=VMIN-0.03*DIFFY
      DX=DIFFX/20.
      XX=ALOG10(DX)+100.
      KX=XX
      KX=KX-100
      RX=DX/(10.0**KX)
      PX=1.0
      IF(RX.GT.1.4)  PX=2.0
      IF(RX.GT.3.3)  PX=5.0
      IF(RX.GT.7.1)  PX=10.0
      DELU=PX*DX/RX
      LABEL=5
      IF(RX.GT.3.3.AND.RX.LE.7.1) LABEL=4
      DY=DIFFY/20.
      YY=ALOG10(DY)+100.
      KY=YY
      KY=KY-100
      RY=DY/(10.0**KY)
      PY=1.0
      IF(RY.GT.1.4)  PY=2.0
      IF(RY.GT.3.3)  PY=5.0
      IF(RY.GT.7.1)  PY=10.0
      DELV=PY*DY/RY
      CALL        SCALNG(UMIN,UMAX,VMIN,VMAX)
      CALL BORDER(UMIN,UMAX,VMIN,VMAX,DELU,DELV,ITITLE,LABU,LABV,LABEL)
      CALL GRAPH (U,V,N,IDASH)
      RETURN
      END


      SUBROUTINE SCALNG(UMIN,UMAX,VMIN,VMAX)
      COMMON/SCALE/A,B,C,D,YT,YB,XR,XL
C THIS SUBROUTINE SETS UP THE SCALING BETWEEN (U,V) AND (X,Y)
C (U,V) ARE (ABSCISSA,ORDINATE) AND (X,Y) ARE IN INCHES ON CRT.
C THE RELATIONS ARE   X=A*U+B, Y=C*V+D
C EQUAL SCALE FACTORS (A AND C) ARE USED IF THE GRAPH IS NEARLY SQUARE.
      A=6.5/(UMAX-UMIN)
      C=4.75/(VMAX-VMIN)
      R=A/C
      IF(R.GT.1.5.OR.R.LT.0.7) GO TO 10
      A=AMIN1(A,C)
      C=A
   10 CONTINUE
      B=4.0-0.5*A*(UMAX+UMIN)
      D=2.9-C*0.5*(VMAX+VMIN)
      YT=C*VMAX+D
      YB=C*VMIN+D
      XL=A*UMIN+B
      XR=A*UMAX+B
      RETURN
      END
```

```
      SUBROUTINE GRAPH(U,V,N,IDASH)
       COMMON/IOBS/IOBS(10),IQB
      COMMON/SCALE/A,B,C,D,YT,YB,XR,XL
      DIMENSION U(N),V(N),I(6),H(6)
      X=A*U(1)+B
      Y=C*V(1)+D
      CALL PLOT(X,Y,3)
      JDASH=IABS(IDASH)
      IF(JDASH.LE.9) GO TO 200
C COUNT NUMBER OF DIGITS IN IDASH
      NDIGIT=6
      IF(JDASH.LE.99999) NDIGIT=5
      IF(JDASH.LE.9999) NDIGIT=4
      IF(JDASH.LE.999) NDIGIT=3
      IF(JDASH.LE.99) NDIGIT=2
C DECOMPOSE INTO FOUR INTEGERS
      NDEN=100000
      NUM=JDASH
      DO 99 K=1,6
      I(K)=NUM/NDEN
      NUM=NUM-I(K)*NDEN

      NDEN=NDEN/10
   99 CONTINUE
C MINIMUM SPACING IS 1/128 INCH .
      DO 100 K=1,6
      IF(I(K).GT.7) I(K)=7
  100 CONTINUE
      NFIRST=7-NDIGIT
      DO 101 NI=NFIRST,6
      H(NI)=1.0/(2.0**I(NI))
  101 CONTINUE
C INITIALIZE
      LEVEL=NFIRST
      EXCESS=H(NFIRST)
      DO 103 K=2,N
C DRAW DASHED LINE TO NEXT POINT IN ARRAYS.
      XOLD=A*U(K-1)+B
      YOLD=C*V(K-1)+D
      XNEW=A*U(K)+B
      YNEW=C*V(K)+D
      XDIFF=XNEW-XOLD
      YDIFF=YNEW-YOLD
      TOTAL=SQRT(XDIFF*XDIFF+YDIFF*YDIFF+0.0000001)
      XCOS=XDIFF/TOTAL
      YSIN=YDIFF/TOTAL
      TOGO=TOTAL
      X=XOLD
      Y=YOLD
C NEXT SECTION OF LINE
  102 CONTINUE
      ITEST=LEVEL+NDIGIT
      IPEN=2
      IF(((ITEST/2)*2).EQ.ITEST) IPEN=3
      P=AMIN1(EXCESS,TOGO)
      X=X+P*XCOS
      Y=Y+P*YSIN
      CALL PLOT(X,Y,IPEN)


      TOGO=TOGO-P
      EXCESS=EXCESS-P
      IF(EXCESS.LT.0.005) LEVEL=LEVEL+1
      IF(LEVEL.GT.6) LEVEL=NFIRST
      IF(EXCESS.LT.0.005) EXCESS=H(LEVEL)
      IF(TOGO.GT.0.005) GO TO 102
C OTHERWISE GO TO NEXT POINT IN ARRAY AND CONTINUE
  103 CONTINUE
      RETURN
C SOLID LINE GRAPH WHEN IDASH HAS ONLY ONE DIGIT.
  200 CONTINUE
       IQB=1
      DO 10 K=2,N
      X=A*U(K)+B
      Y=C*V(K)+D
      IF(K.EQ.IOBS(IQB))1000,1001
 1000 CALL PLOT(X,Y,3)
       IQB=IQB+1
       GO TO 10
 1001 CONTINUE
      CALL PLOT(X,Y,2)
   10 CONTINUE
      RETURN
      END
```

```
      SUBROUTINE BORDER(UMIN,UMAX,VMIN,VMAX,DU,DV,ITITLE,LABU,LABV,INC)
      DIMENSION ITITLE(5),LABU(2),LABV(2)
      COMMON/SCALE/A,B,C,D,YT,YB,XR,XL
C THIS SUBROUTINE DRAWS A RECTANGULAR BORDER, TICK MARKS AT DU,DV
C INCREMENTS ALONG ABSCISSA, ORDINATE, THEN LABELS EVERY INC TICK MARKS.
C ITITLE IS WRITTEN ALONG THE TOP, LABU,LABV ALONG THE ABSCISSA,
C ORDINATE AXES. THE FIRST FOUR ARGUMENT ARE TRANSFERED TO SET.
      CALL        SCALNG(UMIN,UMAX,VMIN,VMAX)
      ULAB=DU*INC
      VLAB=DV*INC
      IFLAG=0
C DRAW BORDER   (XR,YB) TO (XR,YT) TO (XL,YT) TO (XL,YB) TO (XR,YB)
      CALL PLOT(XR,YB,3)
      CALL PLOT(XR,YT,2)
      CALL PLOT(XL,YT,2)
      CALL PLOT(XL,YB,2)
      CALL PLOT(XR,YB,2)
C NUMBER OF FIGURES TO RIGHT OF DECIMAL POINT
      NRU=1.5-ALOG10(ULAB)
      NRV=1.5-ALOG10(VLAB)
      IEU=0
      IEV=0
      IF(NRU.GE.4) IEU=2-NRU
      IF(NRV.GE.4) IEV=2-NRV
      IF(NRU.GE.4) NRU=2
      IF(NRV.GE.4) NRV=2
      QU=AMAX1(ABS(UMAX),ABS(UMIN))
      MU=ALOG10(QU)
      IF(MU.GE.4) IEU=MU
      IF(MU.GE.4) NRU=2
      QV=AMAX1(ABS(VMAX),ABS(VMIN))
      MV=ALOG10(QV)
      IF(MV.GE.4) IEV=MV
      IF(MV.GE.4) NRV=2
C SCALING FACTORS FOR U AND V .
      FU=10.0**IEU
      FV=10.0**IEV
      NCHU=NRU
      IF(NRU.LT.0) NCHU=-1
      NCHV=NRV
      IF(NRV.LT.0) NCHV=-1
C TICK MARKS ALONG ABSCISSA
      I=(UMAX+DU)/DU
      U=I*DU
      U=U+0.0000001*DU
   20 CONTINUE
      U=U-DU
      I=I-1
      IF(U.LE.UMIN) GO TO 30
C OTHERWISE DRAW TICK MARKS
      X=A*U+B
C DRAW LINE FROM (X,YB) TO (X,YB+0.1)
      TICK=0.04
      IF(((I/INC)*INC).EQ.I) TICK=2.5*TICK
      YBB=YB+TICK
      CALL PLOT(X,YB,3)
      CALL PLOT(X,YBB,2)


C DRAW LINE FROM (X,YT) TO (X,YT-0.1)
      YTT=YT-TICK
      CALL PLOT(X,YT,3)
      CALL PLOT(X,YTT,2)
      IF(((I/INC)*INC).NE.I) GO TO 20
C OTHERWISE, WRITE U BELOW TICK MARK
C NUMBER OF FIGURES TO LEFT OF DECIMAL POINT

      NLU=1
      UU=U/FU
      IF(ABS(UU).LT.0.01) GO TO 25
      NLU=ALOG10(ABS(UU))+1
   25 CONTINUE
```

```
      IF(NLU.LE.1) NLU=1
      NT=NLU+NCHU
      XLAB=X-0.07*NT
      YLAB=YB-0.2
      IF(NCHU.GT.-1.AND.NCHU.LT.1) NCHU=0
      CALL NUMBER(XLAB,YLAB,0.14,UU,0.,NCHU)
      GO TO 20
   30 CONTINUE
      IF(XLAB.LT.XL) IFLAG=1
C TICK MARKS ALONG ORDINATE
      J=(VMAX+DV)/DV
      V=J*DV
      V=V+0.000001*DV
   40 CONTINUE
      J=J-1
      V=V-DV
      IF(V.LE.VMIN) GO TO 50
C OTHERWISE DRAW TICK MARKS
      Y=C*V+D
C DRAW LINE FROM (XL,Y) TO (XL+0.1,Y)
      TICK=0.04
      IF(((J/INC)*INC).EQ.J) TICK=2.5*TICK
      XLL=XL+TICK
      CALL PLOT(XL,Y,3)
      CALL PLOT(XLL,Y,2)
C DRAW LINE FROM (XR,Y) TO (XR-0.1,Y)
      XRR=XR-TICK
      CALL PLOT(XR,Y,3)
      CALL PLOT(XRR,Y,2)
      IF(((J/INC)*INC).NE.J) GO TO 40
C OTHERWISE, WRITE V NEXT TO TICK MARK.
C NUMBER OF FIGURES TO LEFT OF DECIMAL POINT
      NLV=1
      VV=V/FV
      IF(ABS(VV).LT.0.01) GO TO 26
      NLV=ALOG10(ABS(VV))+1
   26 CONTINUE
      IF(NLV.LE.1) NLV=1
      NT=NLV+NCHV
      XLAB=XL-0.06
      YLAB=Y-0.07*NT
C ELIMINATE LAST LABEL WHEN OVERLAP COULD OCCUR AT CORNER.
      IF(IFLAG.EQ.1.AND.YLAB.LT.YB) GO TO 50
      IF(NCHV.GT.-1.AND.NCHV.LT.1) NCHV=0
      CALL NUMBER(XLAB,YLAB,0.14,VV,90.,NCHV)
      GO TO 40


   50 CONTINUE
C WRITE IN TITLE ON TOP BORDER, ABSCISSA AND ORDINATE LABELS
      HT=0.14
      X=0.4
      Y=YT+0.2
      CALL SYMBOL(X,Y,HT,ITITLE,0.,50)
      ISCL=8H( X10   )
      X=XL+0.4
      Y=YB-0.5
      CALL SYMBOL(X,Y,HT,LABU,0.,20)
      IF(IEU.EQ.0) GO TO 60
C OTHERWISE, WRITE SCALING FACTOR
      X=XL+3.2
      CALL SYMBOL(X,Y,HT,ISCL,0.,8)
      X=XL+3.8
      Y=Y+0.1
      Q=-IEU
      CALL NUMBER(X,Y,0.07,Q,0.,-1)
   60 CONTINUE
      X=XL-0.3
      Y=YB+0.2
      CALL SYMBOL(X,Y,HT,LABV,90.,20)
      IF(IEV.EQ.0) GO TO 61
C OTHERWISE, WRITE SCALING FACTOR
      Y=YB+3.0
      CALL SYMBOL(X,Y,HT,ISCL,90.,8)
      X=X-0.1
      Y=Y+0.6
      Q=-IEV
      CALL NUMBER(X,Y,0.07,Q,90.,-1)
   61 CONTINUE
      RETURN
```

VII. Apalachicola Bay

1. Nature of Inputs

St. George Island is part of a barrier island chain in the Apalachicola Bay region of northwest Florida (see Figure 5). Because of its location it is subject on the average to low-to-moderate wave energy levels. Waves propagating from deep water toward the island pass over a broad, shallow continental shelf region and experience bottom friction damping, the degree of which depends directly on the wave height and period (equivalently, wavelength) i.e., the higher, longer waves are attenuated more rapidly. The net energy loss can be substantial when integrated over the total travel time from intermediate depth water to the point of incipient breaking. Other means by which energy can be subtracted from a wave train are the presence of adverse winds and shear currents, and non-linear wave-wave interactions (including dissipation due to capillary waves). In shallow water the wave energy density increases, competing effectively against bottom friction to enhance the wave height and induce breaking. An exception may occur on very mild slopes where bottom damping is sufficient to extinguish the wave. Depending upon the bathymetry, refraction and diffraction can augment or reduce the local wave height.

Walton (1973) in a study on the distribution of littoral drift along the entire Florida shoreline considered deep-water wave data as his source of wave information and incorporated in

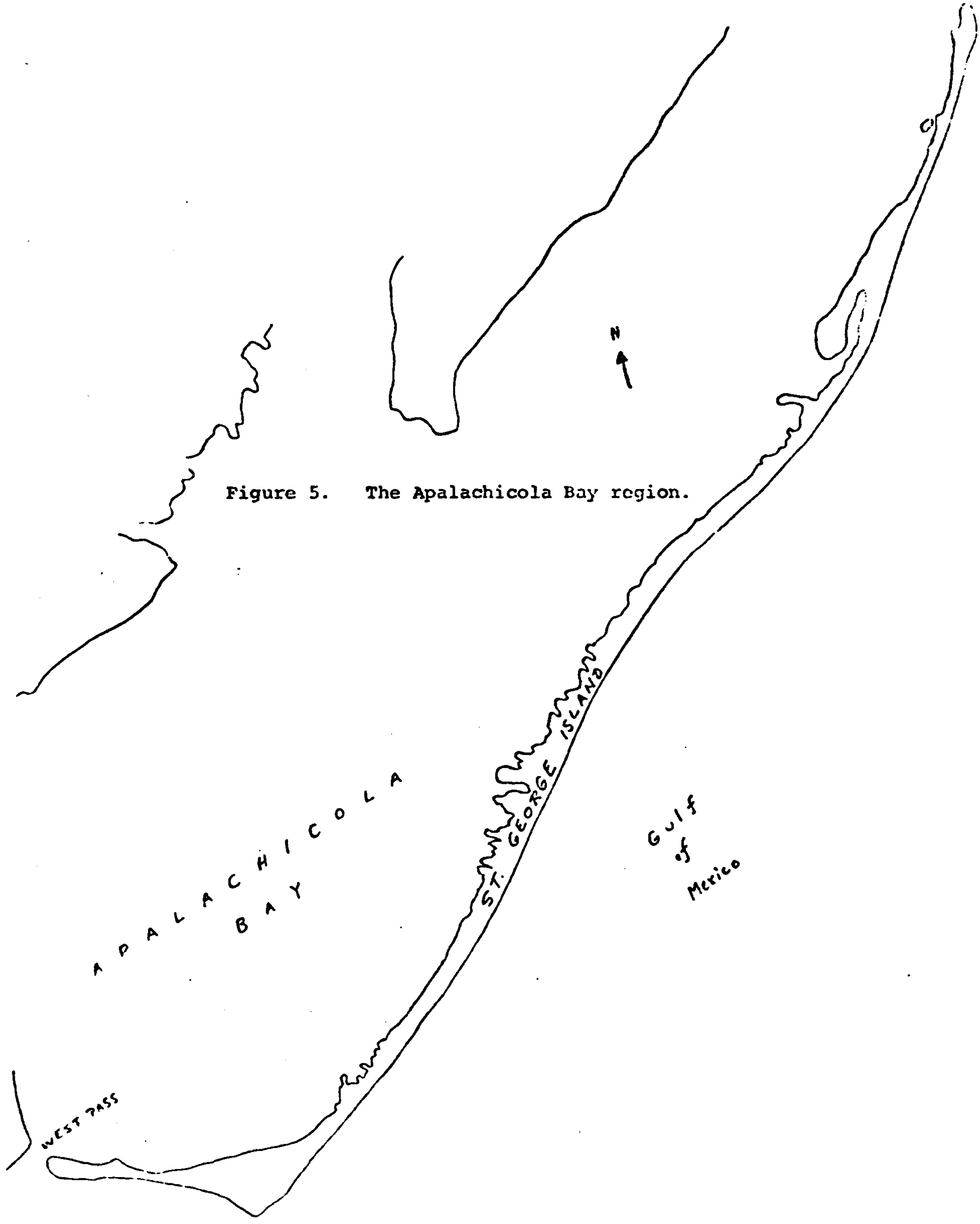

Figure 5. The Apalachicola Bay region.

his model the influences of bottom friction, shoaling and refraction. We have chosen to utilize Walton's model on wave modification in shallow water as the means by which we generate the breaker data essential to our model, $\phi_b(\vec{y})$ and $H_b(\vec{y})$, the breaker angle and height as functions of longshore position. We will not detail Walton's work, since he has provided a thorough explanation of his methodology, but rather outline his general approach and the changes we introduce.

The wave data source is the U.S. Naval Weather Service Command, Summary of Synoptic Meterological Observations available from the NOAA Environmental Data Service, National Climatic Center, Asheville, N.C. These are shipboard observations of meterological and sea conditions made by ships in passage. The drawbacks inherent in such data are many (we shall not enumerate) but they represent the best general compilation of marine data at present. The record extends through the years 1865-1971 with eighty percent of the observations occurring during the period 1954-1971. The pertinent annually averaged tables are Table 18, which gives the percent frequency of wind direction versus sea heights, and Table 19, which gives the percent frequency of wave height versus wave period. Using these tables several bits of information are computed. The frequency of occurrence of a wave of a given height, period and direction of propagation is determined and expressed as a fraction of the total time of record and is subsequently adjusted according to the following formula: the geographical oceanic region which is assumed to contribute waves to a specific coastal area is divided into "data squares"; this necessitates that data from adjacent squares be weighted. Walton used 2°-4° data squares as shown in Figure 6 to blanket the Florida coastline and linearly interpolated the wave climate between adjacent squares. We chose a set of finer resolution 1° squares in the Gulf of Mexico (Figure 7) because of the high density of data in each square and the coverage of the Florida Panhandle. Our method of weighting, somewhat different from Walton's, is illustrated in Figure 8. A reference line is drawn due south of St. George Island. Additional lines are drawn to the center of each 1° square and the angle, δ, between these lines and the reference line is measured. A weighting term, d, with respect to δ_2, is determined from the formula

$$d\,|\delta_2| \sum_{i=1}^{7} |\delta_i|^{-1} = 1 \qquad (52)$$

where δ_i = 28°, 8°, -17°, -36°, -51°, -58°, -64°, i = 1,7 so that d = 0.417. The individual weighting factors,

$$|\delta_2| / |\delta_i|$$

are then applied to each wave type in the respective squares to ascertain the contribution from each square to the mean frequency (the fraction of time over which a specific wave endures). At this point a set of deep-water input data has been established.

The next step is to track each wave component into shore monitoring its change in direction due to refraction and its change in amplitude due to shoaling, refraction, bottom friction and percolation through the sand grains. Walton's numerical model to accomplish this has the following structure:

Figure 6. Data squares used in Walton (1973).

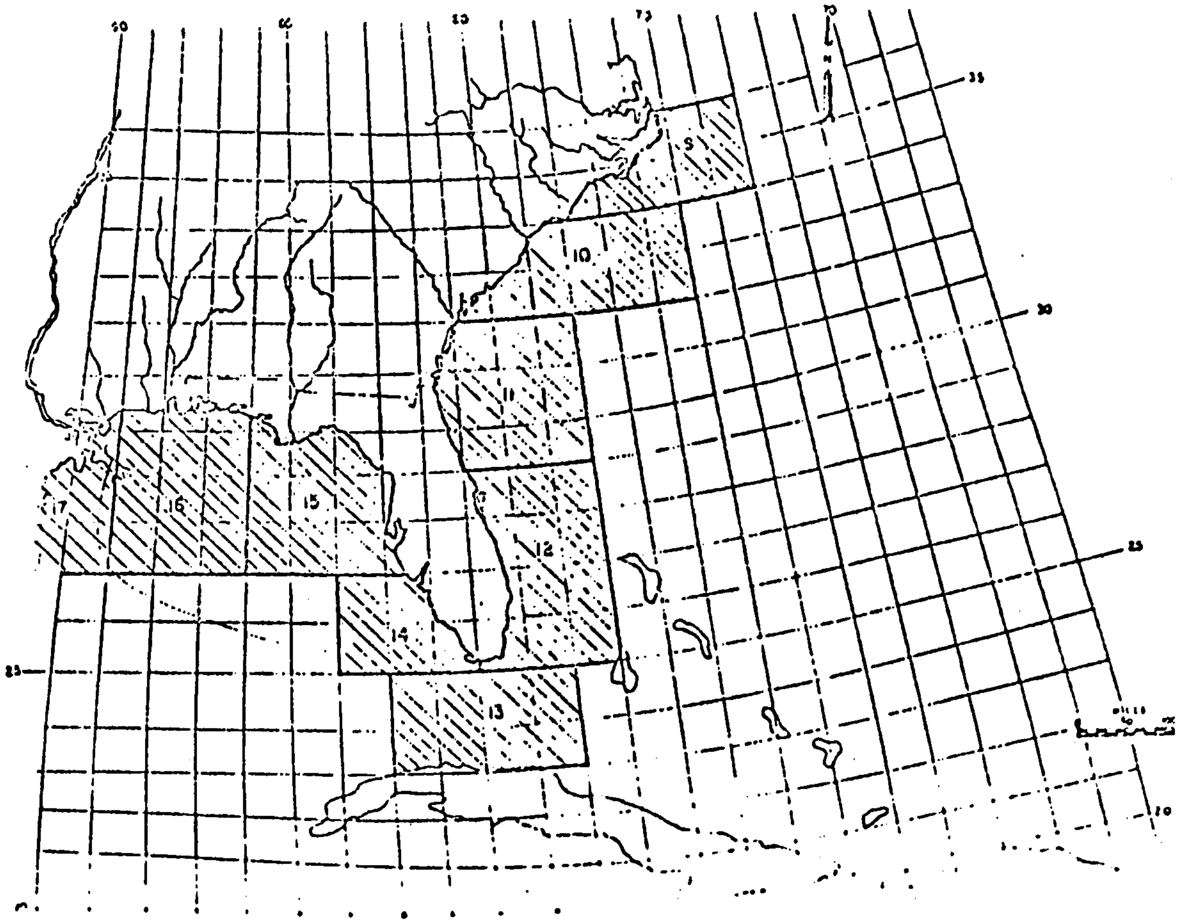

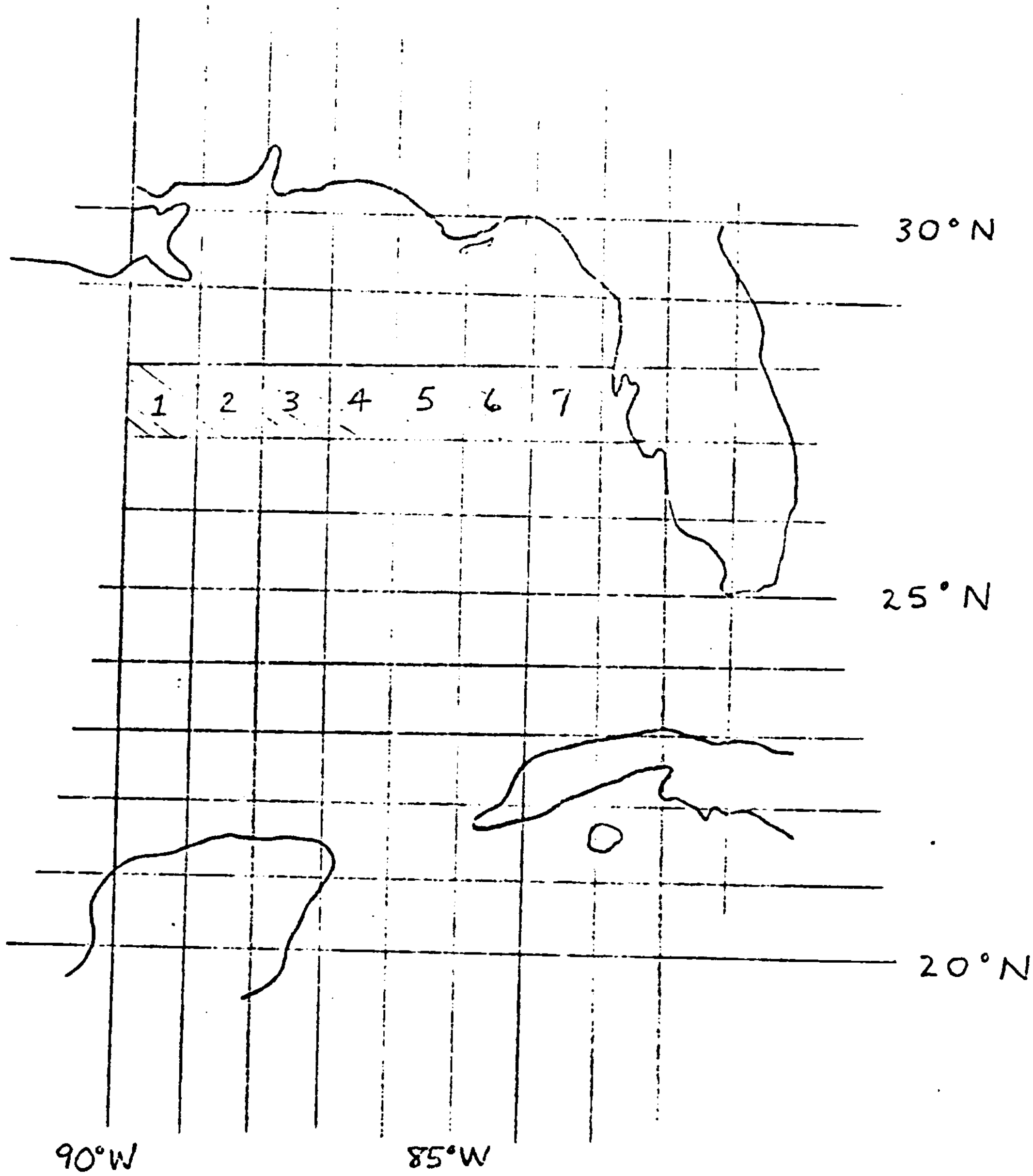

Figure 7. Data squares used in present study.

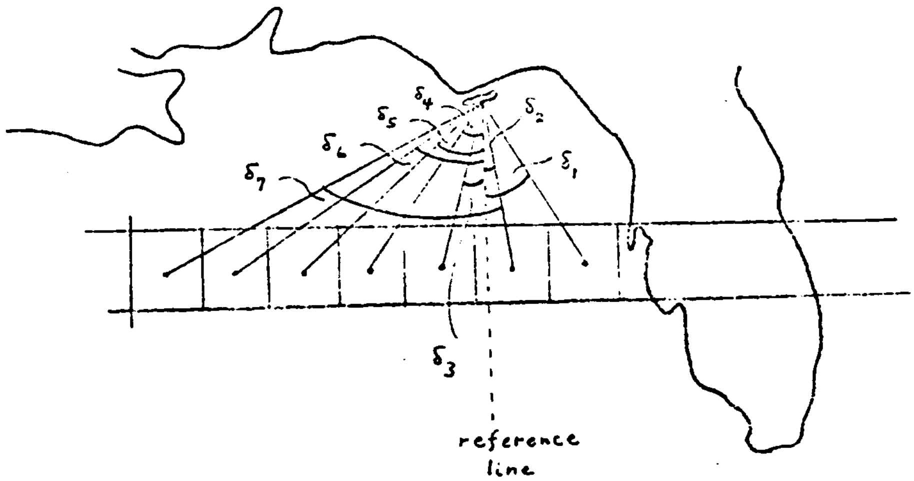

Figure 8. Geometric weighting of annually-averaged data from each square.

1. The orientation of the wave fronts as they approach shore is computed using Snell's law of refraction for a bottom topography composed of straight and parallel bottom contours. The refraction and shoaling coefficients are calculated concomitantly.

2. The computation of the coefficients of bottom friction and percolation follows the work of Bretschneider and Reid (1954). Required inputs are the lengths and slopes of a series of bottom sections comprising a bottom profile normal to the stretch of shoreline being considered (rather than the true profile over which the waves pass). In our model we consider seven profiles coincident with the seven lines in Figure 8 and weight the results in the same manner as before.

The product of these calculations is the breaker height, the breaker angle and the fractional duration of each deep-water wave type for a segment of beach. Repeating this process for each beach segment of interest we obtain a longshore distribution of breaker heights and angles, each of these quantities contributing independently to the magnitude of the longshore current, e.g., a decreasing angle of incidence longshore could be offset by an increasing wave height and vice-versa. The reader is referred to Walton (1973) for a more complete discussion of the assumptions, approximations and limitations underlying the above data reduction and analyses.

The application of our numerical model requires that we discretize the strandline in a coordinate system established with reference to some semi-permanent landmark. A feature which is present on all the bathymetric sheets of the U.S. Hydrographic Office that we have used (which provide us with a progressive history of the St. George shoreline) is the St. George lighthouse on Cape St. George (see Figure 5). Stapor (1971) has indicated that the lighthouse, constructed in 1847, has a margin of error associated with its position on the charts which falls within accepted map standards. The lighthouse is the origin of our coordinate system which, for convenience, has its ordinate running due north and its abscissa due east. The shoreline of 1873 as depicted on smooth sheet No. 1184 is divided into 57 segments; the northwest tip of the island is beach point 1, the northeast tip beach point 58. The points are irregularly spaced, being packed more closely where the beach exhibits large horizontal curvature; the maximum spatial increment is 840 m (in the mildly concave middle section), the minimum about 320 m (in the area of Cape St. George). Resolving each beach point into vertical (x) and horizontal (y) coordinates, the separation between points and the angular orientation of each segment is straightforward to calculate. This information, when fed into the wave modification program previously discussed, ultimately determines the longshore variation of breaker height and angle. Supplementary information on the Apalachicola Bay region is provided by smooth sheets H1265 (1974), H5794-5 (1935), H5819 (1935), 2265 (1896), 6788 (1943). The 1873 strandline serves as the baseline for the predictive model. If the present (circa 1970) strandline can be generated, even qualitatively, then the model could be used, albeit cautiously, for future projections.

2. Long-time Integration of Predictive Equations

The integration of (43a,b), as they apply to St. George Island, cannot be accomplished blindly. One must be aware of any special features that contribute to the dynamic balance of the island.

St. George Island in 1873 was composed of three parts separated by two hurricane-cut inlets (the bay side of the island is marked by hurricane washover deposits). In Figure 9 is a schematic diagram identifying the major sections and the inlets. The stability of tidal inlets is a complex problem which we do not treat here (see O'Brien and Dean, 1972; Dean and Walton, 1975). The littoral drift past an inlet can be interrupted and sand deposited, leading to closure of the inlet. The question of closure rests on knowledge of the inlet cross-sectional area, the tidal velocities, the wave climate, the magnitude of bottom and side friction and the level of littoral drift. We assume that the rate of sediment transport across the inlet is reduced relative to its upstream value by some fraction. Since Sand Island Pass and New Inlet Pass both eventually close, an estimate of the volume of material contained in these inlets, the period over which closure progresses (assumed to be unidirectional) and an average upstream littoral drift rate can yield a value for this fraction. An alternative method for determining the rate at which the longshore

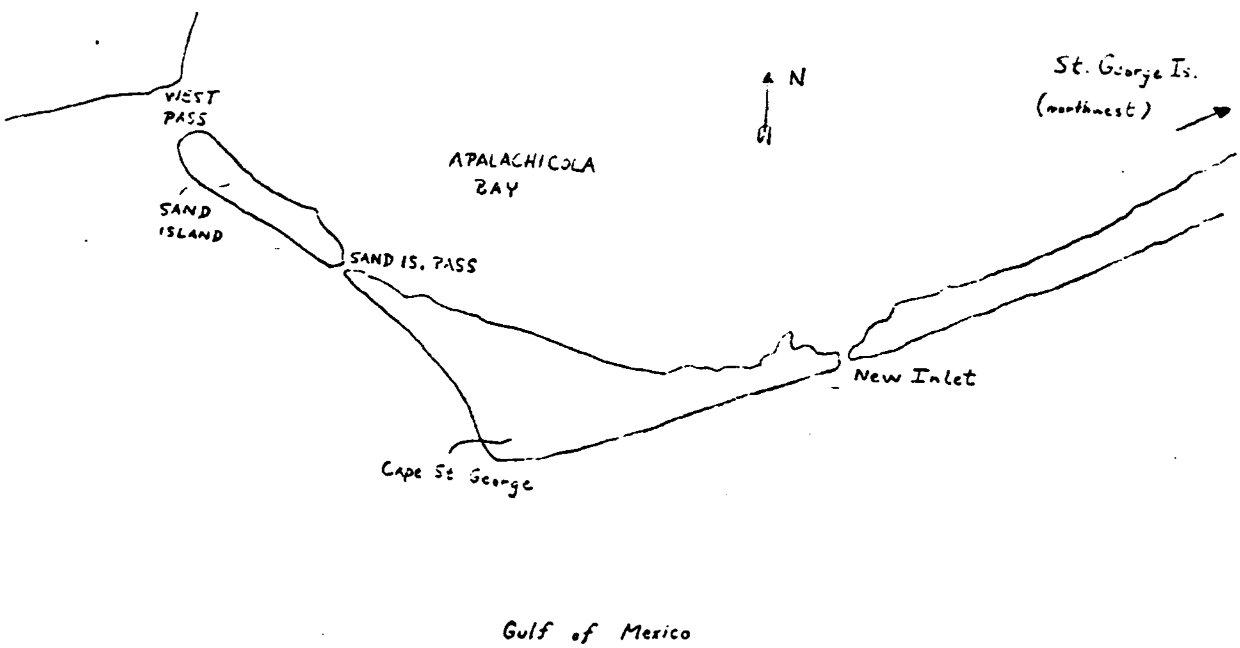

Figure 9. The southwest portion of St. George Island, 1873.

drift is trapped in the vicinity of an inlet is to obtain an independent measure of the growth rate of the shoals inside and outside the channel. In the absence of such information we simply assume that the transport rate across the mouth of the inlets is the average of the upstream and downstream values. This is an unwarranted assumption if the inlet does not bypass a substantial portion of the longshore sediment load for, then, the downstream shore is likely to be cut back due to sand deprivation.

Due south of Cape St. George is an extensive series of shoals projecting some 8 kilometers into the Gulf of Mexico. These shoals are focus areas for incoming wave energy and, consequently, the breaker energy expended on the shore to move sediment is reduced. This submarine relief will attenuate, re-direct, or even block waves propagating toward the Cape. We expect that the level of wave activity in the vicinity of the Cape, as computed previously, will tend to be an overestimate, at least, in relation to the energy levels at contiguous portions of the beach. We, therefore, reduce the energy input to this region, due to waves from the south and southwest, by about 25%; this figure is arrived at by considering the degree of wave damping over this special bottom relief and the percentage of waves that are likely to break far from shore.

Off the northwest tip of Sand Island is a rather permanent shallow, submarine feature, the East Bank. The tidal ebb flow through West Pass has transported local material seaward and the wave levels have been too low to reverse this trend and confine the sediment to the littoral zone. This shoal, which sweeps to the south and west, almost attaches itself to the shoreline. With the Cape St. George Shoals intercepting waves from the southeast and the East Bank doing the same for waves from the southwest, it is anticipated that the levels and periods of wave activity in the area of Sand Island will be diminished compared to those values computed in disregard of these prominent shoals. As before, we reduce the transport figures, accordingly. In addition, much of the longshore drift toward West Pass is likely to be diverted to the East Bank by tidal currents in the presence of low incident wave levels, i.e., only small quantities of sand will be deposited at the tip of Sand Island. This situation will prescribe the boundary condition at the northwest end of St. George Island in our model.

It should be noted that there is an overall bias toward low wave energy in this study. Since ships tend to avoid bad weather our deep-water wave observations are on the low side. Also, major storms, such as hurricanes, can cause rapid and marked fluctuations in a beach system. We are presuming that over a long period (e.g., greater than 50 years) there is a "smoothing" effect that works to reverse sudden and violent changes, i.e., a shoreline responds to long-term forcings (e.g., hurricane breaches in a barrier island on a tidal sea are usually repaired on a relatively short time scale).

To be specific, the integration of the governing equations for St. George Island over the period 1873-1970 was carried out according to the following procedure:

1. The wave characteristics at the breaker line (height, angle, fraction of a year over which a particular wave acts), as generated by Walton's program, serve as input to our model. A

cumulative frequency of occurrence of all waves yields the time, expressed as a fraction of a year, during which onshore waves are expected, e.g., for St. George Island it was found that on-shore (breaking) waves are present about half the time, the exact number being 0.51. Thus over a 98 year interval relatively calm periods prevailed for approximately 48 years. The sets of breaker data are inserted in random order into the model to compute the forcing function for the longshore motions. Equations (23a,b) are integrated for a number of time steps equivalent to 1 year. This process is repeated for as many years as desired, i.e., one year does not differ from any other year inasmuch as the deep-water wave climate remains unchanged (although the breaker angles do change in response to the evolving beach shape).

2. In (24a,b) it is found by trial that choosing a step size of $\Delta t = 50$ hours and applying the corrector <u>twice</u> is the most efficient compromise, i.e., the truncation error is kept small and the integration proceeds fairly rapidly.

3. As mentioned in section V special care must be taken at endpoints. We see in Figure 4 that for point j, Q_{j-1}, β_j and Δ_j must be defined differently than the same quantities as they apply to the interior points. By "endpoints" we mean those points at the extremities at or near which the longshore transport approaches zero (i.e., $Q = 0$). This definition is offered in lieu of more detailed information about the tidal, wave, and current dynamics in these areas. A more formal consideration

of the sediment flux at the tips of St. George Island would entail finer wave refraction and diffraction computations, a knowledge of the magnitude of the tidal streams and of the leakage of sand from the island to offshore shoals. By referring to the boat sheets and noting where the shoreline begins to curve inward away from the predominant wave direction we choose the endpoint positions and measure manually the effective beach angles, β, at these points. These angles are important in that they determine the direction in which the ends prograde or recede; they are adjusted as the integration proceeds. The initial β at the northeast tip of the island is $2\pi/3$ (radians), at the northwest tip it is $3\pi/2$. The endpoint Δ is twice the distance between the endpoint and its neighboring point.

4. Other parameters in the model assume the following values:

$K_o = 0.4$

$N = 0.05$

It was found that the magnitude of the sand transport was not particularly sensitive to variations in N.

Results are displayed in Figures 10-15. St. George Island is viewed in 3 sections: 1) the Cape St. George region, 2) the long, arc-like middle section, and 3) the elongating northeast tip. Supporting evidence is provided by Stapor (1971) who determined the areas of erosion and accretion for shorelines in the Apalachicola Bay region. He considered the redistribution of the bathymetric contours to be indicative of the direction and

Figure 10. Southwest St. George Island as recorded in 1873 and 1970.

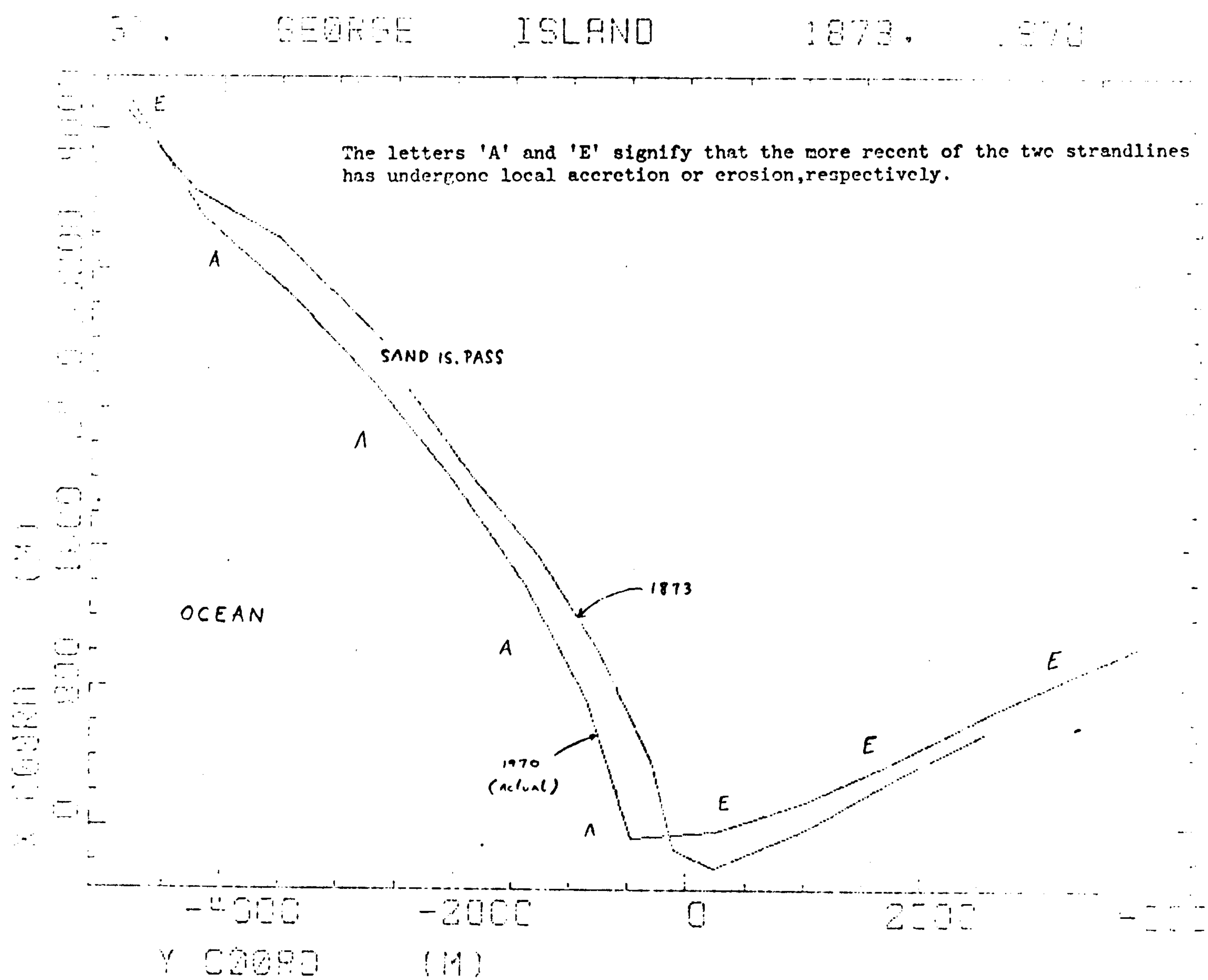

Figure 11. A comparison of southwest St. George Island in 1873 and 1970 (predicted).

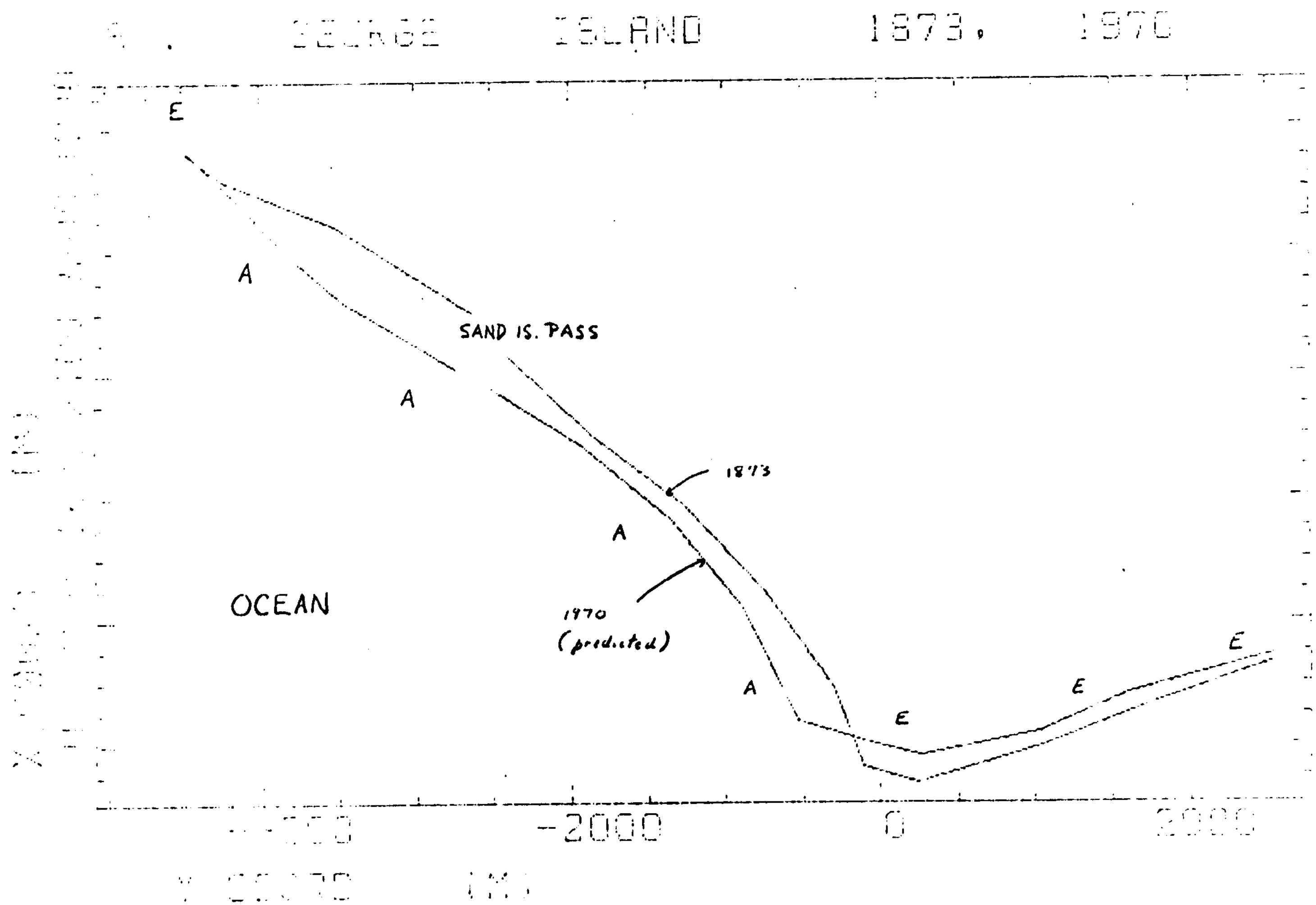

Figure 12. The middle section of St. George Island as recorded in 1873 and 1970.

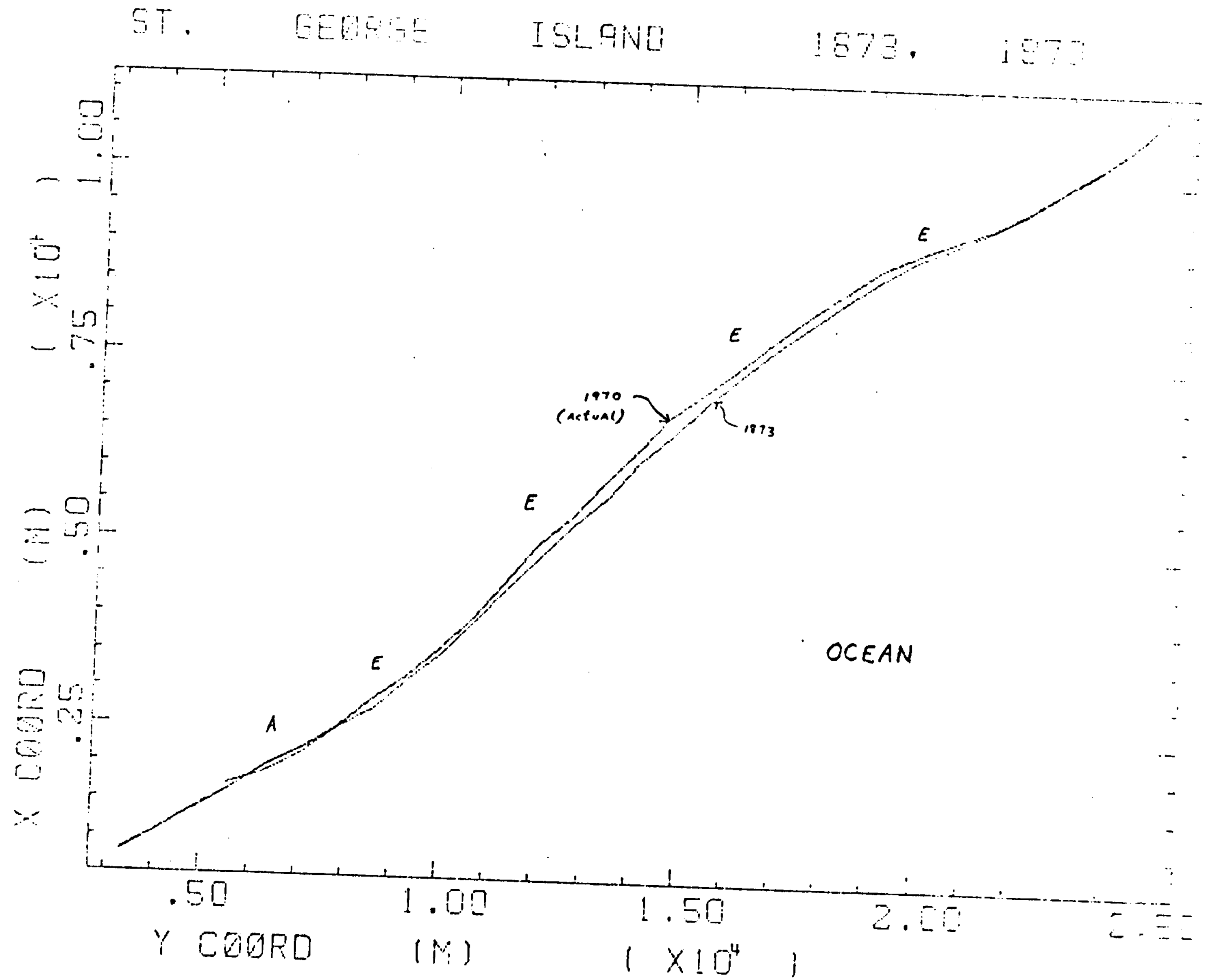

Figure 13. A comparison of the middle section of St. George Island in 1873 and 1970 (predicted).

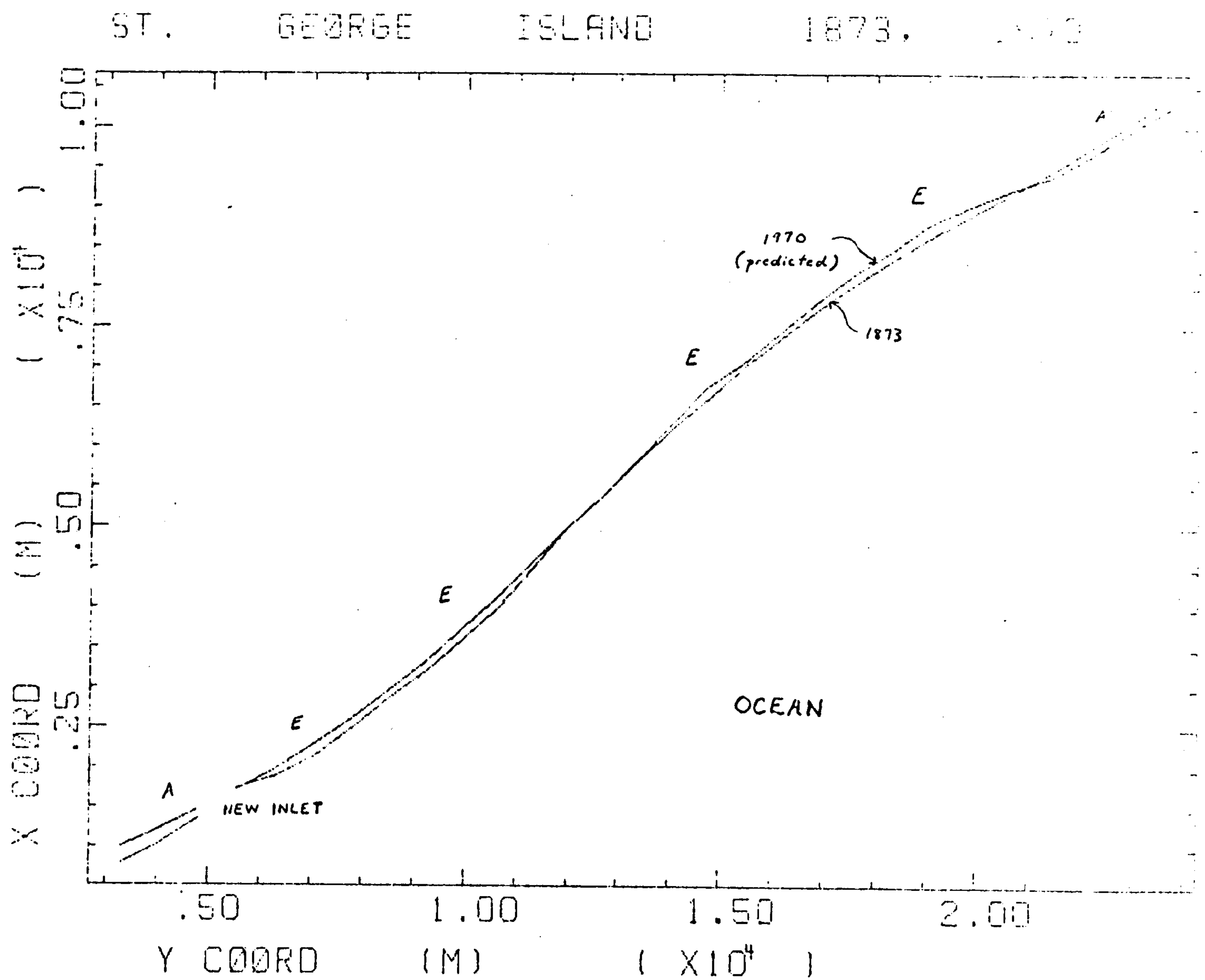

Figure 14. Northeast St. George Island as recorded in 1873 and 1970.

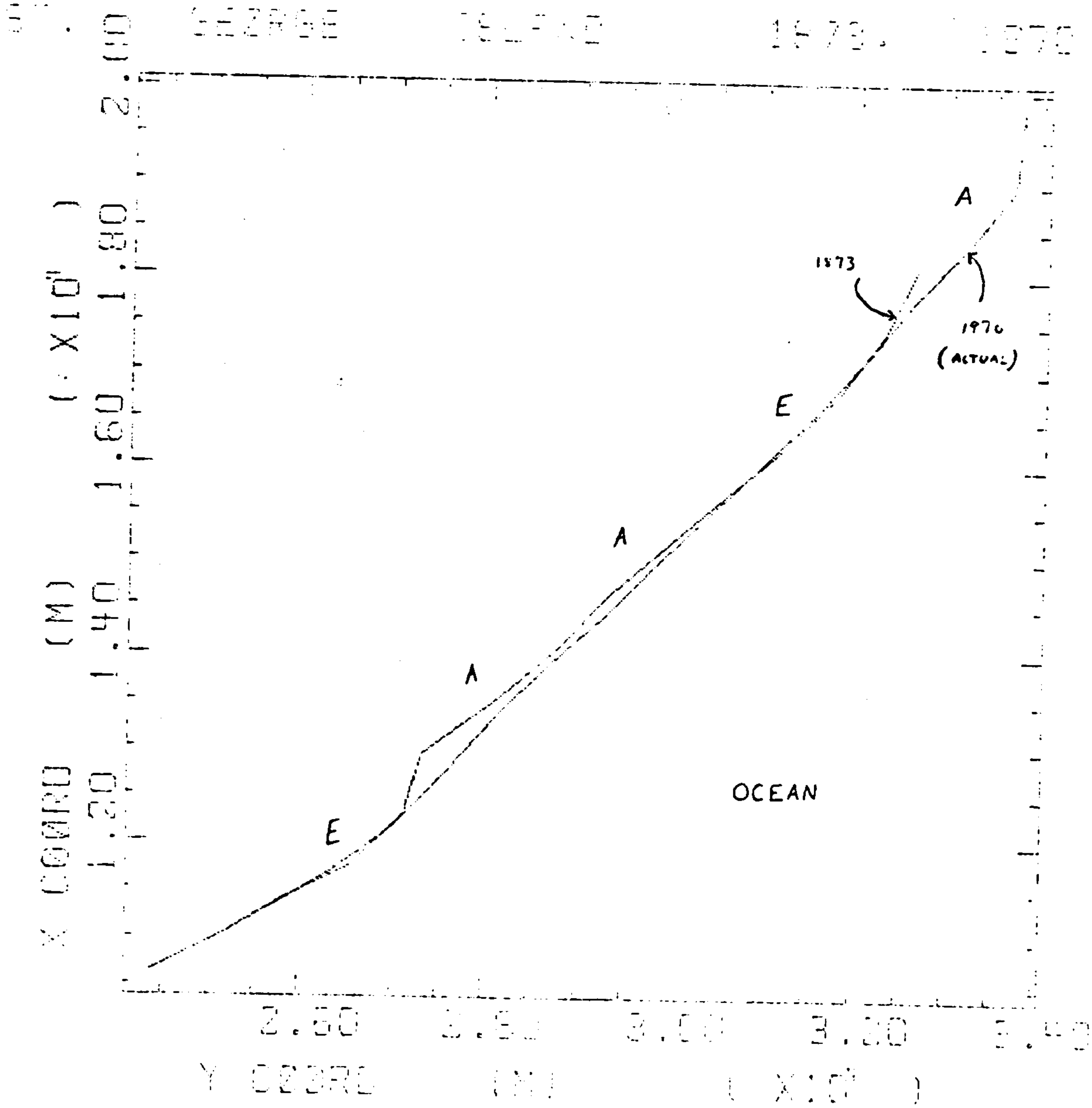

Figure 15. A comparison of northeast St. George Island in 1873 and 1970 (predicted).

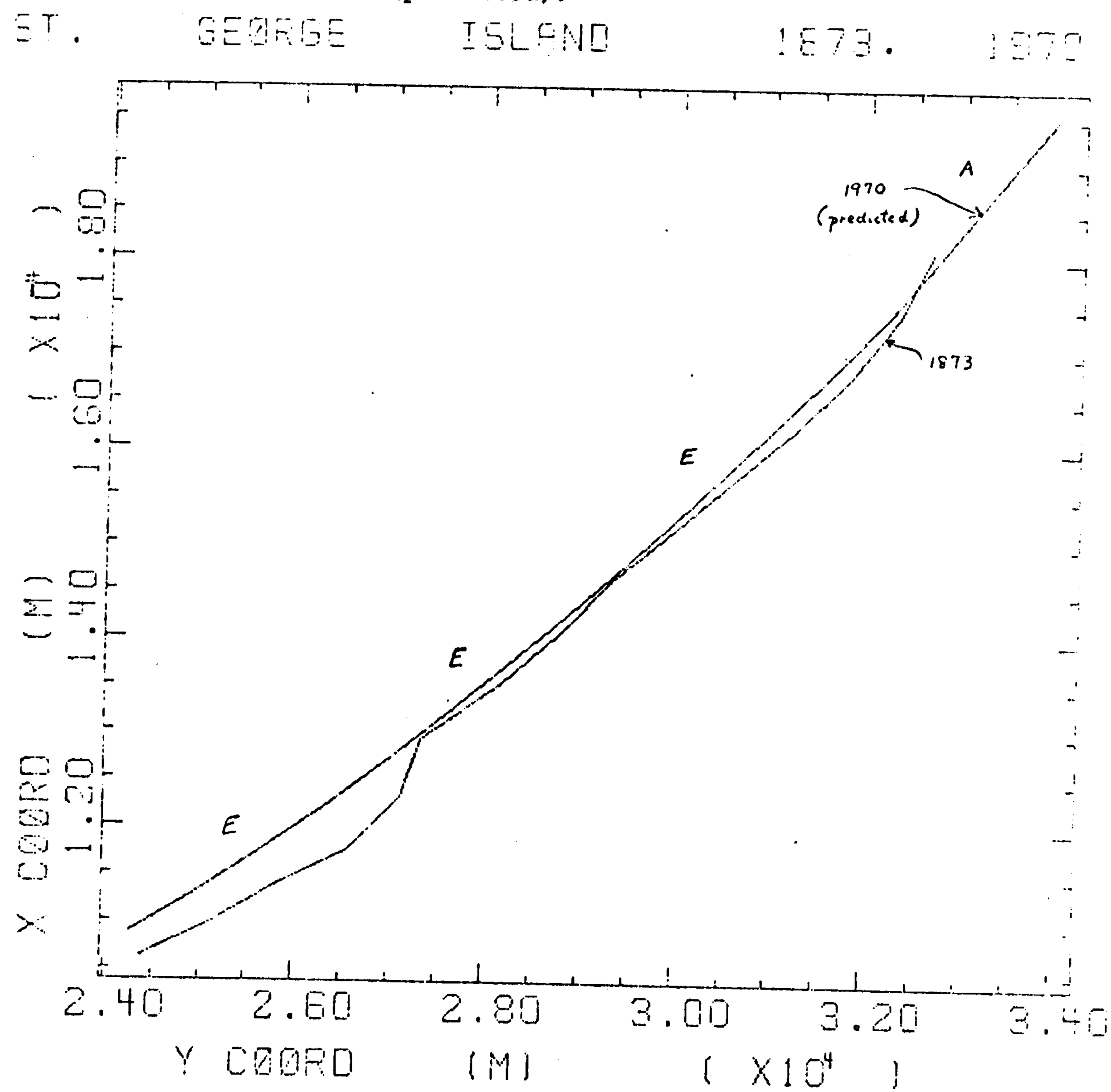

and volume of sediment transport. By subtracting isobaths as given on old and new boat sheets and contouring the results Stapor was able to compute and approximate sand budget for St. George Island and adjacent areas over a 70-80 year period.

The salient differences between the actual plan profiles of 1970 and those of 1873 (Figures 10,12,14) are:

1. The Cape St. George area undergoes a lateral shift of its strandline to the north and west, i.e., there is erosion to the east of the Cape and accretion to the west. The northwest tip of the island is cut back slightly. Sand Island Pass is closed. These features are confirmed by Stapor's computations as seen in Figures 16 and 17, where, in addition, sand deposition is observed on the East Bank and the Cape St. George Shoals. Our predictions (Figure 11) show the same trends as Figure 10 with the exception of the inlet closure (note: since we have not modelled the inlet dynamics it is not expected that the mouth of the inlet will enlarge, diminish, or migrate appreciably.

2. The long, middle section of the island, over most of its length, experiences erosion (Figure 12). Stapor (Figure 18) indicates a sand transport direction away from the concave middle: $76 \times 10^3\ m^3/yr$ to the southwest and $60 \times 10^3\ m^3/yr$ to the northeast. By expanding our concept of 'control volume' to include <u>any</u> length of shoreline we can compute a net volume drift rate for a <u>particular</u> stretch of beach acted on by a <u>particular</u> wave climate. By summing over the difference between successive transport rates, i.e.,

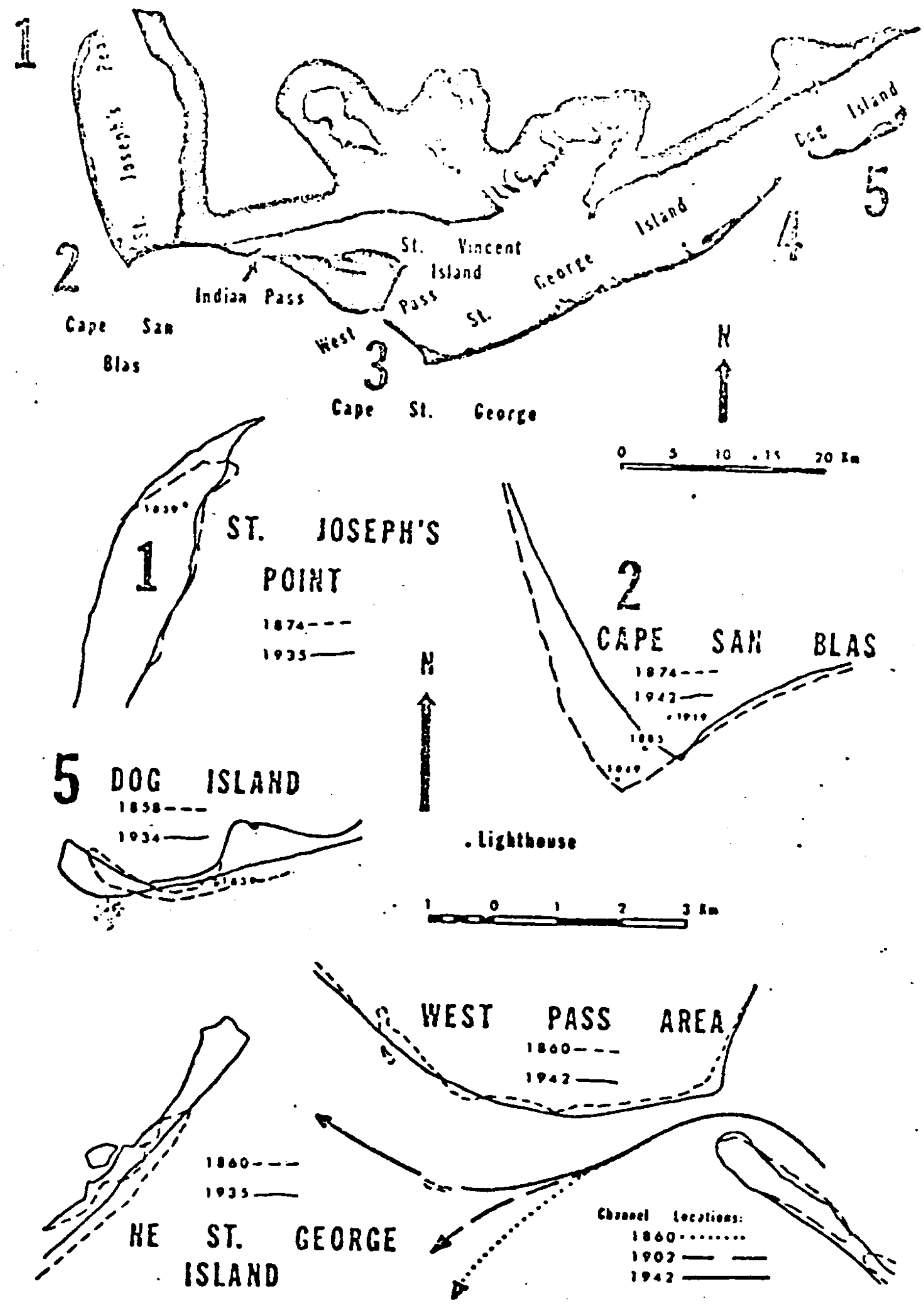

Figure 16. Shoreline changes, Apalachicola Bay (Stapor 1971)

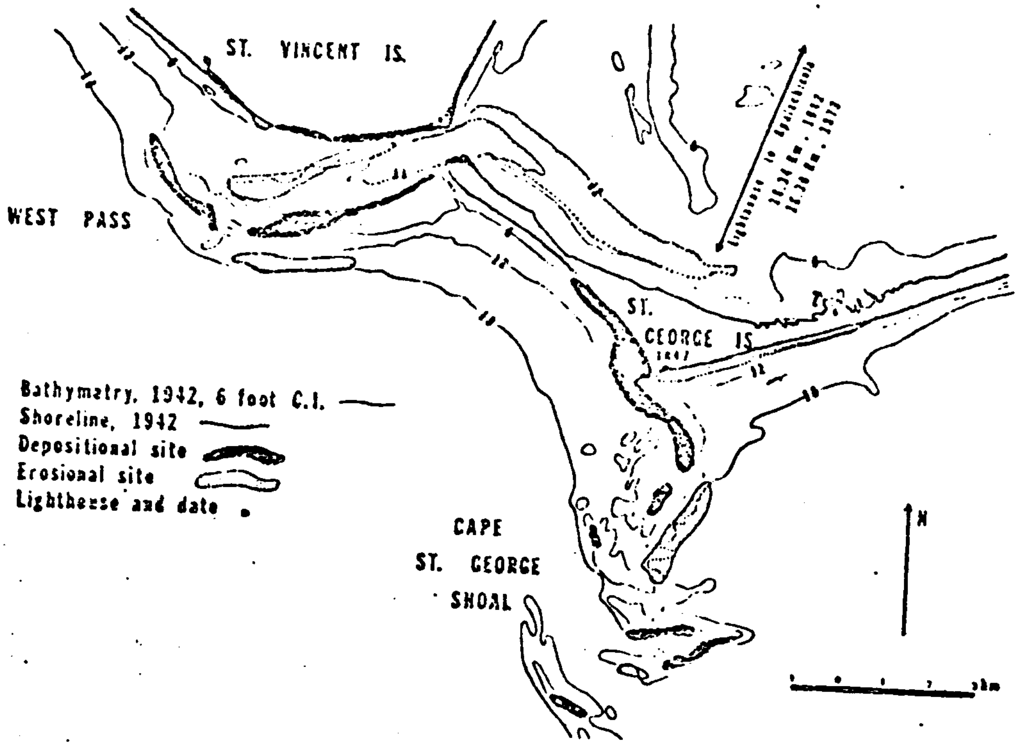

Figure 17. Erosion and deposition patterns, West Pass Area (Stapor 1971).

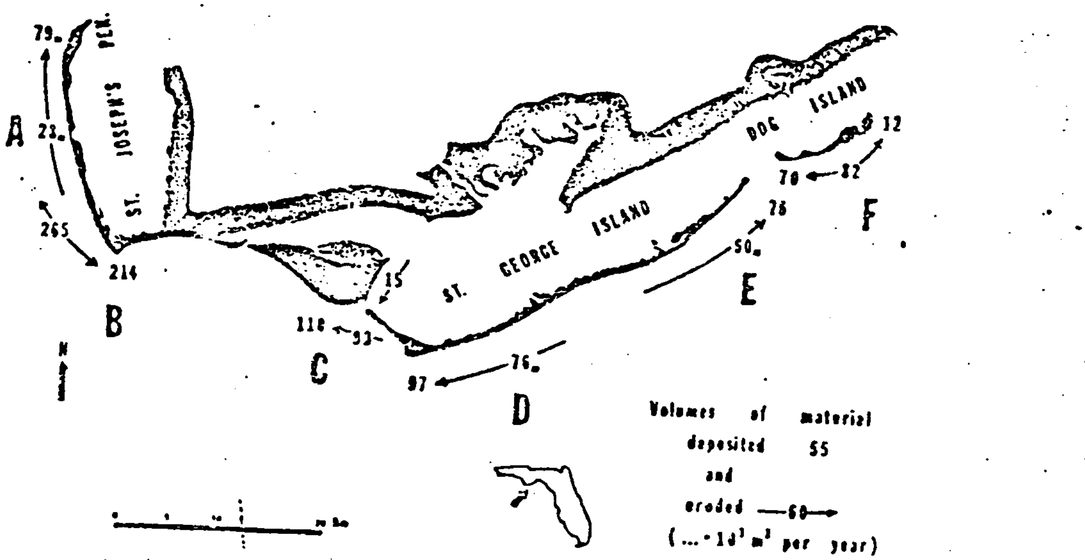

Figure 18. Transport figures for St. George Island and adjacent coastline (Stapor 1971).

$$\sum_{i=n_1}^{i=n_2} \left(Q_i - Q_{i-1} \right) \tag{53}$$

(see SUBROUTINE ADJUST in computer program), for our range of wave parameters, we obtain figures, corresponding to Stapor's, of 4-25 m^3/hour (approximately 35 x 10^3 - 220 x 10^3 m^3/year). Figure 13 displays an overall erosive pattern but differs from Figure 12 in the degree of shoreline retreat and the position of maximum change.

3. According to Figures 14 and 16 the northeast end of the island has been growing (a spit-like feature). Figure 14 indicates that areas adjacent to the expanding tip have advanced seaward interrupted only by a few smaller pockets of erosion. Figure 15 predicts a substantial growth at the endpoint although not the eventual sharp veering to the north (away from the dominant direction of wave approach) seen in Figure 14. In addition the prediction shows the shoreline being cut back along the entire stretch of beach upstream of the endpoint, i.e., the tip of the island is being fed sand from nearby beaches as well as from the island's middle section. This contrasts with Figure 14 which shows the middle section to be the major contributor of sand.

Because the wave data is averaged on an annual basis and extraordinary wave conditions (e.g., hurricane-produced) are filtered out it is not expected that future trends will differ significantly from those occurring in the past. Using the observed strandline of 1970 the nearshore wave field is re-computed and a 20-year projection is made. The results (Figures 19,20,21) exhibit patterns similar to those computed before, such as the erosion of the concave middle, which makes it susceptible to breaching. The exception is the northeast tip of the island which now turns inward as well as prograding northward, i.e., the beach reacts to the incident waves in such a way as to minimize their erosive effects. In the presence of an ample sand supply and low wave energy it is unlikely that the end of the island will curl in appreciably; rather, its excursions in a westerly direction should be intermittent, being counteracted by sand deposits sufficient to direct the tip's advance to the north and east. Figure 21 again points to erosion immediately upstream of the tip with accretion farther west.

The foregoing predictions in most cases are in reasonable agreement qualitatively with observed strandline changes. For the results to be more pleasing quantitatively certain improvements are obvious: (1) the quality of the wave observations could be enhanced by *in situ* recording of swell *and* local sea (shallow water wave generation is not accounted for in this study); (2) rather than considering the depth contours to be straight and parallel offshore of each beach segment, a formal refraction analysis using the actual bathymetry should lead to better forecasting of nearshore wave conditions; (3) an attempt could be made to model the effects of severe storms (hurricanes). Strictly speaking, this falls outside the outline of the present report

Figure 19. Southwest St. George Island, 1970 and 1990 (predicted).

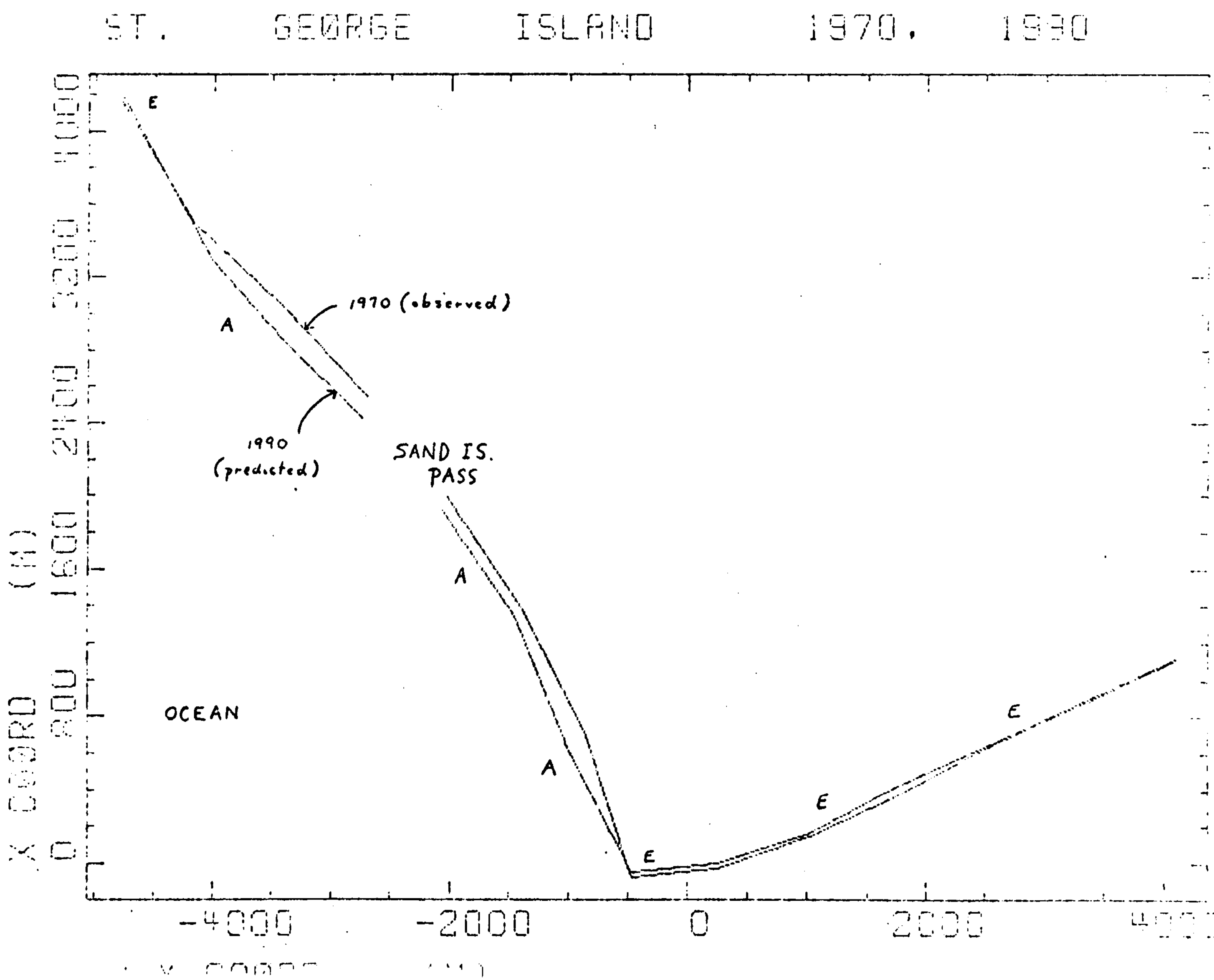

Figure 20. Middle section of St. George Island, 1970 and 1990 (predicted).

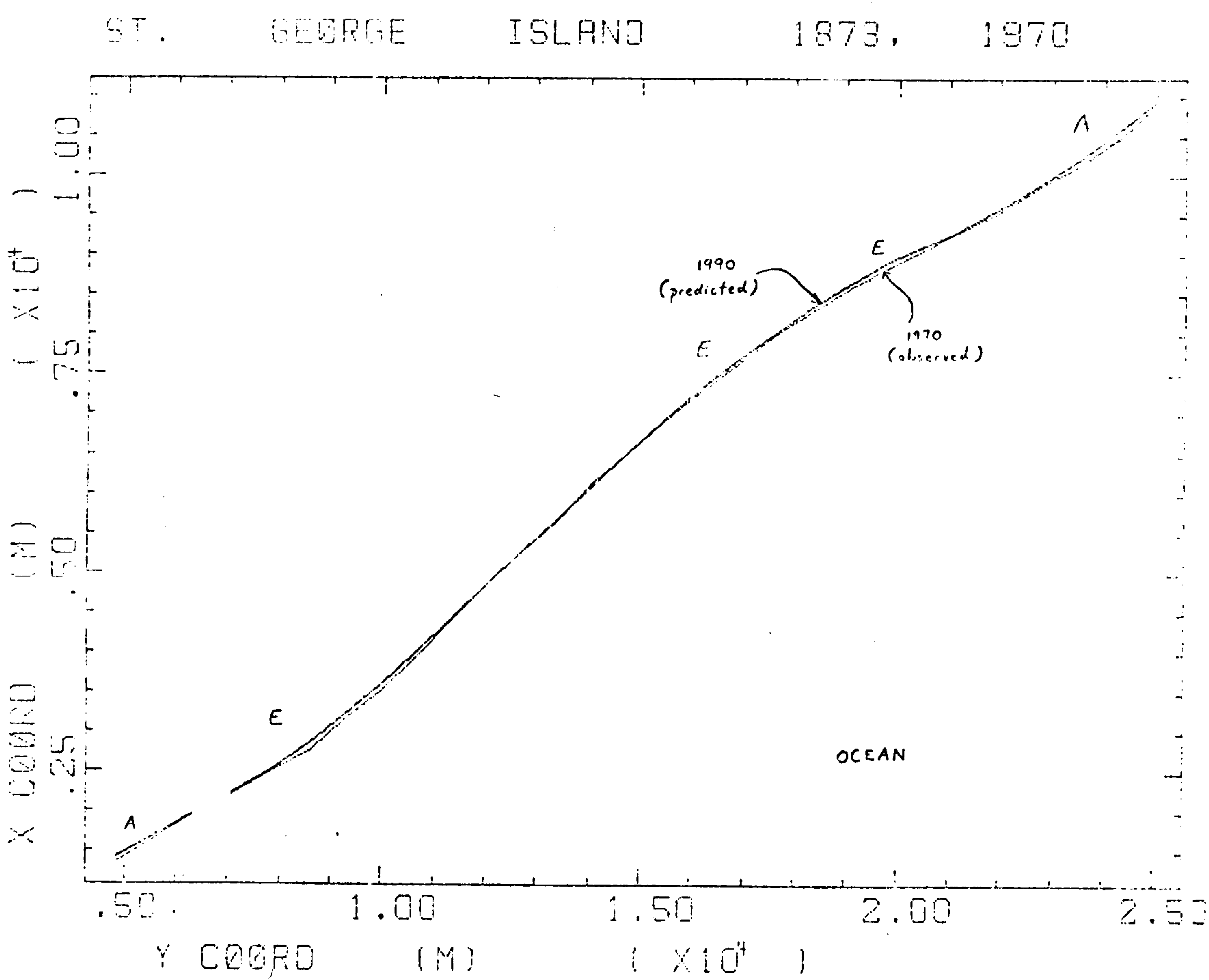

Figure 21. Northeast St. George Island, 1970 and 1990 (predicted).

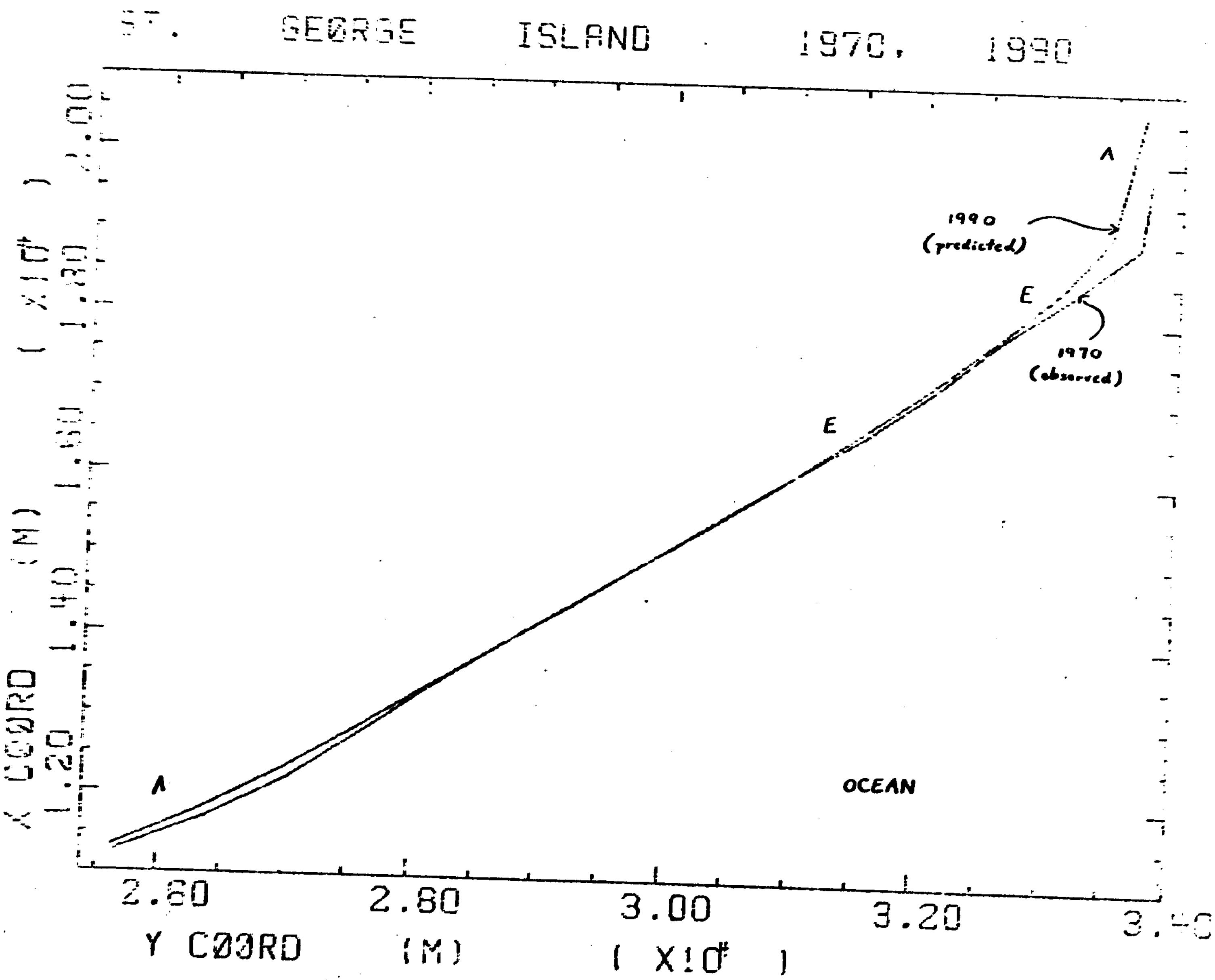

because longshore drift would then only be one of the important components of motion--the offshore-onshore movement of sediment associated with high water levels and high waves would be very significant. The present model could be used to monitor a beach after it has incurred heavy damage to ascertain what contribution the longshore transport makes to restoration.

In addition, for a coastal region with complex endpoint boundary conditions (e.g., islands, spits, capes, penisulas) a packing of the beach points at the ends is advantageous if it is accompanied by a finer resolution of the wave field. Since nearshore wave measurements are usually lacking this would have to be accomplished by more careful refraction and diffraction analyses. The diffraction analysis could be based on experimental data or be an approximation to the existing mathematical theory for ideally shaped barriers. Furthermore, in such regions where there is sharp curvature of the wavefront the longshore gradients in the breaker wave amplitude and incident angle may drive a non-negligible longshore current. Shoreline change is often manifested most dramatically at endpoints; this dictates that we treat these boundaries in special ways.

VIII. Jupiter Island

The Jupiter Island phase of this research was undertaken in cooperation with the Coastal Engineering Laboratory of the University of Florida. Jupiter Island, about 15 miles north of West Palm Beach, is the site of a recent beach restoration project.

During its duration wave, wind, and beach profile data were recorded by a University of Florida contingent. Figure 22 shows the island bordered on the north by St. Lucie Inlet and on the south by Jupiter Inlet. The project limits are marked. Figure 23 is a photograph of the construction site and Figure 24 a diagram of the beach nourishment area showing the location of the sand fill which is placed on alternate sides of the public beach. Its movement and redistribution within the project limits is monitored by beach profiling (a sample is shown in Figure 25).

The wave height and period are recorded at only one point along the beach in 20 feet of water. The breaker angle, in the absence of more than one wave pressure sensor for directional resolution, is logged visually at approximately the same longshore site. Shore-normal profiles of the beach are taken before the placement of the fill, at the time of fill, and from 6 months to 1 year afterward at varying points along the beach.

In this study we have the benefit of *in situ* wave observations, albeit at one point, and finer bathymetric data. In order to generate the necessary longshore breaker data we employ a refraction program (Dobson, 1967) and, by working outward from the position of the one wave guage, a deep-water wave climate is established. The details of such an approach are contained in Mogel, *et al.* (1970). Suffice it to say, a fan of wave rays of different periods is tracked seaward from this one nearshore point across a bathymetry which is represented by a fine inner grid of depth points and a larger coarse outer grid. The inner grid width is determined by the longshore distance

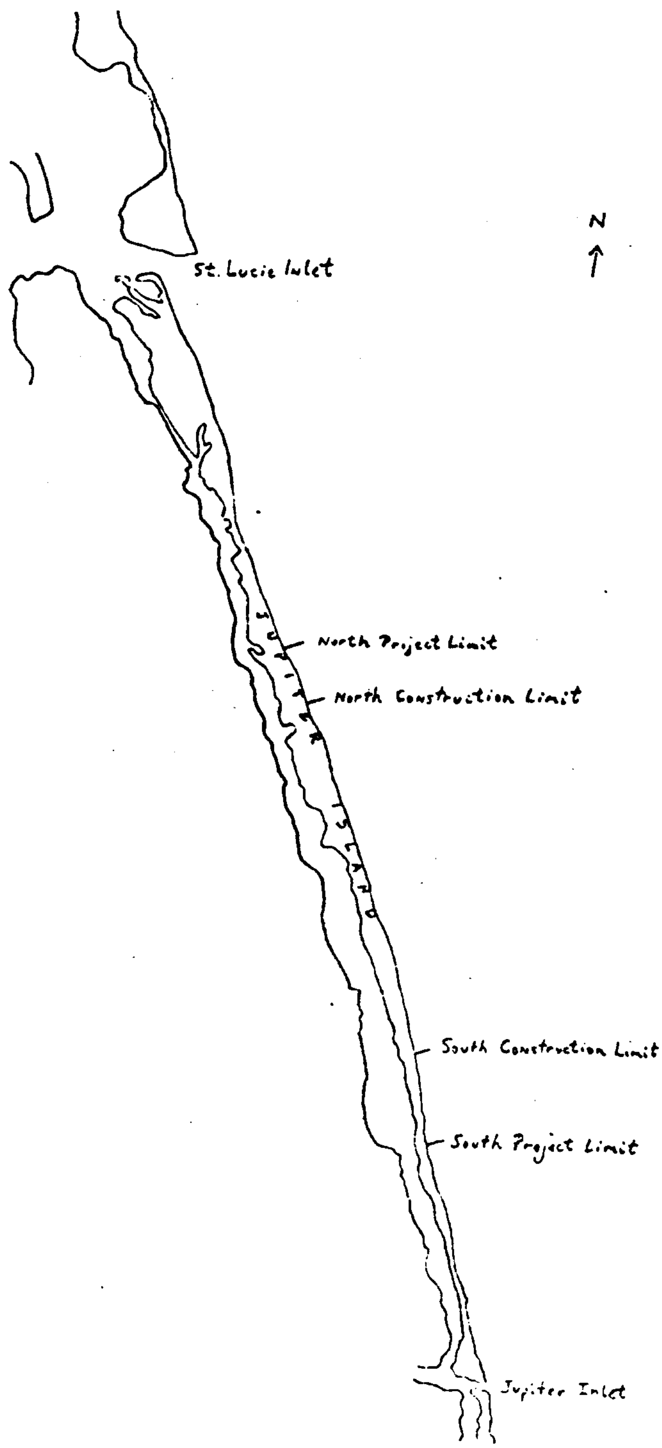

Figure 22. Jupiter Island.

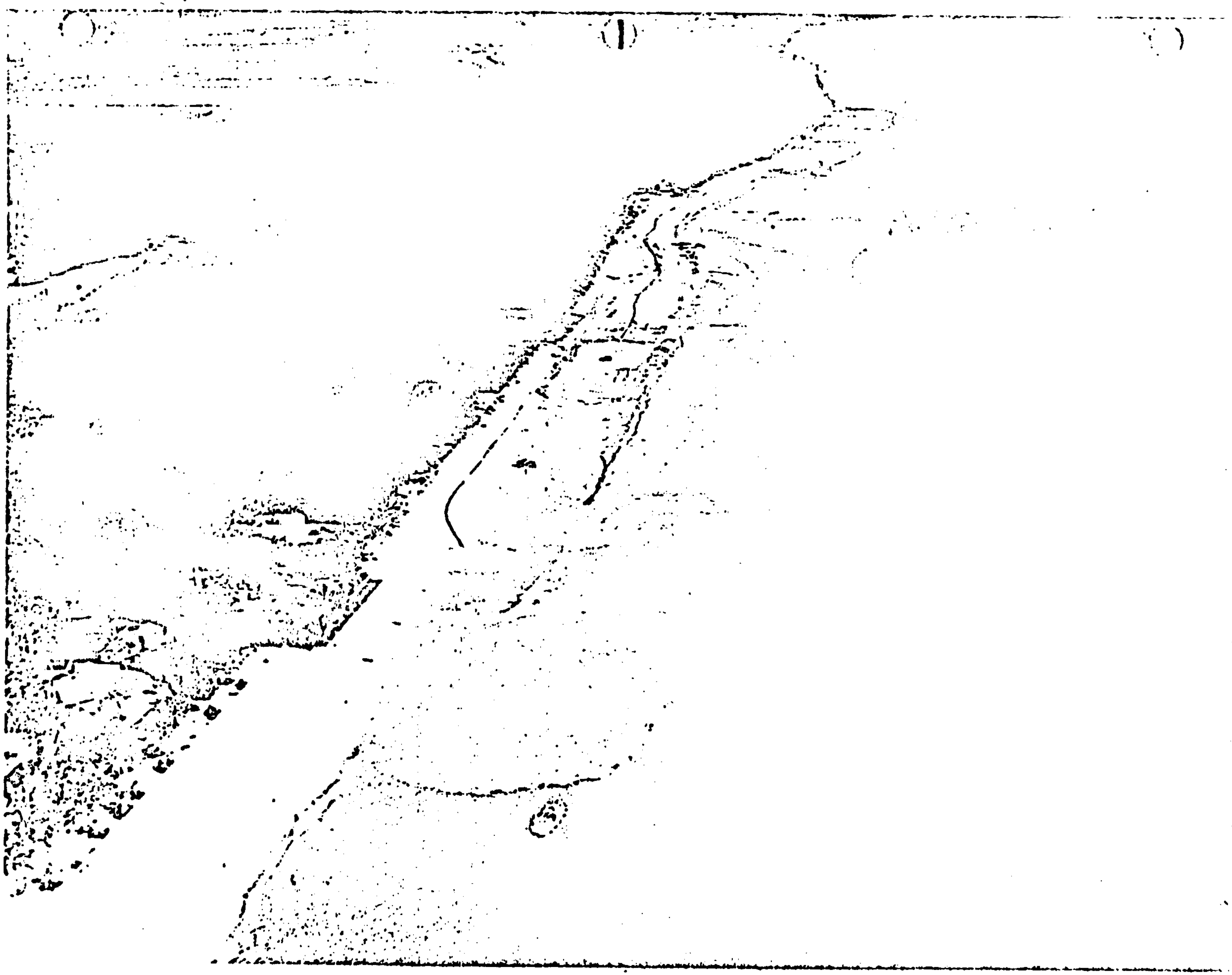

Figure 23. An aerial photograph of the fill area, Jupiter Island.

Figure 24. Dates and longshore extent of beach fill.

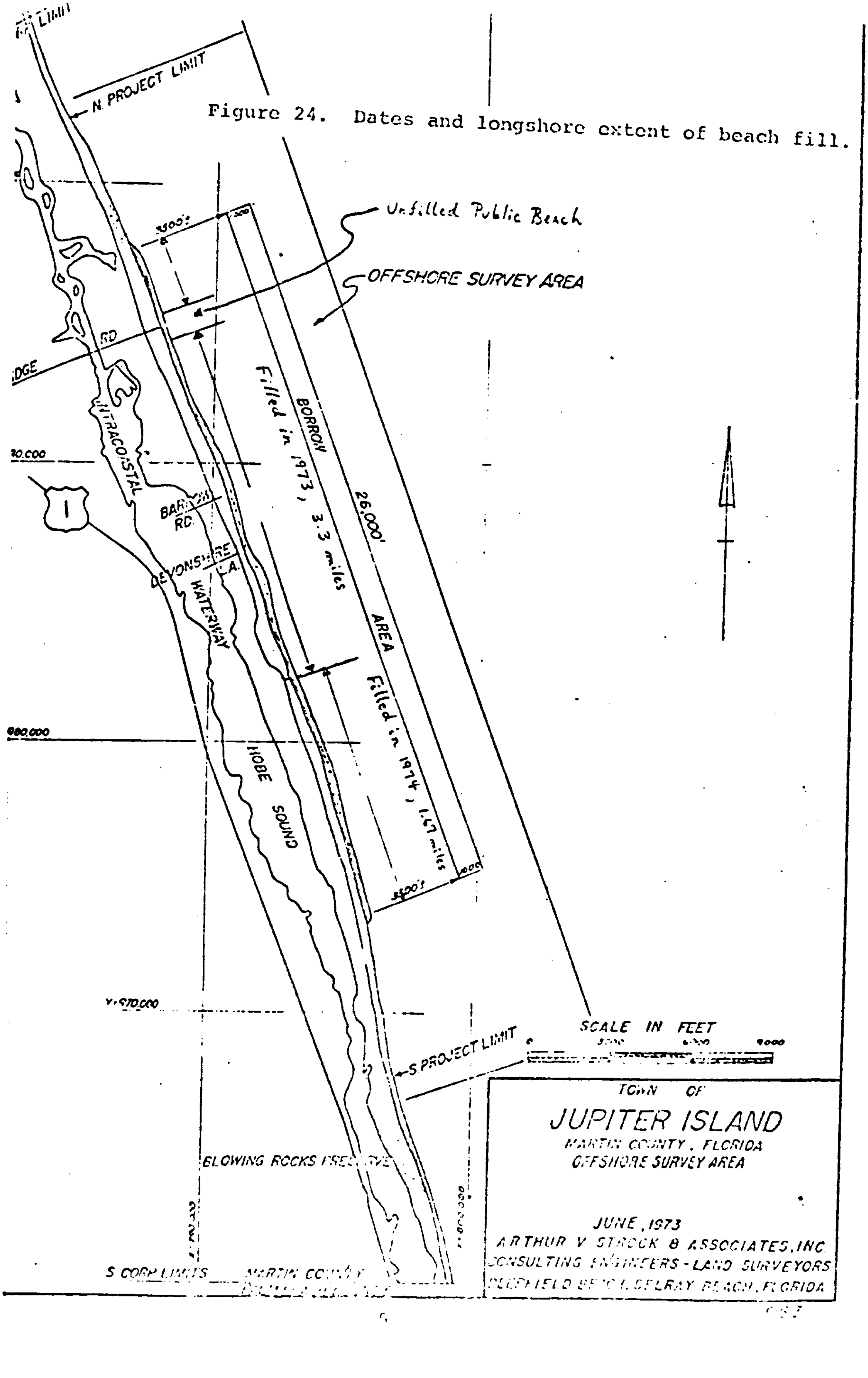

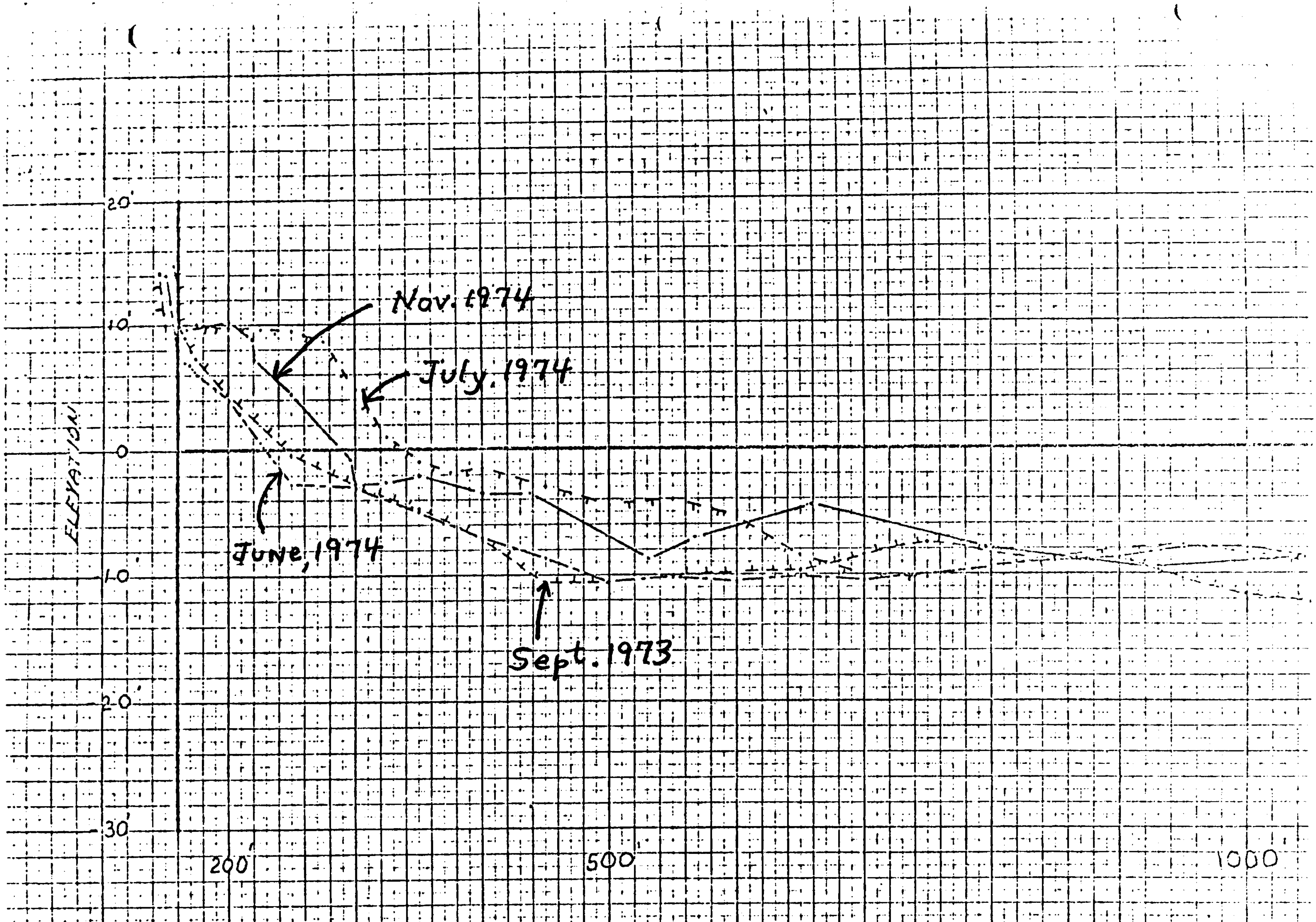

Figure 25. A sample of a set of beach profiles at one location.

between the transverse beach profiles as recorded in the field (400 feet); these profiles extend to about a 30 foot depth, this contour marking the outer limit of the inner grid. The outer grid has a width of 2500 feet. The resulting deep-water wave field serves, subsequently, as initial data (wave periods and directions) for a refraction analysis. By packing the wave rays densely we recover, for each wave type, the longshore distribution of H_b and ϕ_b at longshore intervals of about 400 feet.

The beach points defining the strandline coincide with the profile locations which number 94, spanning the distance from the north project limit to the south project limit. A coordinate system is established with its origin slightly north of the north project limit; the y-axis runs due south, the x-axis due east. All profile lines are 67.3° south of north. The lateral shift in the mean still water line as evidenced in the beach profiles is assumed to be indicative of erosion or accretion (a note for emphasis: in this report the terms 'erosion' and 'accretion' are synonymous with shoreline retreat and advance, respectively; a stricter approach would treat the sediment distribution normal to shore from the berm plateau to some maximum depth of wave influence, e.g., 30 feet--that is, local accretion may not necessarily be accompanied by a prograding shoreline and vice-versa).

The history of the nourishment project is indicated in Figure 24. In the summer of 1973 approximately 2.4 million cubic yards of fill was placed on a 3.3 mile stretch of shoreline; with the exclusion of the public beach. Profiles were recorded prior to this fill, at the time of fill and in May-June, 1974 just before the second fill of 1 million cubic yards covering 1.67 miles. A subsequent profile was taken in November, 1974. The fill area extends 5.0 miles along the beach, the study area 6.82 miles.

The period of wave record is marked by abnormally low wave energy levels. During the winter when storm waves from the northeast would be expected to enter the study area the maximum breaking waves rarely exceeded 5 feet in height. The predominant direction of wave approach was from the northeast and east. The data is averaged on a weekly basis.

The procedure for using the numerical model parallels that for St. George Island with the following modifications and comments:

1. The step size, Δt, is set equal to 15 hours and the corrector is applied only once.

2. The endpoints lie a fair distance away from the beach fill (the region where the most rapid change is anticipated) so that the transport rate does not fluctuate markedly in magnitude nor sign within a few grid lengths of the ends. We, therefore extrapolate the directional tendency of those interior points immediately adjacent to the ends in order to derive suitable boundary conditions (note: there is no requirement that $Q = 0$ at the boundaries). If the left boundary is denoted point 1 then the 'effective' angle β_1 is

$$\beta_1 = (\theta_1 + \theta_0)/2 \qquad (54)$$

where

$$\theta_0 = \theta_1 - (\theta_2 - \theta_1) \tag{55}$$

Similarly, for the right boundary, denoted point M,

$$\beta_M = (\theta_M + \theta_{M-1}) / 2 \tag{56}$$

where

$$\theta_M = \theta_{M-1} - (\theta_{M-2} - \theta_{M-1}) \tag{57}$$

In the plots displayed the coordinate axes have been rotated 20° counterclockwise for clarity-the vertical coordinate is exaggerated with respect to the horizontal. Figure 26 shows the beach shape before the first fill and soon thereafter. Figure 27 shows the first fill profile and the beach shape at the time of the second fill. Figure 28 shows how the beach evolved from the time of the first fill to just prior to the second fill. Figure 29 is a predictive comparison for the case $K_o = 0.3$ (Figure 30 is the forecast for $K_o = 0.5$). It predicts fairly well the sites where the shoreline recedes and advances but underestimates the degree of the erosion. The answer for this discrepancy, at least partially, lies in the profiles. A volumetric analysis of the profiles (Ceylanli, University of Florida) points to a balanced sand budget for the beach system within the project limits, i.e., by considering the sand distribution to a depth of 20-25 feet it is found that there is actually a slight net gain to the system; a portion of the

Figure 26. Prefill and fill, 1973.

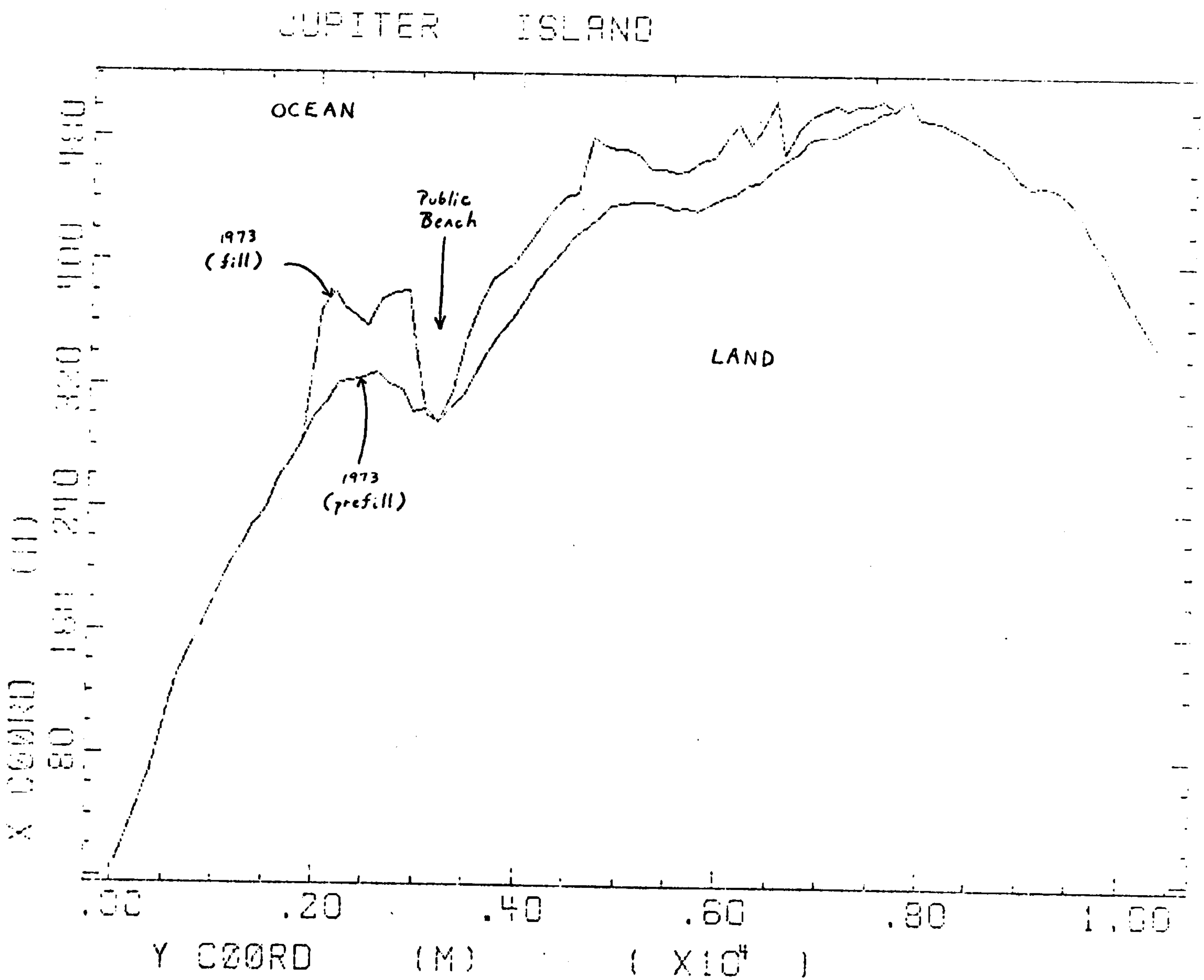

Figure 27. Fill 1973 and fill 1974.

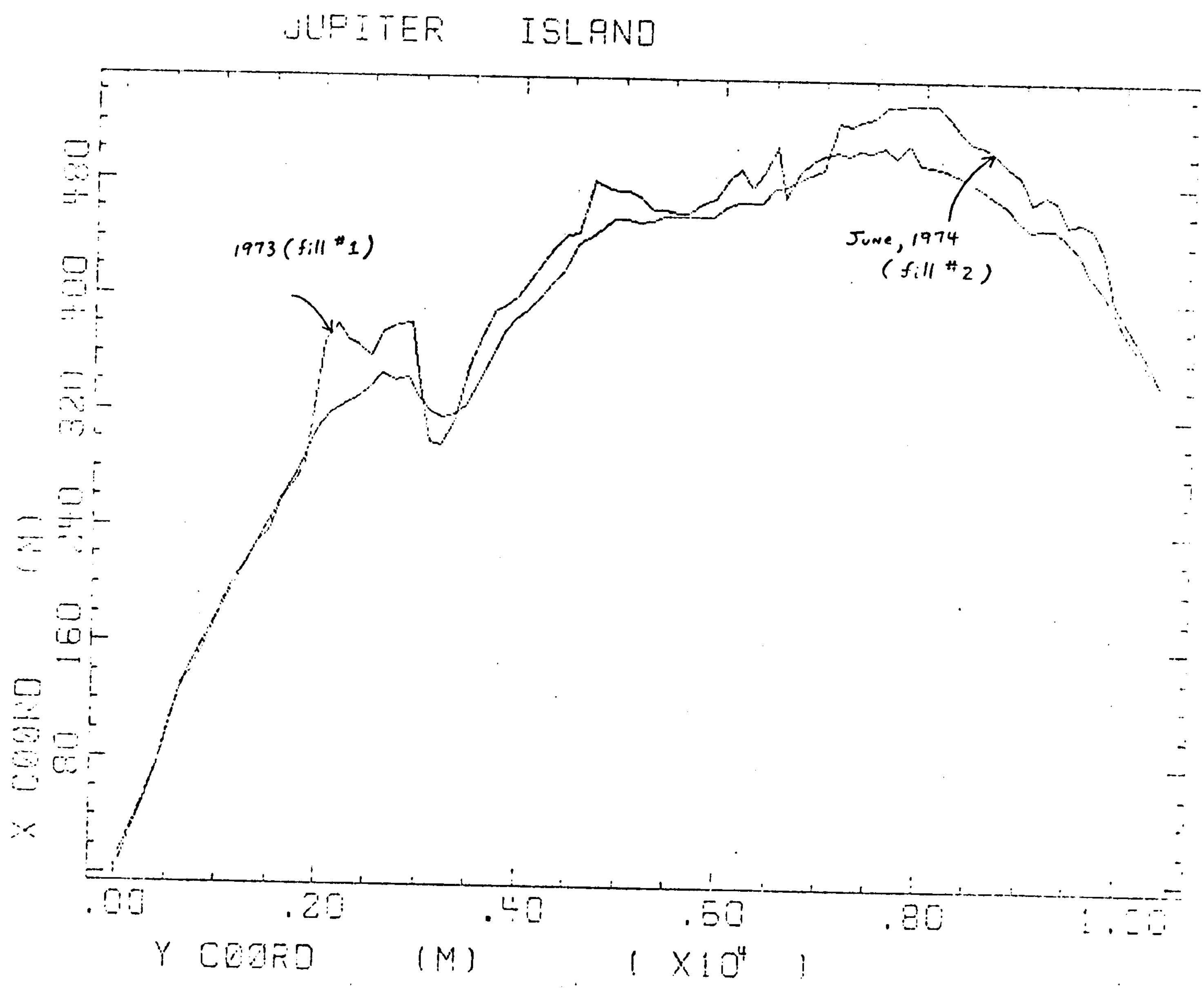

Figure 28. Development of the 1973 fill.

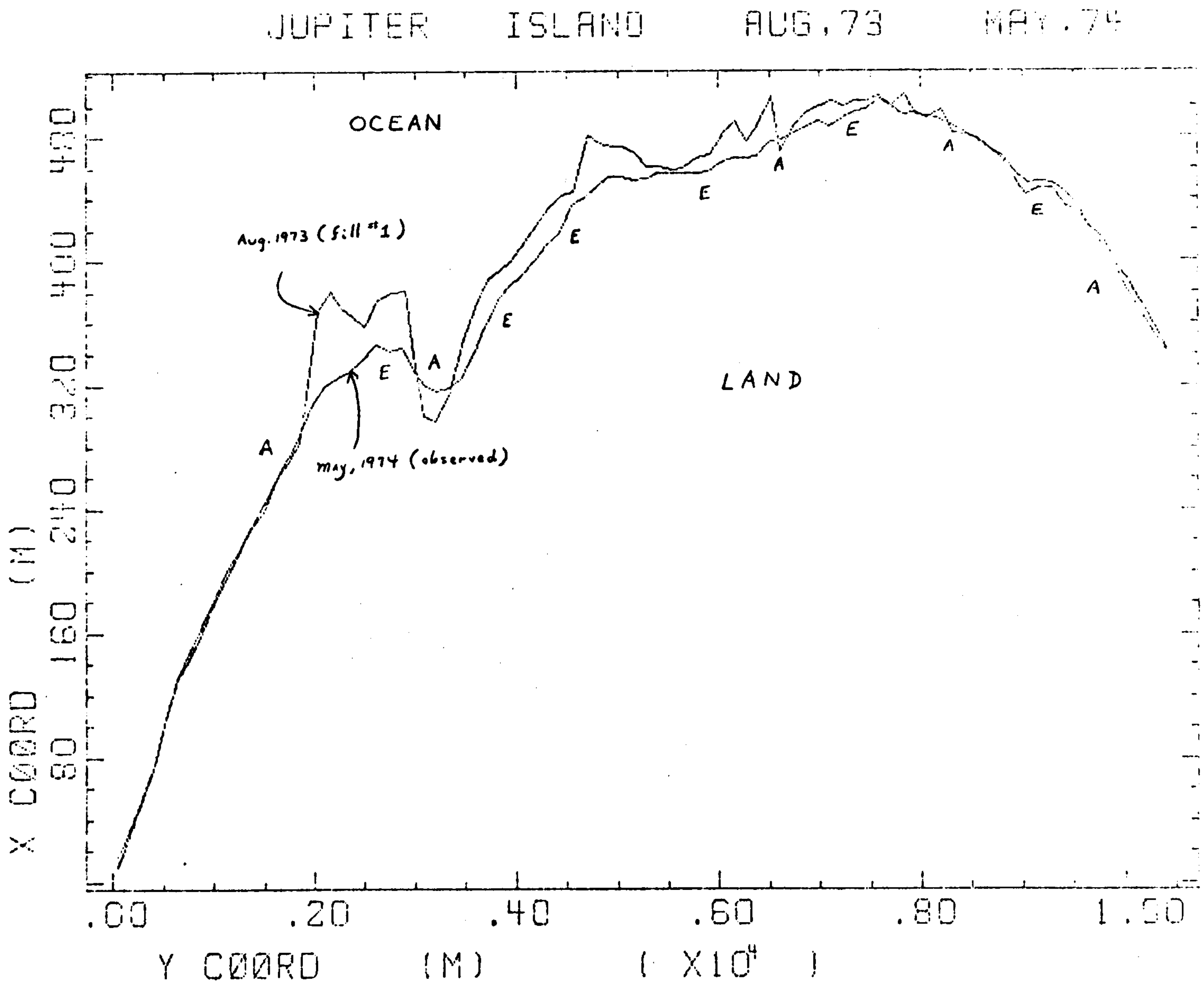

Figure 29. A prediction of the development of 1973 fill ($K_o = 0.3$).

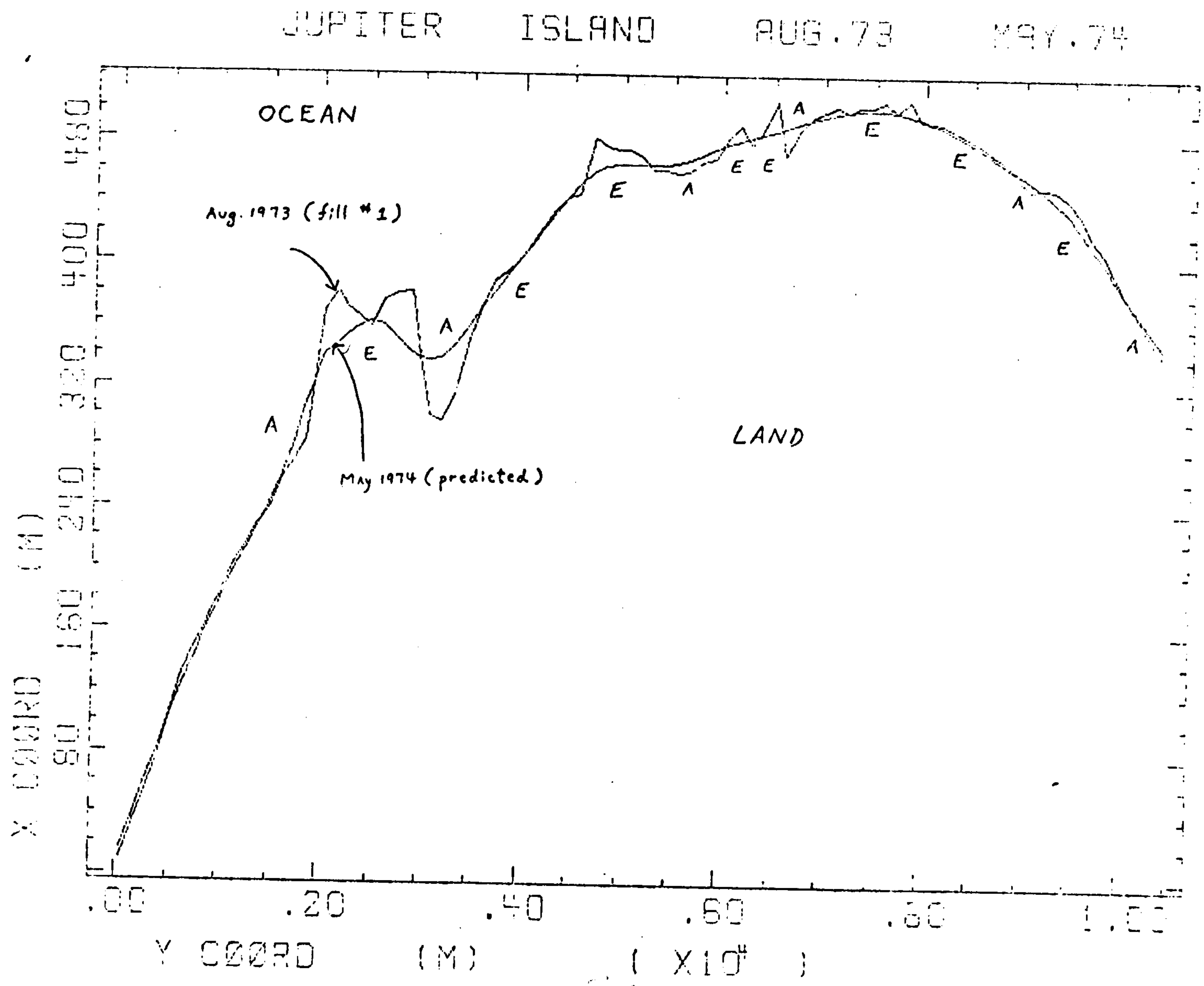

Figure 30. A prediction of the development of the 1973 fill ($K_o = 0.5$).

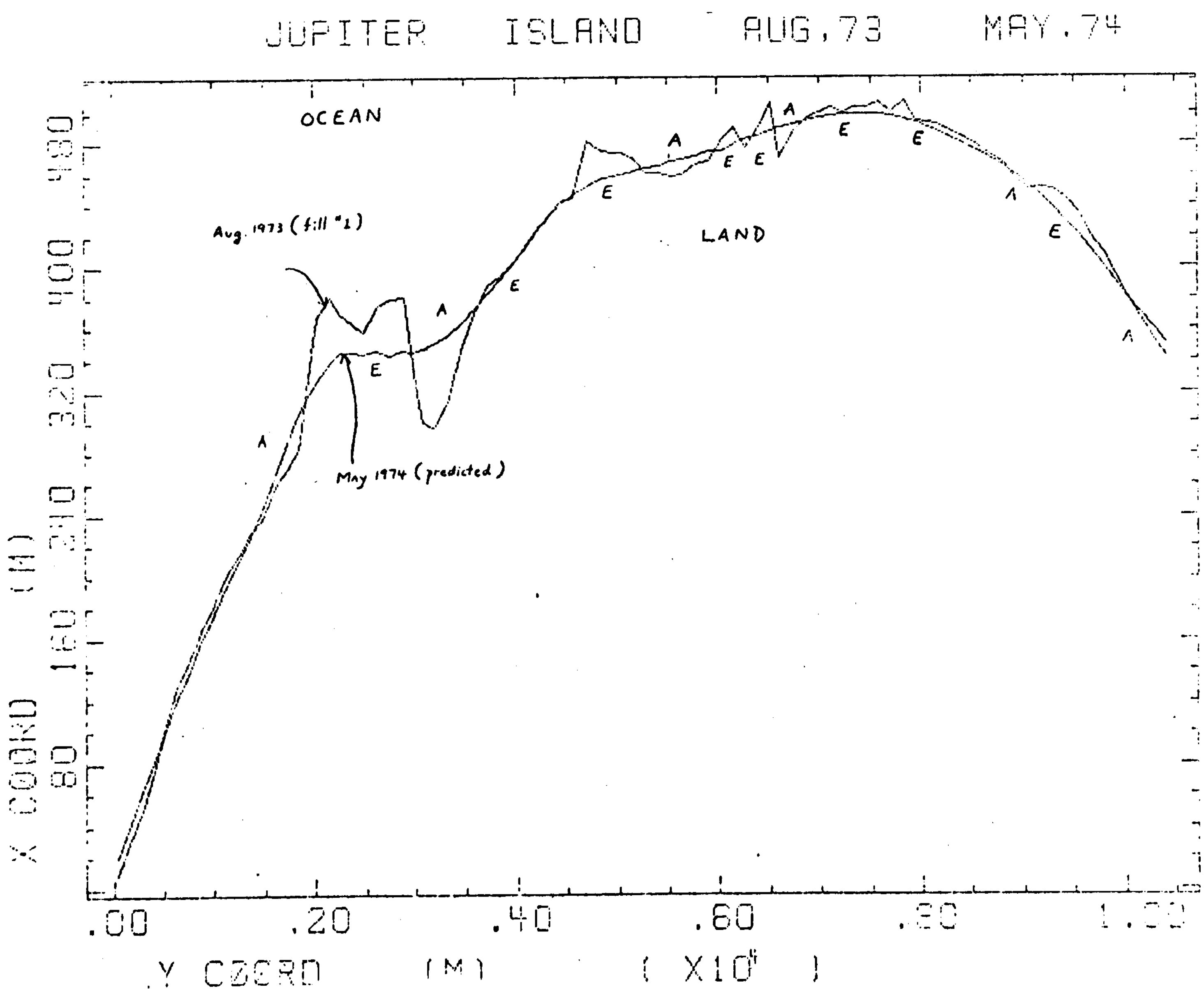

material lost from the subaerial beach (a decrease in surface area) is re-deposited in offshore shoals. Our calculation of the surface area change (see subroutine AREA in the computer program) is about 30 per cent of the actual change. The conclusion we draw is that the longshore mode, although present, is not predominant in this case.

The fate of the second fill is shown in Figure 31. The seaward protuberance that is the fill is smoothed out. However, the sand is not re-distributed along the shore to any significant degree. The beach face exhibits an overall erosive trend over most of its length - even the public beach area, which might be expected to trap some of the longshore drift, is cut back (accretion occurs only on the southern flank of the public beach). The beach system, though, remains fairly stable. A volumetric analysis points to a loss of 7×10^4 cubic meters of sand between June and November, less than 10 per cent of the volume of the second fill. Furthermore between August, 1973 and November, 1974 there was actually a small net gain of 4×10^4 cubic meters of material to the system as a whole. The prediction (Figure 32) shows the shoreline to be generally receding but at a slower rate than that recorded. The public beach is partly filled in which is contrary to observation. Again, the neglect of the onshore-offshore mode of motion is proved unjustified.

If, on an annual basis, it can be shown that there exists an equilibrium in the onshore-offshore direction then an integration over several years would be instructive. This has not been demonstrated conclusively for Jupiter Island. Figure 33 is a 5-year prediction beyond the last set of profiles of

Figure 31. Development of the 1974 fill.

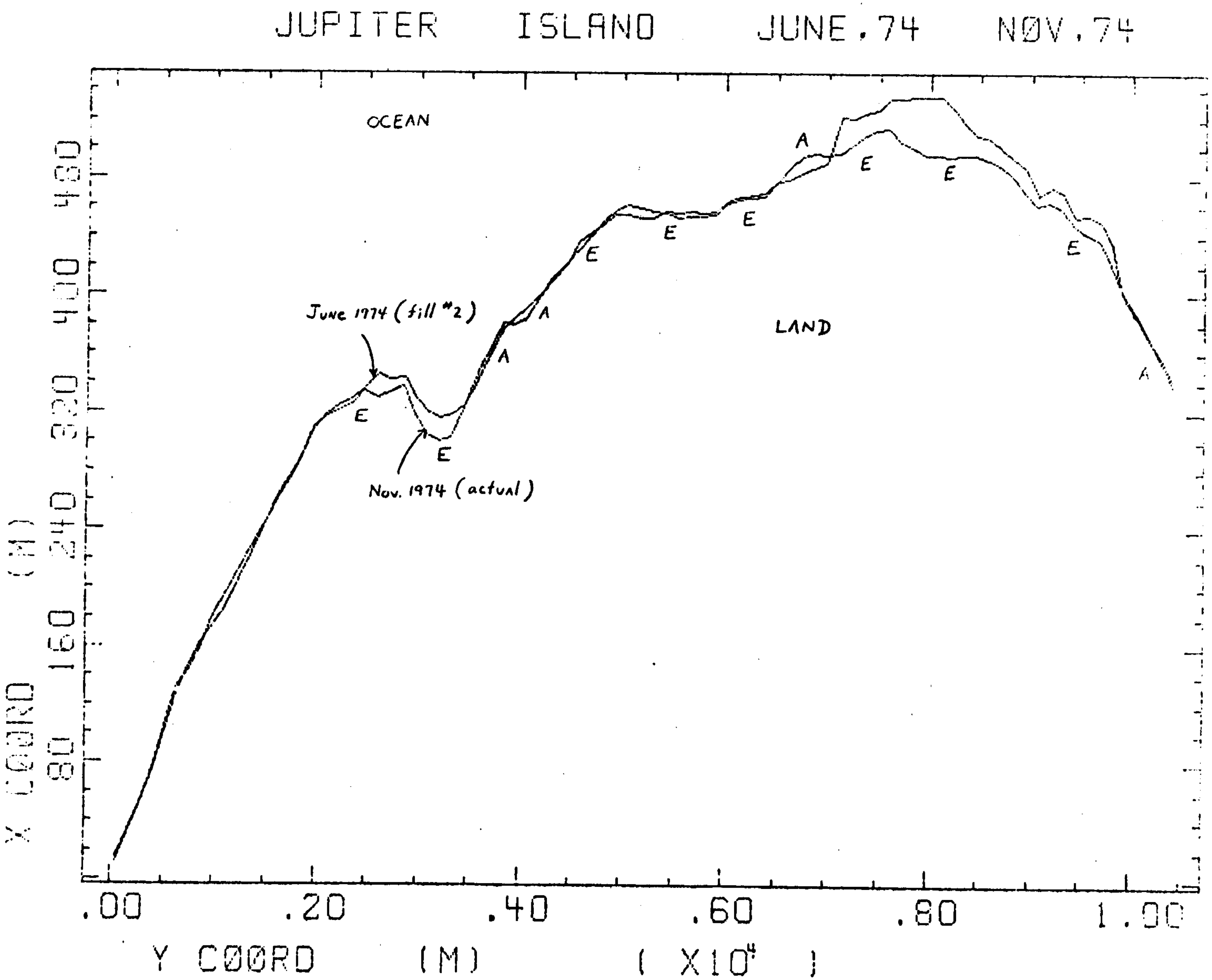

Figure 32. A prediction of the development of the 1974 fill.

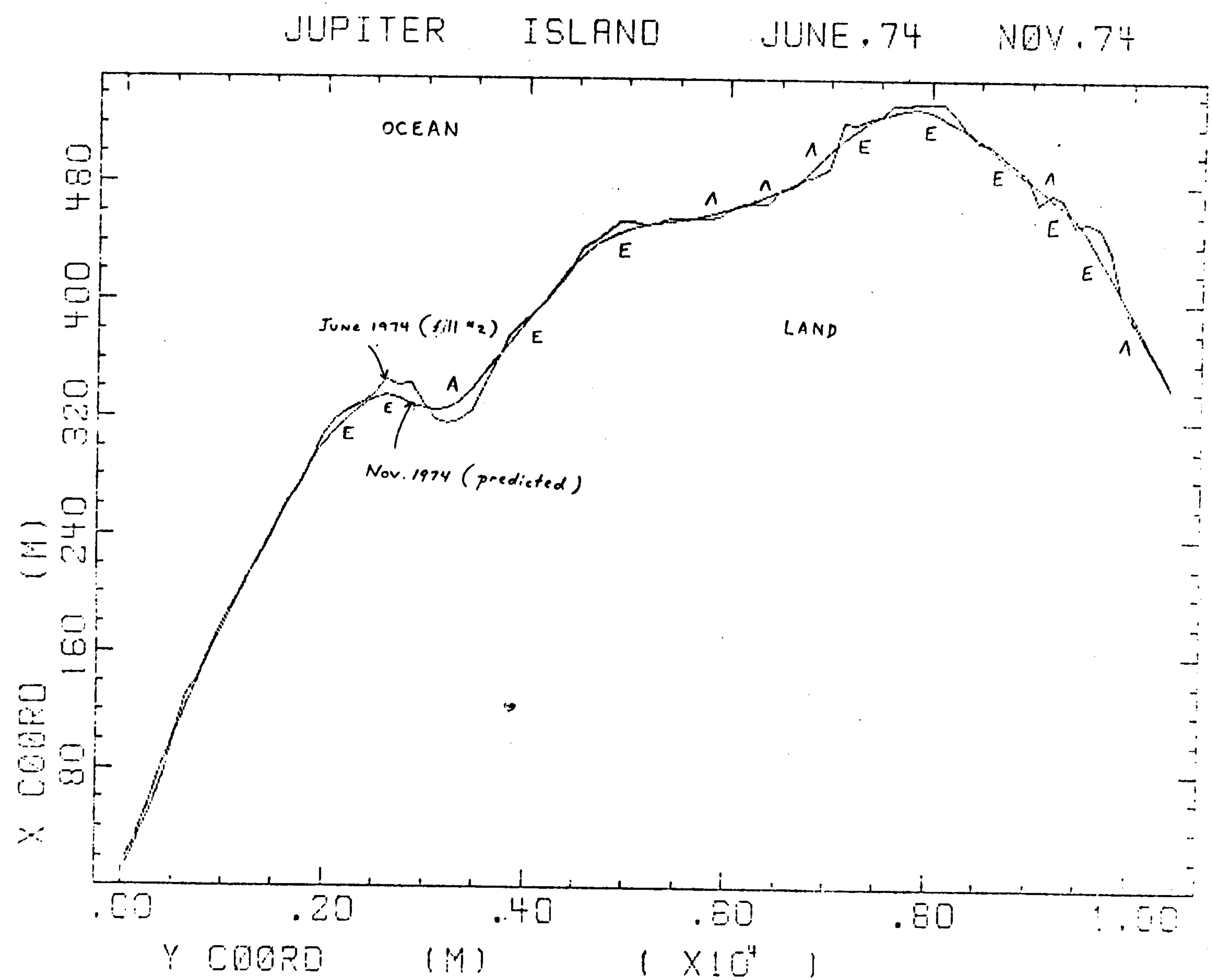

Figure 33. A 5 year prediction beyond the last profile set, November, 1974.

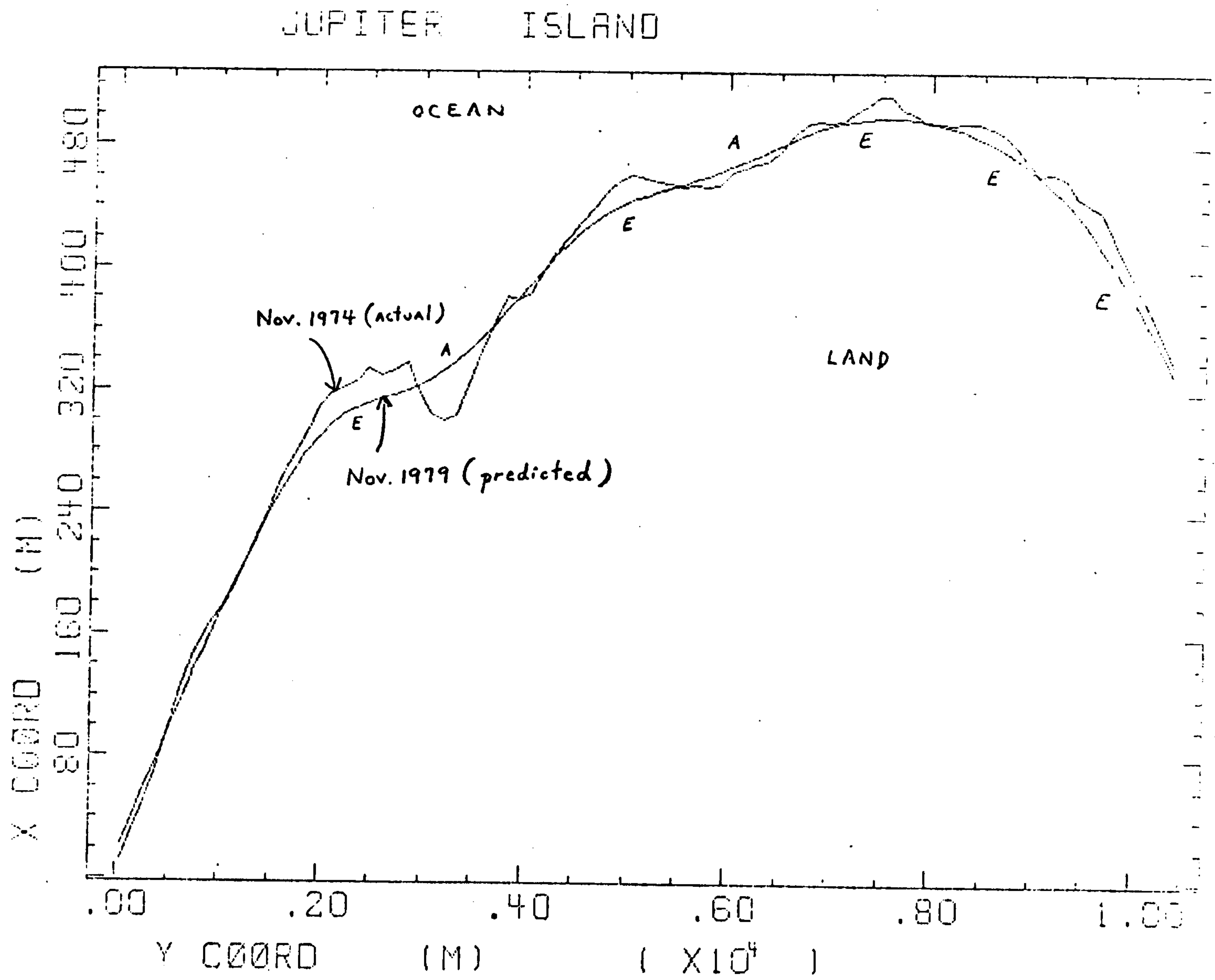

November, 1974. A loss of 5×10^4 square meters of berm area is predicted due to longshore drift out of the project limits. The loss is greater if the wave energy levels are increased (the presently recorded levels are anomalously low).

Figure 34 is a comparison of the strandline before the placement of any fill with the most recently recorded strandline position (November, 1974). Most of the shoreline undergoes a seaward advance. To be noted is the resistance of the public beach region to change. To the area of the berm has been added about 9×10^4 square meters of sediment.

A critical question which arises is whether the sand stored offshore is available for shoreward transport by natural agents. The answer lies in the compatibility of the fill material with local sand type and dynamic conditions. The movement of the fill is a function of the grain density and diameter (especially so for the suspended load) and of the wave type. A fine sand deposited on the beach may be dispersed offshore and reside there semi-permanently.

Figure 34. The Jupiter Island strandline before the placement of any fill and at the time of the final profiling(November,1974).

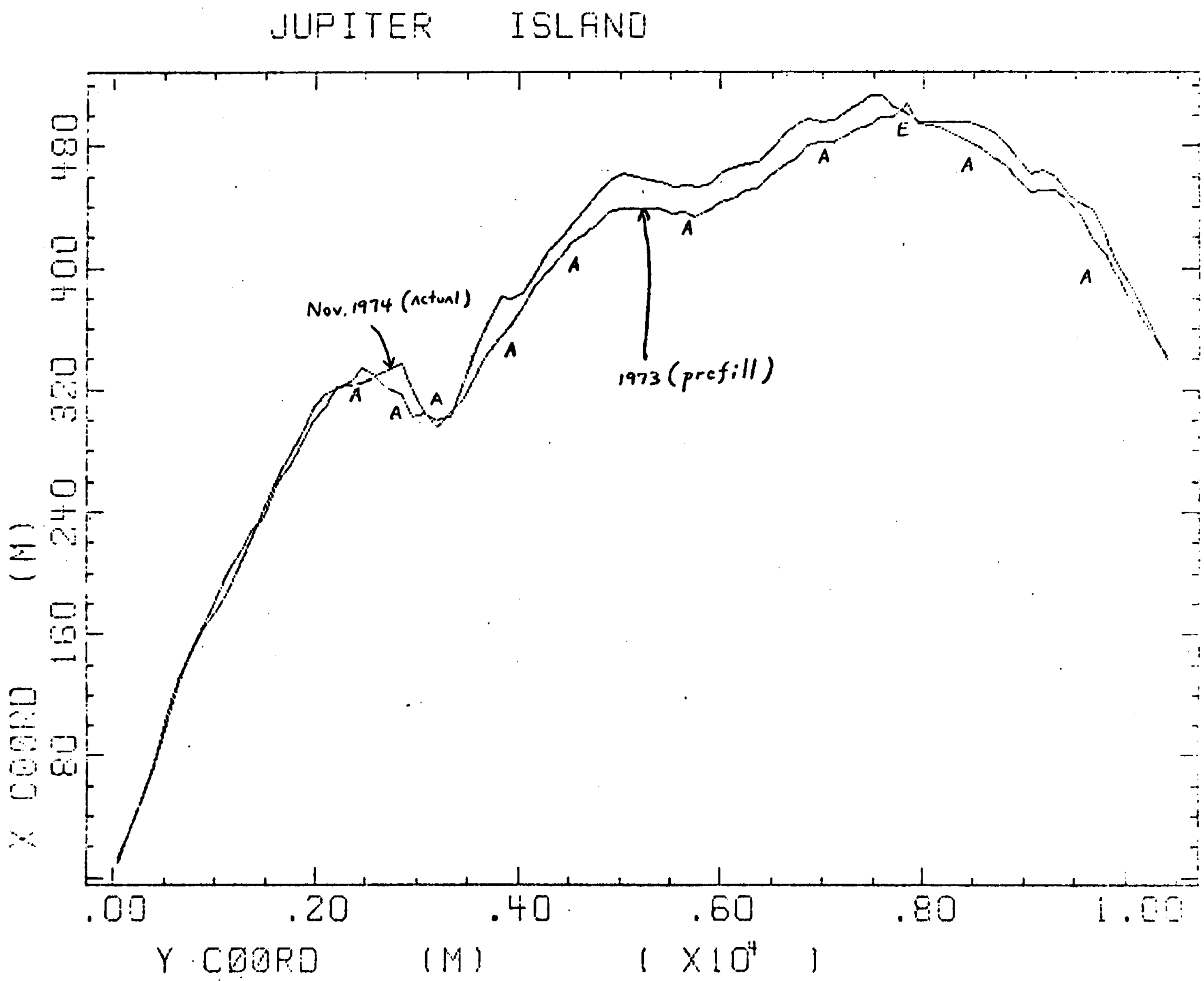

IX. Comments and Suggestions

1. Our preliminary studies indicate that a reasonable range for the coefficient, K_o, is $0.2 < K_o < 0.6$, that the uncertainty attached to it is less than an order of magnitude.

2. Our simple-minded approach, correlating differential sand transport with the lateral movement of a plane-sloping beach, has its drawbacks. In light of measurements (Goldsmith, et al., 1972) which demonstrate that migration of the strandline is not necessarily directly proportional to local sand loss or gain, as well as our experience in the Jupiter Island project, an improvement of the present model to include the onshore-offshore component of sand flow would make it more generally applicable, especially for short-term predictions.

3. It has been found that there is a critical dependence on the conditions specified on endpoint boundaries. The sediment, interior to these points, is redistributed and re-worked but its passage across the boundaries is what determines the sand budget of the beach system being examined. The nature of the boundaries points to how they should be treated. For example a jetty perpendicular to shore imposes a zero flux condition, i.e., $Q = 0$, at least until it is overtopped or bypassed by the sand flow; an open groin allows a fraction (empirical) of the sand to pass; some of the sand supplied to the tip of an island can be deposited in the sheltered lee region, in offshore shoals and/or contribute to a prograding end, a complex partioning of the available sand; etc. Because information generated on the

boundaries propagates into the interior careful attention must be paid to the endpoint conditions unique to a particular beach.

4. The present model is a viable predictor of shoreline change if the longshore mode of transport is dominant and the nearshore wave field is adequately resolved.

References

Baer, F. and T. J. Simons, Computational stability and time truncation of coupled nonlinear equations with exact solutions, Monthly Weather Review, 98, 665-679, 1970.

Bagnold, R. A., Mechanics of marine sedimentation in The Sea, edited by M. N. Hill, Vol. 3, 963 pp., Interscience Publishers, New York, 1963.

Barcilon, A. and J. Lau, A model for formation of transverse bars, J. Geophys. Res., 78, 2656-2664, 1973.

Battjes, J. A., Set-up due to irregular waves, Proc. 13th Conf. Coastal Engr., 1993-2003, 1972.

Bowen, A. J., The generation of longshore currents on a plane beach, J. Mar. Res., 27, 206-215, 1969.

Bretschneider, G. L. and R. O. Reid, Modification of wave height due to bottom friction, percolation, and refraction, Beach Erosion Board, Tech. Memo. 45, 36 pp., 1954.

Das, M. M., Longshore Sediment Transport Rates: A compilation of Data, U.S. Army Corps of Engineers, Coastal Engineering Research Center, Miscellaneous Paper No. 1-71, Sept., 1971.

_____, Suspended sediment and longshore sediment transport data review, Proc. 13th Conf. Coastal Engr., 1027-1048, 1972.

Dean, R. G., Heuristic models of sand transport in the surf zone, presented at the Conf. on Engr. Dynamics in the Surf Zone, Sydney, Australia, 1973.

_____, and T. L. Walton, Jr., Sediment transport processes in the vicinity of inlets with special reference to sand trapping, in Estuarine Research, Vol. 2, edited by L. E. Cronin, Academic Press, 1975.

Dobson, R. S., Some applications of a digital computer to hydraulic engineering problems, Tech. Rep. 80, Dept. Civ. Engr., Stanford University, 1967.

Dolan, R., Sand waves, Cape Hatteras, North Carolina, Shore and Beach, 38, 23-25, 1970.

_____, Coastal landforms: crescentic and rhythmic, Geol. Soc. of Am. Bull., 82, 177-180, 1971.

Earle, M. D., Longshore currents generated by waves with a Rayleigh wave amplitude distribution, presented at annual AGU meeting, Washington, D.C., April, 1974.

Galvin, C. J., Longshore current velocity: a review of theory and data, Rev. Geophys., 5, 287-304, 1967.

_____, Wave breaking in shallow water, in Waves on Beaches and Resulting Sediment Transport, 462 pp., Academic Press, New York, 1972.

_____, and P. S. Eagleson, Experimental study of longshore currents on a plane beach, U.S. Army Coast. Engr. Res. Center, Tech. Memo. 10, 1-80, 1965.

Goldsmith, V., J. M. Colonell, and P. N. Turbide, Forms of erosion and accretion on Cape Cod Beaches, Proc. 13th Conf. Coastal Engr., 1277-1291, 1972.

Hamming, R. W., Numerical Methods for Scientists and Engineers, McGraw-Hill, New York, 1962.

Inman, D. L., R. J. Tait, and C. E. Nordstrom, Mixing in the surf zone, J. Geophys. Res., 76, 3493-3514, 1971.

Johnson, J. W., Scale effects in hydraulic models involving wave motion, Trans. AGU, 30, 517-527, 1949.

Komar, P. D., Computer models of delta growth due to sediment input from rivers and longshore transport, Geol. Soc. Amer. Bull., 84, 2217-26, 1973.

_____, and D. L. Inman, Longshore sand transport on beaches, J. Geophys. Res., 75, 5914-27, 1970.

Kurihara, Y., On the use of implicit and iterative methods for the time integration of the wave equation, Monthly Weather Review, 93, 33-46, 1965.

LeBlond, P. H., Formation of spiral beaches, Proc. 13th Conf. Coastal Engr., 1331-46, 1972.

Lilly, D. K., On the computational stability of numerical solutions of time-dependent non-linear geophysical fluid dynamics problems, Monthly Weather Review, 93, 11-26, 1965.

Longuet-Higgins, M. S., Longshore currents generated by obliquely incident sea waves, 1. J. Geophys. Res., 75, 6778-89, 1970.

_____, Longshore currents generated by obliquely incident sea waves, 2. J. Geophys. Res., 75, 6790-801, 1970.

_____, Recent progress in the study of longshore currents, in Waves on Beaches and Resulting Sediment Transport, 462 pp., Academic Press, New York, 1972.

_____, and R. W. Stewart, Changes in the form of short gravity waves on long waves and tidal currents, J. Fluid Mech., 8, 565-83, 1960.

_____, _____, The changes in amplitude of short gravity waves on steady non-uniform currents, J. Fluid Mech., 10, 529-49, 1961.

_____, _____, Radiation stress and mass transport in gravity waves, with application to 'surf beats', J. Fluid Mech., 13, 481-504, 1962.

_____, _____, Radiation stresses in water waves: a physical discussion with applications, Deep-Sea Res., 11, 529-62, 1964.

Mogel, T. R., R. L. Street, and B. Perry, Computation of alongshore energy and littoral transport, Proc. 12th Conf. Coastal Engr., 899-918, 1970.

Noda, E. K., State of the art of littoral drift measurements, Shore and Beach, 39, 35-41, 1971.

O'Brien, M. P. and R. G. Dean, Hydraulics and sedimentary stability of coastal inlets, Proc. 13th Conf. Coastal Engr., 761-780, 1972.

O'Rourke, J. G., and P. H. LeBlond, Longshore currents in a semi-circular bay, J. Geophys Res., 77, 444-52, 1972.

Price, W. A., K. W. Tomlinson and D. H. Willis, Predicting changes in the plan shape of beaches, Proc. 13th Conf. Coast. Engr., 1321-30, 1972.

Ralston, A., A first course in numerical analysis, 578 pp., McGraw-Hill Inc., New York, 1965

Rector, R. L., Laboratory study of equilibrium profiles of beaches, Beach Erosion Board, Tech. Memo. 41, Washington, 1954.

Saville, T., Jr., Model Study of sand transport along an infinitely long straight beach, Trans. of Am. Geophys. Union, 31, 555-65, 1950.

_____, Scale effects in two dimensional beach studies, Proc. of Conf. of the International Association of Hydraulic Research, Lisbon, 1957.

Scott, T., Sand movement by waves, Beach Erosion Board, Tech. Memo. 48, Washington, 1954.

Sonu, C. J., Field observation of nearshore circulation and meandering currents, J. Geophys. Res., 77, 3232-47, 1972.

Stapor, F. W., Sediment budgets on a compartmented low-to-moderate energy coast in northwest Florida, Mar. Geol., 10, M1-M7, 1971.

Thornton, E. B., Longshore current and sediment transport, Tech. Rep. No. 5, Dept. of Coastal and Oceanographic Engr., University of Florida, 1969.

Vincent, L., Quantification of Shoreline Meander, Tech. Rep. No. 7, Dept. of Environmental Sciences, University of Virginia, 1973.

Walton, T. L., Jr., Littoral drift computations along the coast of Florida by means of ship wave observations, Coastal and Oceanographic Engineering Laboratory, University of Florida, Tech. Rep. No. 15, 1973.

```
      SUM=0.
      DO 2 I=J,L1
    2 SUM=SUM+DELXY(I)
      DELNEW=SUM/(L1-J+1)
      I=J
C**** EXECUTE THE PROCEDURE AS DESCRIBED IN THE TEXT FOR THE
C     TRANSLATION OF THE BEACH POINTS I.E. MOVE THE FIRST POINT
C     ALONG THE BEACH SEGMENT TO ITS LEFT UNTIL THE DISTANCE BETWEEN
C     IT AND THE POINT ON ITS LEFT IS DELNEW,REDEFINE THE SEGMENT
C     BETWEEN THIS NEW POSITION AND THE POINT IMMEDIATELY TO ITS RIGHT
C     AND MOVE THIS SECOND POINT ALONG THE NEW SEGMENT...ETC.
   23 IF(DELNEW-DELXY(I))10,20,30
   10 X(I+1)=X(I+1)+(DELNEW-DELXY(I))*SIN(THETA(I))
      Y(I+1)=Y(I+1)+(DELNEW-DELXY(I))*COS(THETA(I))
      GO TO 21
   30 X(I+1)=X(I+1)+(DELNEW-DELXY(I))*SIN(THETA(I+1))
      Y(I+1)=Y(I+1)+(DELNEW-DELXY(I))*COS(THETA(I+1))
   21 DELXY(I+1)=SQRT((X(I+2)-X(I+1))**2+(Y(I+2)-Y(I+1))**2)
   20 I=I+1
      IF(I.EQ.L1)GO TO 22
      GO TO 23
   22 ICOUNT=ICOUNT+1
      IF(ICOUNT.NE.NUMTI) GO TO 11
CHECK TO SEE IF THE DISTANCE BETWEEN ADJACENT POINTS IS APPROXIMATELY
      EQUAL.
      WRITE(6,25)(DELXY(I),I=J,L1)
   25 FORMAT(2X,5(3X,F10.1))
      RETURN
      END


      SUBROUTINE RESULTS(X,Y,Z2,Z1,LIM,MAX)
C
C**** RESULTS PRINTS OUT SOME OF THE MORE IMPORTANT NUMBERS GENERATED
C     BY SHORLIN.
      DIMENSION Z1(90),Z2(90),X(90),Y(90)
      COMMON DEL(90),BETA(90),THETA(90)
      COMMON    X0(90),X1(90),X2(90),X3(90),Y0(90),Y1(90),Y2(90),Y3(90)
      COMMON DY0(90),DX0(90),DY1(90),DX1(90),DY2(90),DX2(90),DY3(90),
     $DX3(90)
      COMMON/BLK1/XX(90),YY(90)
      COMMON/BLOC2/LIMIT,LIM1,LIM2
      COMMON/BLOC5/Q0,Q(90)
      COMMON/BLOC7/IV,DT
      COMMON/BLK2/PHI0,PHI(90)
      TIME=IV*DT
      DAYS=TIME/24.
      YEARS=DAYS/365.
      PRINT 1,IV,DT,TIME,DAYS,YEARS
    1 FORMAT(3X,* NO.TIME STEPS(IV)=*,I4,5X,*TIME INCREMENT(DT)=*,F4.1,
     $1X,*HRS.*,5X,*ELAPSED TIME(IVXDT)=*,F10.1,1X,*HRS.=*,F8.1,1X,
     $*DAYS=*,F5.2,1X,*YEARS*)
      PRINT 2
    2 FORMAT(//5X,*POINT*,13X,*X(TIME=0)*,10X,*Y(TIME=0)*,10X,*X(TIME=
     $IVXDT)*,10X,*Y(TIME=IVXDT)*,5X,*X(PRESENT)*,5X,*Y(PRESENT)*/17X,
     $*METERS*,13X,*METERS*,13X,*METERS*,18X,*METERS*,15X,*METERS*,
     $10X,*METERS*)
      IF(MAX.GT.LIM)  K=MAX
      IF(MAX.LE.LIM)  K=LIM
      DO 4  I=1,K
    4 WRITE(6,3)I,X(I),Y(I),Z2(I),Z1(I),XX(I),YY(I)
    3 FORMAT(3X,1H ,I3,3X,3(7X,F10.2),16X,F10.2,8X,F10.2,5X,F10.2)
      PRINT 5
    5 FORMAT(//2X,*POINT*,10X,*BEACH ANGLE*,10X,*WAVE ANGLE*,10X,*BEACH
     $POINT SEPARATION* ,5X,*TRANSPORTS*/17X,*DEGREES*,14X,*DEGREES*,13X
     $,*METERS*,22X,*CUBIC METERS/HR*)
C**** CONVERT FROM RADIANS TO DEGREES.
      DO 8 I=1,LIMIT
      J=I-1
      PHI(J)=CVRT2*PHI(J)
    8 THETA(J)=CVRT2*THETA(J)
      DO 6  I=1,LIMIT
      J=I-1
    6 WRITE(6,7)J,THETA(J),PHI(J),DEL(J),Q(J)
C**** CONVERT FROM DEGREES BACK TO RADIANS.
      DO 10 I=1,LIMIT
      J=I-1
      PHI(J)=CVRT1*PHI(J)
   10 THETA(J)=CVRT1*THETA(J)
    7 FORMAT(1H ,2X,I3,7X,F10.2,9X,F10.2,13X,F10.2,25X,F10.2)
      CALL ERROR(X,Y,Z2,Z1,LIM,MAX)
      RETURN
      END
```

```
      SUBROUTINE GRAPH(U,V,N,IDASH)
       COMMON/IUBS/IUBS(10),IQB
      COMMON/SCALE/A,B,C,D,YT,YB,XR,XL
      DIMENSION U(N),V(N),I(6),H(6)
      X=A*U(1)+B
      Y=C*V(1)+D
      CALL PLOT(X,Y,3)
      JDASH=IABS(IDASH)
      IF(JDASH.LE.9) GO TO 200
C COUNT NUMBER OF DIGITS IN IDASH
      NDIGIT=6
      IF(JDASH.LE.99999) NDIGIT=5
      IF(JDASH.LE.9999) NDIGIT=4
      IF(JDASH.LE.999) NDIGIT=3
      IF(JDASH.LE.99) NDIGIT=2
C DECOMPOSE INTO FOUR INTEGERS
      NDEN=100000
      NUM=JDASH
      DO 99 K=1,6
      I(K)=NUM/NDEN
      NUM=NUM-I(K)*NDEN

      NDEN=NDEN/10
   99 CONTINUE
C MINIMUM SPACING IS 1/128 INCH .
      DO 100 K=1,6
      IF(I(K).GT.7) I(K)=7
  100 CONTINUE
      NFIRST=7-NDIGIT
      DO 101 NI=NFIRST,6
      H(NI)=1.0/(2.0**I(NI))
  101 CONTINUE
C INITIALIZE
      LEVEL=NFIRST
      EXCESS=H(NFIRST)
      DO 103 K=2,N
C DRAW DASHED LINE TO NEXT POINT IN ARRAYS.
      XOLD=A*U(K-1)+B
      YOLD=C*V(K-1)+D
      XNEW=A*U(K)+B
      YNEW=C*V(K)+D
      XDIFF=XNEW-XOLD
      YDIFF=YNEW-YOLD
      TOTAL=SQRT(XDIFF*XDIFF+YDIFF*YDIFF+0.0000001)
      XCOS=XDIFF/TOTAL
      YSIN=YDIFF/TOTAL
      TOGO=TOTAL
      X=XOLD
      Y=YOLD
C NEXT SECTION OF LINE
  102 CONTINUE
      ITEST=LEVEL+NDIGIT
      IPEN=2
      IF(((ITEST/2)*2).EQ.ITEST) IPEN=3
      P=AMIN1(EXCESS,TOGO)
      X=X+P*XCOS
      Y=Y+P*YSIN
      CALL PLOT(X,Y,IPEN)


      TOGO=TOGO-P
      EXCESS=EXCESS-P
      IF(EXCESS.LT.0.005) LEVEL=LEVEL+1
      IF(LEVEL.GT.6) LEVEL=NFIRST
      IF(EXCESS.LT.0.005) EXCESS=H(LEVEL)
      IF(TOGO.GT.0.005) GO TO 102
C OTHERWISE GO TO NEXT POINT IN ARRAY AND CONTINUE
  103 CONTINUE
      RETURN
C SOLID LINE GRAPH WHEN IDASH HAS ONLY ONE DIGIT.
  200 CONTINUE
       IQB=1
      DO 10 K=2,N
      X=A*U(K)+B
      Y=C*V(K)+D
      IF(K.EQ.IUBS(IQB))1000,1001
 1000 CALL PLOT(X,Y,3)
       IQB=IQB+1
       GO TO 10
 1001 CONTINUE
      CALL PLOT(X,Y,2)
   10 CONTINUE
      RETURN
      END
```